INVESTIGATING THE ROLE OF VACCINIA VIRUS-DERIVED SMALL EXTRACELLULAR VESICLE CARGO IN INFECTION

Hayley Elizabeth McKay

A thesis submitted to the Faculty of Graduate and Postdoctoral Studies
in partial fulfillment of the requirements for the degree of

Master of Science in Microbiology and Immunology

Department of Biochemistry, Microbiology, and Immunology
Faculty of Medicine
University of Ottawa

Supervisor: Dr. Carolina Ilkow

ABSTRACT

Poxviruses, such as vaccinia virus, encode a variety of proteins that inactivate their host's antiviral response. Small extracellular vesicles (sEV), including exosomes and microvesicles, contain a variety of proteins, lipids, and nucleic acids that enable intercellular crosstalk. Recent evidence suggests that viruses can hijack these sEV pathways upon infection and use them to their advantage. Here, we found that upon vaccinia virus infection of a variety of cancer cell lines, sEV production and release increases drastically. We hypothesized that these VacV-infected cell sEVs contain RNA molecules that may play an important role in VacV's virulence. We identified two VacV mRNAs with enriched reads in the small RNA-Seq analysis of MiaPACA-2 cells and sEVs following VacV infection. By qPCR analysis, we confirmed that these two immunomodulatory VacV mRNAs, B19R and C12L, were present in sEVs. With the use of a Vaccinia Virus lacking functional B19R and an exosome-deficient 786-O cell line, we have shown that sEV-associated B19R is functionally present in exosomes and plays a role in dampening the antiviral response prior to infection. This is the first time a poxvirus has been shown to enhance sEV production, packaging viral mRNAs into sEVs, and potentially exploit sEVs for their own advantage.

ACKNOWLEDGEMENTS

I would like to acknowledge and thank my supervisor Dr. Carolina Ilkow for her personal and scientific guidance throughout my time in her research group and for the wonderful opportunities she has provided me within and outside the laboratory. I would like to thank my fellow lab members for their contributions to this project, and for their constant support, ideas, and feedback. Thank you to the members of the Ilkow lab, the 3rd Floor, and the BMI Department for their friendship. I would like to thank my Thesis Advisory Committee members, Dr. Marceline Cote and Dr. Ian Lorimer, for their time, guidance, and constructive feedback throughout my MSc. Finally and most importantly, I would like to thank my family for their never-ending love and support in all that I do.

TABLE OF CONTENTS

Abstract ii

Acknowledgements iii

Table of Contents iv

List of Abbreviations viii

List of Figures xi

List of Tables xii

1. Introduction 1

1.1 Vaccinia Virus 1

1.1.1 Vaccinia Virus and the Eradication of Small Pox 1

1.1.2 Orthopoxviruses: Origins, Clinical Manifestations, and Epidemiology 2

1.1.3 Vaccinia virus as a laboratory model: Understanding Orthpoxviruses 4

1.1.4 Vaccinia Virus Genetic Nomenclature 5

1.1.5 Vaccinia Virus Replication Cycle 6

1.1.6 Host Defences and VacV Counter-Defences 13

1.1.7 Vaccinia virus as an Oncolytic Virus 22

1.1.8 Vaccinia virus as a Next-Generation Vaccine 23

1.1.9 The Importance of Studying Vaccinia Viruses 24

1.2 Extracellular Vesicles and Viral Infections 25

1.2.1 Extracellular Vesicles: Exosomes, Microvesicles, and Apoptotic Bodies 25

1.2.2 sEV Biogenesis Pathways 27

1.2.3 The Sorting of Cargo into sEVs 30

1.2.4 sEV Uptake into Recipient Cells 31

1.2.5 sEV Biodistribution 32

1.2.6 sEVs in Health and Disease 33

1.2.7 Immunostimulatory and Immunomodulatory sEVs 34

1.2.8 Viruses Hijack SEVs 35

1.2.9 sEVs and VacV 37

1.3 Study Rationale, Hypothesis, and Aims 38

2. Materials and Methods 39

2.1 Cells 39

2.2 Viruses 39

2.3 Poxvirus Amplification 40

2.4 Rhabdovirus Amplification 40

2.5 Poxvirus Plaque Assay 41

2.6 Rhabdovirus Plaque Assay 41

2.7 sEV Isolation from VacV-infected and Mock Cells 41

2.8 Nanoparticle Tracking Analysis (NTA) 42

2.9 Nanoscale Flow Cytometry (NFC) 42

2.10 Western Blotting and sEV 43

2.11 Western Blotting of Whole Cell Lysates 44

2.12 Crystal Violet Staining and Quantification for Cell Viability 45

2.13 Small RNA-Seq 45

2.14 Quantitative Real-Time PCR of sEV RNA 46

2.15 Assay 1: sEV Pre-Treatment of 786-Os 47

2.16 Assay 2: sEV Post-Treatment of 786-Os 48

2.17 Assay 3: sEV Treatment in the Absence of VSVΔ51 infection 48

2.18 CRISPR-Cas9-mediated Rab27a Knockout 49

2.19 Isolation of Confirmation of a 786-O ΔRab27a Monoclonal Cell Line 50

2.20 Statistical Analyses 50

3. Results **51**

3.1 VacV-infected cells release more small extracellular vesicles than uninfected cell 51

3.2 B19R and C12L RNAs are present in sEVs following infection with VacV 55

3.3 CRISPR-Cas9-mediated targeting of Rab27a in 786-O cells 59

3.4 Small extracellular vesicle-associated B19R RNA augments VSVΔ51-induced cytotoxicity 64

3.5 sEV-associated B19R RNA does not augment VSVΔ51-GFP replication 24 hours following infection 69

3.6 Small extracellular vesicle-associated B19R RNA cytotoxicity is VSVΔ51-dependent 69

4. Discussion **72**

4.1 The Effect of VacV Infection on sEVs 72

4.2 The Effect of VacV Infection on sEV Cargo 73

4.3 Characterization of a 786-O ΔRab27a Cell Line 75

4.4 Potential Effect of sEV-Associated C12L in Infection 77

4.5 The Functional Effect of sEV-Associated B19R in Infection 77

4.6 Future Directions 80

5. Conclusions **81**

References Cited **82**

Contributions from Collaborators **101**

Appendix **102**

Curriculum Vitae **103**

LIST OF ABBREVIATIONS

Bak	BCL-2 Homologous Antagonist/Killer
CEV	Cell-Associated Enveloped Virion
CFSE	Carboxyfluorescein succinimidyl ester
cGAS	Cyclic GMP-AMP Synthase
Cop	Copenhagen Strain
CMC	Carboxymethyl Cellulose
CV	Crystal Violet
DC	Dendritic Cell
DNA-PK	DNA-Dependent Protein Kinase
dsRNA	Double-Strand Ribonucleic Acid
EBV	Epstein Barr Virus
EEV	Extracellular Enveloped Virion
ESCRT	Endosomal Sorting Complex Required for Transport
ER	Endoplasmic Reticulum
EV	Extracellular Vesicles
EV71	Enterovirus 71
FBS	Fetal Bovine Serum
gRNA	Guide Ribonucleic Acid
HBV	Hepatitis B Virus
HCV	Hepatitis C Virus
HRP	Horseradish Peroxidase
IEV	Intracellular Enveloped Virions
IL	Interleukin

ILV	Intraluminal Vesicles
IMV	Intracellular Mature Virion
IRF	Interferon Regulatory Factor
ISG	Interferon Stimulated Genes
lEV	Large Extracellular Vesicle
KSHV	Kaposi's Sarcoma-Associated Herpesvirus
lncRNA	Long Non-Coding Ribonucleic Acid
MDA-5	Melanoma Differentiation-Associated Protein 5
MHC	Major Histocompatibility Complex
miRNA	Micro Ribonucleic Acid
MLKL	Mixed Lineage Kinase Domain Like Pseudokinase
MOI	Multiplicity of Infection
mRNA	Messenger Ribonucleic Acid
MVA	Modified Virus Ankara
MVB	Multivesicular Body
Nef	Negative Regulatory Factor
NF-κB	Nuclear Factor Kappa-light-chain-enhancer of activated B cells
NK	Natural Killer
NFC	Nanoscale Flow Cytometry
NTA	Nanoparticle Tracking Analysis
NYVAC	New York Vaccinia Copenhagen
PAMP	Pathogen-Associated Molecular Pattern
PKR	Protein Kinase R
PRR	Pattern Recognition Receptor

qPCR	Quantitative Polymerase Chain Reaction
Rab	Ras-Related Proteins in Brain
RBP	RNA-Binding Protein
RIG-I	Retinoic Acid-Inducible Gene I
RLR	Rig-I-Like Receptor
rRNA	Ribosomal Ribonucleic Acid
sEV	Small Extracellular Vesicle
STAT	Signal Transducer and Activator of Transcription
TLR	Toll-Like Receptor
TNF	Tumour Necrosis Factor
TSG101	Tumour Susceptibility Gene 101
VacV	Vaccinia Virus
VSV	Vesicular Stomatitis Virus 2
ZBP1	Z-DNA Binding Protein 1

LIST OF FIGURES

Figure 1. Vaccinia Virus Replication Cycle. 9

Figure 2. Small Extracellular Vesicle Biogenesis Pathways 28

Figure 3. Characterization of sEVs following VacV infection 53

Figure 4. Small RNA-Seq experiment reveals B19R and C12L RNA are present in VacV-infected cell sEVs. 56

Figure 5. B19R and C12L RNA detection in VacV-infected cell-derived sEVs by Quantitative Real-Time PCR. 58

Figure 6. Validation of an exosome-deficient ΔRab27a 786-O monoclonal cell line. 60

Figure 7. ΔRab27a 786-O cells produce less sEVs and less exosomes than parental 786-O cells. 62

Figure 8. sEV-B19R augments VSVΔ51-dependent cytotoxicity. 66

Figure 9. VacV sEVs are virion-free. 67

Figure 10. sEV-B19R does not increase VSVΔ51-GFP viral titers at 24 hours post-infection. 70

Figure 11. sEV-B19R treatment did not reduce cell viability in the absence of VSVΔ51-GFP infection. 71

LIST OF TABLES

Table 1. qPCR and PCR primers used in this study. 102

Table 2. Human Rab27a gRNA design and cloning strategy. 102

1. INTRODUCTION

1.1 Vaccinia Virus

Vaccinia virus (VacV) is the prototypical orthopoxvirus. It has been used for over 80 years as a model to study its more pathogenic relatives; including variola virus, the causative agent of smallpox. VacV's claim to fame was as the small pox vaccine, culminating with the World Health Organization's announcement in May 1980 that smallpox had been officially eradicated (Fenner *et al.* 1988, WHO). Though smallpox has been eradicated, VacV is a promising oncolytic virus and vaccine candidate for the prevention of emerging infectious diseases.

1.1.1 Vaccinia Virus and the Eradication of Small Pox

Throughout the WHO-led Global Immunization Campaign, many different VacV strains were used. These VacV variants, named after the geographical regions in which they were used, were propagated in the skin of livestock and became more evolutionarily distinct over time (Qin *et al.* 2015, Journal of Virology). These first-generation wildtype VacV strains included Wyeth, Bern, Copenhagen, Tian Tian, NYCBH (New York City Board of Health), Lister, Paris, Tashkent, Ankara, and Dairen (Qin *et al.* 2015, Journal of Virology). The use of live animals for viral propagation presented several complications, including a high probability of the microbial contamination of vaccines (Jacobs *et al.* 2009, Antiv. Res.). Second-generation vaccines were those in which these wildtype VacV strains were propagated in cell culture or in embryonated chicken eggs. In these culturing systems, plaque purified VacV variants were selected, increasing the evolutionary divergence of these strains.

Though severe adverse events with first- and second-generation VacV vaccinations were rare, there were reports of myopericarditis and encephalopathy, sometimes resulting in death (Greenberg and Kennedy 2008, Expert Opinion on Investigational Drugs). This drove the development of third-generation attenuated VacV vaccines near the end of the eradication program, prepared through sequential passaging of wildtype VacV strains in cell culture or in embryonated chicken eggs (Fenner *et al.* 1988, WHO). Three widely-used third-generation VacV vaccine candidates include LC16m8 (Lister), NYVAC (Copenhagen), and MVA (Ankara). These third-generation VacVs all contain large deletions in host-range genes and are either replication-deficient or have reduced replicative abilities in human cells (Kidokoro *et al.* 2005, PNAS, Meyer *et al.* 1991, Journal of Virology, Tartaglia *et al.* 1992, Virology). These strains are very safe, with very few reported moderate to severe adverse events (Artenstein 2008, Reviews in Medical Virology). With the more recent advances in our ability to modify the VacV genome through the insertion of interruption cassettes, the fourth generation VacV vaccines are being produced. These vaccines are attenuated by interrupting specific host-range genes, and their immunogenicity can be enhanced by the expression of immunomodulatory genes to ensure a robust cross-reactive immune response against variola virus, the causative agent of small pox (Jacobs *et al.* 2009, Antiviral Res.).

1.1.2 Orthopoxviruses: Origins, Clinical Manifestations, and Epidemiology

Several orthopoxviruses infect humans, including variola, vaccinia, monkeypox, and cowpox. Most orthopoxvirus infections of humans are considered accidental, as variola virus is the only orthopoxvirus whose natural reservoir is humans. Most orthopoxviruses are

named after the host from which they were isolated, but VacV's origin was controversial and speculative for many years (Baxby 1977, Archives of Virology). Originally, before orthopoxviruses had been sequenced, VacV was thought to have evolved from the cowpox virus (Baxby 1977, Archives of Virology). It was only after sequencing each of the orthopoxvirus species that VacV's evolutionary beginning was proposed to have stemmed from the horsepox virus (Tulman *et al.* 2006, Journal of Virology, Hatcher *et al.* 2014, Journal of Virology, Qin *et al.* 2015, Journal of Virology). Orthopoxvirus speciation has now been attributed to reductive evolution, through recombination, gene fragmentation, and selective retention of genes required for virion production (Hatcher *et al.* 2014, Journal of Virology, Qin *et al.* 2015, Journal of Virology).

Orthopoxviruses infect their hosts through the skin. If the virus is then able to spread to the lymphatic system, viremia will occur and the virus will disseminate throughout the host's body. Clinically, smallpox manifests as the sudden onset of flu-like symptoms, followed by the presence of pock lesions in the oropharynx region and on the extremities (Fenner *et al.* 1988, WHO). Lesions progress towards the patient's trunk and other serious complications arise, including encephalopathy and blindness. After several weeks, in the roughly 70% of patients who survive smallpox, scars develop in the place of these lesions and they are no longer contagious (Fenner *et al.* 1988, WHO). On the other hand, VacV inoculation of the skin results in a localized pock lesion, and viremia only occurs in immunosuppressed patients infected with unattenuated strains (Kretzschmar *et al.* 2006, PLoS Medicine).

While variola virus no longer represents a threat for humans, other pathogenic orthopoxviruses still present a challenge worldwide, as they have not been eradicated from their natural reservoirs. Monkeypox virus is endemic to the Republic of Congo and presents similarly to variola virus (Jezek *et al.* 1986, The Journal of Infectious Diseases). There have been several monkeypox virus outbreaks in the Republic of Congo (Meyer *et al.* 2002, Journal of Clinical Microbiology), and one outbreak was reported in Wisconsin in 2003 (Reed *et al.* 2004, NEJM). Cowpox virus infects similarly to vaccinia virus, causing localized lesions, and viremia only in those who are immunocompromised (Singh *et al.* 2012, Indian Journal of Virology). Several other pathogenic strains, referred to as vaccinia-like viruses (VLVs), have been identified in Brazil, India, Nepal, Pakistan, Egypt, and Indonesia (Nagasse-Sugahara *et al.* 2004, Rev. Inst. Med. Trop. São Paulo, Singh *et al.* 2012, Indian Journal of Virology, Venkatesan *et al.* 2010, Vet. Ital.).

1.1.3 Vaccinia virus as a laboratory model: Understanding Orthpoxviruses

There are several factors that make VacV an important laboratory model in the study of orthopoxviruses. First, VacV is relatively safe compared to other orthopoxviruses; even wildtype, first-generation VacV strains can be studied in Biosafety Level-2 laboratories. Second, the ability to isolate recombinant pock lesions from the chorioallantoic membranes of chicken eggs and plaque purify distinct VacV clones in cell culture has allowed us to characterize and compare mutants. These comparisons began in Frank Fenner's laboratory in the 1950s and have improved with advances in sequencing and targeted mutagenesis techniques (Fenner 1958, Quin *et al.* 2011, Journal of Virology, Zhang *et al.* 2013, Vaccine).

Third, the attenuation of VacV for smallpox immunization resulted in a large diversity of strains and their derivatives, which can be compared to decipher the roles of VacV gene products in infection. For example, the attenuation of VacV Ankara to produce MVA (Modified Virus Ankara) was attained by 572 passages in primary chick embryo fibroblasts (Mayr *et al.* 1975, Infection). CVA 382, an Ankara intermediate with four of the six major deletions found in MVA, was isolated during passage number 382 (Mayr *et al.* 1975, Infection). By comparing wildtype Ankara, CVA382, and MVA, Meyer and colleagues (1991, Journal of General Virology) were able to map several host-restriction genes to the VacV terminal repeats.

Orthopoxviruses have high homology, especially in genes encoding for necessary proteins found in the centre of their linear genome (Aguado *et al.* 1992, Journal of General Virology, Aguado *et al.* 1992, Journal of General Virology). Upon comparing the sequences of variola virus (Harvey strain) and VacV (Western Reserve strain – a derivative of NYCBH), more than 96% of their total nucleotide sequence was homologous (Aguado *et al.* 1992, Journal of General Virology). Sequence homology between VacV and either Horsepox or Cowpox are even more highly conserved (Tulman *et al.* 2006, Journal of Virology). Due to the high homology between VacV and the pathogenic orthopoxviruses, VacV is an important tool to gain a better understanding of orthopoxvirus biology.

1.1.4 Vaccinia Virus Genetic Nomenclature

In 1990, the VacV Copenhagen strain was the first VacV strain to be fully sequenced (Goebel *et al.* 1990, Virology). They found that VacV genes were compactly organized and

contained very few non-coding regions. For this sequencing, they first used several restriction enzymes (BamHI, KpnI, SalI, SacI, PstI, SmaI, and HindIII) to cut the VacV genome and then subsequently cloned each region into a plasmid vector. These inserts were then sequenced and the organization of the VacV genome was determined. The nomenclature used for VacV genes and proteins is based on the HindIII restriction map generated in this VacV Copenhagen sequencing study (Goebel *et al.* 1990, Virology). The HindIII-mediated cutting of the VacV genome resulted in 16 fragments labeled A to P, with the order based on the order that they were sequenced and not based on their position in the VacV genome. Within each of these fragments, they identified between 0 and 29 genes. These genes were then numbered starting with 1 on the 5' end of each fragment. Finally, the direction of the gene within the genome (left or right) is where the R or L in VacV nomenclature originated. For example, A11R was the 11th gene in the first sequenced fragment of the HindIII map and is transcribed from left to right (5' to 3') (Goebel *et al.* 1990, Virology). Because the arrangement of genes in Copenhagen differs from other (and later) sequenced VacV strains, the original nomenclature can lead to some confusion. For example, B19R in Copenhagen is B18R in the Western Reserve strain (Prazsak *et al.* 2018, Genome Announcements). Therefore, strain-specific nomenclature is now used when referring to VacV genes and proteins.

1.1.5 Vaccinia Virus Replication Cycle

There are two major VacV virion types: the mature virion and the extracellular virion. The mature virion, also known as the Intracellular Mature Virion (IMV), is composed of a

nucleoprotein core surrounded by a single envelope (Cyrklaff *et al.* 2005, PNAS). IMV visions are released from the cell upon loss of membrane integrity. An alternate mature virion can be produced in which the IMV is wrapped by two more envelopes at the Golgi, resulting in the Intracellular Enveloped Virion (IEV) (Schmelz *et al.* 1994, Journal of Virology). This IEV fuses with the cell membrane and a cell-free Extracellular Enveloped Virion (EEV) or Cell-associated Enveloped Virion (CEV) is released (Smith and Law 2004, Virus Research). The extracellular virion envelope is less stable, and can rupture upon release or attachment, leading to the release of an IMV (Vanderplasschen *et al.* 1998, Journal of General Virology). Mature and extracellular virions differ both antigenically and structurally, as well as in their entry pathways (Fig. 1) (Locker *et al.* 2000, Mol Biol Cell, Doms *et al.* 1990, Journal of Virology). Additionally, there are cell- and strain-specific differences in VacV entry that complicates this further (Bengali *et al.* 2009, Virology, Whitbeck *et al.* 2009, Virology).

VacV IMV entry begins with the attachment of VacV to the cell surface in one of several ways: (1) Envelope proteins A27, D8, and/or H3 bind to host glycosaminoglycans (Bengali *et al.* 2009, Virology, Carter *et al.* 2005, Journal of General Virology); (2) Envelope proteins A26 and/or L1 bind to host cell laminin (Chiu *et al.* 2007, Journal of Virology); or (3) Envelope proteins A14, A17, and/or D8 localize to lipid rafts (Chung *et al.* 2005, Journal of Virology). There are likely to be additional protein-protein interactions that impact the attachment of VacV to the surface. Following attachment, the virion is internalized by either macropinocytosis or membrane fusion. This distinction is dependent on which VacV proteins are present on the surfaces of the virus particle and the host cell, as well as the presence of phosphatidylserine on the IMV surface. When the membrane fusion suppressors A25 and

A26 are present on the IMV envelope, entry can take place through macropinocytosis, in a clathrin- and calveolin-independent but actin- and ATP-dependent manner (Chang *et al.* 2010, Journal of Virology, Huang et al. 2018, Anal. Chem). Additionally, lipid raft-associated proteins CD98, VPEF, and Integrin β1 on the cell membrane are involved in the induction of VacV entry by macropinocytosis, and VacV membrane phosphatidylserine is thought to induce VacV macropinocytosis through apoptotic mimicry, a mechanism used by apoptotic bodies to enter cells in a non-inflammatory manner (Schroeder *et al.* 2012, Journal of Virology, Huang *et al.* 2008, Journal of Virology, Izmailyan *et al.* 2012, Journal of Virology, Mercer and Helenius 2009, Science, Mercer and Helenius 2010, NYAS). Upon macropinocytosis, the mature virion envelope is retained in the macropinosomes until endosomal acidification, when the envelope fuses with the vesicular membrane to release the viral core into the host cytoplasm (Mercer *et al.* 2010, PNAS, Townsley *et al.* 2006, Journal of Virology). If macropinocytosis is not induced, the mature virion penetrates the cell by membrane fusion, where the virion envelope lipids, proteins, and polysaccharides are incorporated into the host cell membrane and the nucleoprotein core is released directly into the cell (Carter *et al.* 2005, Journal General Virology). Several VacV proteins found in the mature virion envelope (A21, A28, H2, L5, L1, A16, G3, G9, and J5) form the entry-fusion complex necessary for VacV entry by membrane fusion, and these proteins are conserved among all poxvirus species (Senkevich and Moss 2005, Journal of Virology, Townsley *et al.* 2005a, Journal of Virology, Townsley *et al.* 2005b, Journal of Virology, Senkevich *et al.* 2005, PNAS, Izmailyan *et al*. 2006, Journal of Virology, Laliberte *et al.* 2011, PLoS Pathogens).

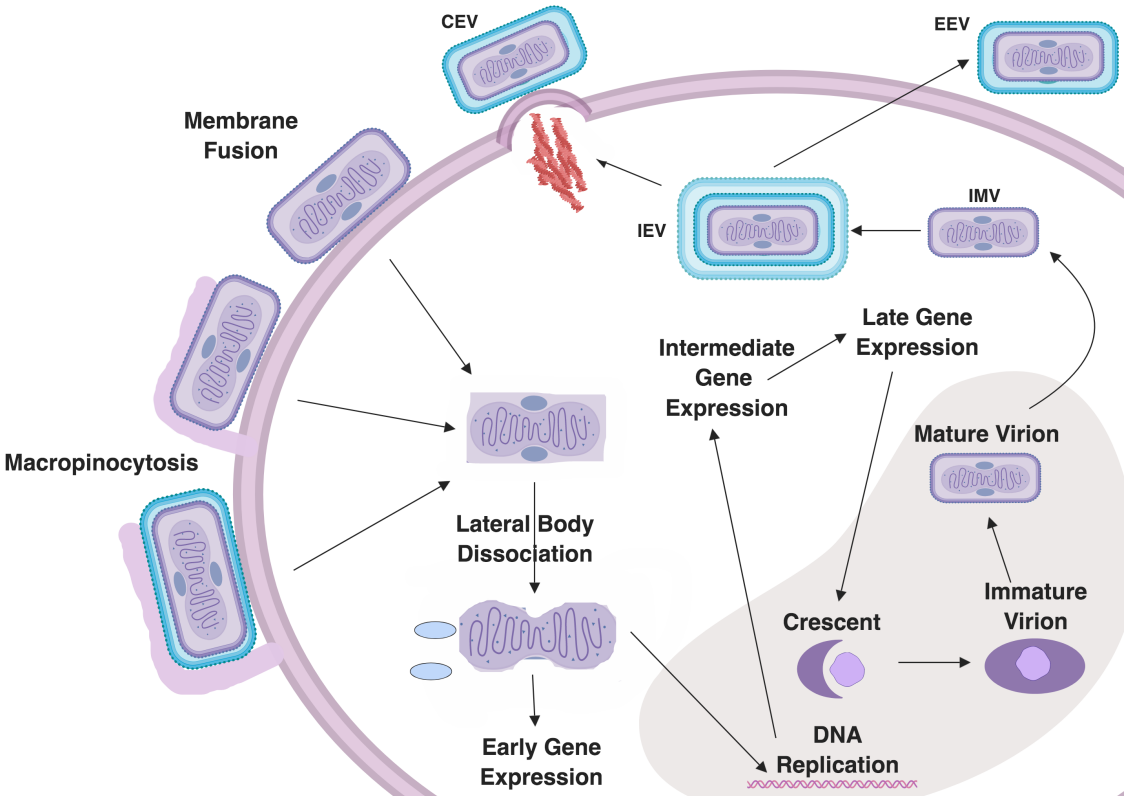

Figure 1. Vaccinia Virus Replication Cycle. First, VacV virions attach to the cell membrane. Extracellular virions (EEV and CEV) enter through macropinocytosis, where their outer envelope is removed within the macropinosome and their inner envelope fuses with the macropinosome membrane, leading to release of the core into the cell. Intracellular mature virions (IMV) enter the cell by macropinocytosis or membrane fusion. Once the core is released into the cytoplasm, the lateral bodies dissociate and the core is activated through conformational changes and an increase in size. This core activation is followed by the release of early gene transcripts for proteins involved in immune modulation, DNA replication, and downstream gene expression. The core is then uncoated and the VacV genome localizes to the viral factory (beige) where DNA replication and intermediate gene expression take place. The core begins to take form and late gene expression allows the formation of the crescent; the virion precursor. The crescent is transformed into the immature vision, which matures into the IMV. IMVs leave the viral factory with some accumulating in the cytoplasm and others become double-wrapped to form intracellular enveloped virions (IEV). These egress on an actin-tail projection (CEV) or through membrane fusion (EEV). Created with biorender.com © Hayley Elizabeth McKay 2019.

Much less is known about the entry of extracellular virions (IEV and CEV). Extracellular virions are more difficult to study because: (1) EEV purification can rupture the outer membrane and release an IMV; (2) EEV/CEV preparations are contaminated with IMV released from lysed cells; and (3) EEV/CEV is much less abundant than IMV (Smith *et al*. 2002, Journal of General Virology). EEV and CEV with an intact outer envelope are internalized exclusively by macropinocytosis (Mercer and Helenius 2009, Nature Cell Biology). This macropinocytosis process involves the uptake of an intact EEV/CEV into the macropinosome, rupturing of the outer envelope by vesicular acidification, and subsequent fusion of the vesicular and virion membrane resulting in the release of the virion core into the host cytoplasm (Ichihashi *et al.* 1996, Schmidt *et al.* 2011, EMBO). The outer envelope of extracellular virions contains several VacV proteins: A33, A34, A56, B5R, and F13 (Lorenzo *et al.* 2000), as well as several cell-derived proteins of trans-golgi network, early endosome, or plasma membrane origin (Vanderplasschen *et al.* 1997, Journal of Virology, Krauss *et al.* 2002, Hiller and Weber 1985, Journal of Virology), but their individual roles in the attachment and macropinocytosis of EEV/CEV is currently unknown.

The VacV biconcave core contains the VacV linear dsDNA genome, as well as several core-specific proteins: L4, A10, A3, A4, J6, A24 and F17 (Pedersen *et al.* 2000, Journal of Virology), and it is surrounded by the outer coat consisting of the inner lipid layer and a discontinuous proteinaceous layer (Easterbrook 1966, Journal of Ultrastructural Research, Cyrklaff *et al.* 2005, PNAS). The nucleoprotein core is flanked by two lateral bodies, anchored to the core's outer layer (Schmidt *et al.* 2013, Cell Reports). Within five minutes of core entry, the lateral bodies disassociate and the core increases in size as core proteins

change shape (Schmidt *et al.* 2013, Cell Reports). The lateral bodies are degraded by the host proteasome and three VacV proteins are released: F17 is a structural protein that is rapidly degraded, G4 is a redox protein that may be involved in lateral body disassembly, and H1 dephosphorylates Stat1, reducing the transcriptional activation of interferon stimulated genes (Teale *et al.* 2009, Journal of Virology, Schmidt *et al.* 2013, Cell Reports). VacV early gene transcription and mRNA processing is carried out by VacV core proteins upon core size increase (Schmidt *et al.* 2013, Cell Reports). More than 100 early mature mRNAs are released through pores in the intact core, and their translation depends on host initiation factors and ribosomes (Kafsafanas and Moss 2007, Cell Host Microbe). These early proteins include intermediate gene transcription factors and proteins needed for core uncoating, DNA replication, and immunomodulation of the host cell's antiviral response (Yang *et al.* 2010, PNAS).

Viral core uncoating, mediated by several VacV early gene products and the cell's ubiquitin-proteasome system, leads to the release of the viral genome (Kilcher *et al.* 2014, Cell Host Microbe, Liu *et al.* 2018, Journal of Virology, Mercer *et al.* 2012, Cell Reports). DNA replication of the VacV genome occurs in viral factories: ER-membrane-enclosed cytosolic sub-compartments (Tolonen *et al* 2001, Molecular Biology Cell). DNA replication is reliant on several early VacV genes that encode proteins involved in nucleotide metabolism and DNA replication (Katsafanas and Moss 2007, Host Cell Microbe, Jones and Moss 1984, Moss 2013, CSH Perspectives). VacV encodes an entire set of DNA replication enzymes, including a DNA Polymerase (E9), Helicase-Primase (D5), and DNA Ligase (A50) (Jones and Moss 1984, Journal of Virology, Roseman and Hruby 1987, Journal of Virology,

Kerr and Smith 1989, Nucleic Acids Research). VacV genome replication results in the formation of concatemeric intermediates (De Silva and Moss 2005, Virology Journal), which are then resolved into unit-length VacV genomes (Culyba *et al.* 2006, Virology, Garcia and Moss 2001). This is followed by the transcription of 53 VacV intermediate genes within viral factories, producing mRNAs encoding late gene transcriptions factors, DNA processing and packaging enzymes, and core-associated proteins (Yang *et al.* 2010, Journal of Virology). Subsequently, 38 late VacV genes, encoding virion morphogenesis/assembly proteins, membrane/structural proteins, and early transcription factors, are transcribed (Yang *et al.* 2011, Journal of Virology).

Virion assembly begins in viral factories about 5-6 hours post-entry with the appearance of crescent-shaped virion membranes of smooth ER, intermediate compartment, and endosomal origin that contain almost all VacV mature membrane proteins (Condit *et al.* 2006, Advances in Virus Research, Risco *et al.* 2002, Journal of Virology, Sodeik *et al.* 1993, JCB, Sodeik and Krijnse-Locker 2002, Trends in Microbiology). These virion crescents are made up of one inner lipid bilayer with embedded viral proteins, surrounded by an outer D13 protein lattice layer that acts as a scaffold for crescent and immature virion formation (Grimley *et al.* 1970, Szajner *et al.* 2005, J. Cell Biology). The spherical, immature virion is formed upon completion of the crescent to encapsidate the nucleoid and the viroplasm, which contains the core proteins (Morgan 1976, Science, Griffiths *et al.* 2001, Journal of Virology). The morphogenesis of an immature virion into a intracellular mature virion (IMV) involves: (1) the proteolytic cleavage of virion core protein precursors; (2) the rearrangement of immature virion components to form an intact core wall and lateral bodies; (3) the

assembly of early gene transcription apparatus within the core; (4) loss of the D13 lattice scaffold; (5) the formation of disulfide bonds with the mature virion membrane proteins; and (6) the addition of other mature membrane proteins (Griffiths *et al.* 2001, Journal of Virology, Mohandas and Dales 1995, Virology, Senkevich *et al.* 2000, Virology, Da Fonesca *et al.* 2000, Journal of Virology, Ansarah-Sobrinho and Moss 2004, Journal of Virology). The majority of mature virions are shuttled on microtubules from the viral factories to cytoplasmic sites of IMV accumulation (Ward 2004, Journal of Virology, McKelvey *et al.* 2002, Journal of Virology). The minority of IMV are shuttled to the Golgi, where they are wrapped with two additional Golgi-derived lipid bilayers, forming IEVs (Schmelz *et al.* 1994, Journal of Virology, Sivian *et al.* 2016, Journal of Virology). The vast majority of these IEVs are then transported to the plasma membrane, where exocytosis occurs, resulting in the release of extracellular virions (Sivan *et al.* 2016, Journal of Virology, Hollinshead *et al.* 2001, JCB). These extracellular virions are either released from the cell as extracellular enveloped virions (EEV) or retained on the cell surface as cell-associated CEV (Smith and Law 2004, Virus Research). CEV induce the accumulation of actin beneath the plasma membrane and are propelled to neighbouring cells on actin-tail projections (Cudmore *et al.* 1995, Nature, Sivan *et al.* 2016).

1.1.6 Host Defenses and VacV Counter-Defenses

Mammalian host cells have evolved many mechanisms by which they can control and combat viral infections. This begins with sensing of the invading pathogen upon the binding of Pathogen-Associated Molecular Patterns (PAMPs) to Pathogen Recognition Receptors

(PRRs). Viral PAMPs, including viral nucleic acids and proteins, are recognized by either plasma membrane, cytoplasmic, or endosomal PRRs, which include the toll-like receptors (TLRs), RIG-I-like receptors (RLRs), and DNA Sensors (Smith *et al.* 2013, Journal of General Virology). PAMP-PRR binding activates a signalling cascade in which Nuclear Factor Kappa B (NF-κB) and Interferon Regulatory Factor 3 (IRF3) are activated and shuttled into the nucleus where they induce the transcription of antiviral chemokines and cytokines. The most crucial cytokine for viral control, IFN-β, is then released from the cell and can bind to the IFN Type I receptor, activating the phosphorylation and heterodimerization of the Signal Transducer And Activator Of Transcription 1 and 2 (Stat1 and Stat2), leading to their translocation into the nucleus and the transcription of interferon stimulated genes (ISGs) (Schoggins *et al.* 2014, Current Opinions in Virology). Activation of ISGs leads to increased PRR stability, degradation of viral mRNA, and inhibition of protein synthesis, ultimately leading to cell death and the inability of the virus-infected cell to produce mature virions (Smith *et al.* 2013, Journal of General Virology). Orthopoxviruses encode many proteins that inactivate host antiviral signalling pathways and their downstream effects. In fact, almost one half of all VacV genes encode immunomodulatory factors that are involved in masking their PAMPs, inactivating PRRs, inhibiting the production of ISGs, inhibiting the activation of cell stress pathways, and inhibiting apoptotic cell death (Gubser *et al.* 2004, Journal of General Virology).

VacV virions contain several potential PAMPs, including a number of glycosylated envelope proteins that stimulate TLR2 and TLR4 upon attachment (Rojas *et al.* 2016, Cell Rep, Hutchens *et al.* 2008, PLoS Pathogens). When TLR2 or TLR4 are activated, they bind

to their adaptor proteins and activate NF-κB. To combat this antiviral signalling, VacV A46 binds to TLR adaptor proteins to inhibit TLR-stimulated signalling (Stack *et al.* 2005, J Exp Med). Once VacV's early mRNA has been released from the viral core, several RNA-sensing PRRs can be activated (Myskiw *et al.* 2011, Virology). Cytoplasmic dsRNA can bind to the Retinoid Acid Inducible Gene (RIG-I) or Melanoma Differentiation-Associated Protein 5 (MDA-5), initiating NF-κB and IRF3 signalling (Kawai *et al.* 2005). Alternatively, cytoplasmic dsRNA can bind to Protein Kinase R (PKR), a kinase that inhibits protein synthesis and ultimately leads to apoptosis (Pham *et al.* 2016, PLoS Pathogens). Endosomal dsRNA can activate TLR3, but again A46 can block its adaptor and inhibit downstream signalling (Kim *et al.* 2014, Protein Science).

VacV has evolved many ways to block the production of interferons by these antiviral pathways. First, VacV minimizes the amount of free viral mRNA through D9 and D10's decapping (Liu *et al.* 2014, Journal of Virology) and E3's dsRNA binding (Chang *et al.* 1992, PNAS). Second, VacV reduces host gene transcription and translation (Katsafanas *et al. 2007*, Cell Host & Microbe). D9 and D10 play a major role in the rapid degradation of host mRNAs, which reduces the production of antiviral proteins (Liu *et al.* 2014, Journal of Virology). Additionally, VacV relies on host translation initiation factors and ribosomes for protein synthesis and recruits this machinery to viral factories, where it is unavailable for host protein production (Walsh *et al.* 2008, Journal of Virology). Third, many VacV proteins block the activation of IRF3 and/or NF-κB, including E3, A46, A52, K7, B14, M2, K1, K3, and A49 (Ferguson *et al.* 2013, Journal of General Virology, Xiang *et al.* 2002, Journal of

Virology, Maluquer de Motes *et al.* 2011, PLoS Pathogens, Graham *et al.* 2008, PLoS Pathogens, Ryerson *et al.* 2017, Journal of Virology, Carroll *et al.* 1993, JBC).

Once the VacV genome is extruded from the virion core, it can activate cytoplasmic DNA-sensing PRRs, including DNA-Dependent Protein Kinase (DNA-PK), Z-DNA-Binding Protein 1 (ZBP1), and Cyclic GMP-AMP Synthase (cGAS), all of which lead to downstream activation of IRF3 in the absence of VacV's C16 protein that blocks this DNA sensing (Peters *et al.* 2013, PLoS Pathogens). Absent in Melanoma 2 (AIM2) also binds to cytosolic DNA and activates NF-κB (Hornung *et al.* 2009, Nature). Additionally, AIM2-DNA activates the inflammasome complex, which in turn activates caspase-1 (Hornung *et al.* 2009, Nature). Caspase-1 then cleaves the pro-inflammatory cytokines Interleukin 1β (IL-1β) and Interleukin-18 (IL-18) to their active forms (Hornung *et al.* 2009, Nature). VacV B13 and F1 inhibit this AIM2-mediated inflammasome formation that would otherwise nurture an inflammatory and immune-activating site of infection (Gerlic *et al.* 2013, PNAS, Kettle *et al.* 1997, Journal of General Virology).

Once Type I IFNs has been released from the virus-infected cell, it can bind to Type I IFN receptors on its cell surface in an autocrine fashion or on the surface of uninfected cells in a paracrine fashion, leading to the downstream activation of ISGs. To block the interferon-stimulated response in infected cells, VacV has evolved two major anti-antiviral mechanisms (Paez and Esteban 1984, Virology). First, VacV encodes B19, a Type I IFN decoy receptor that binds to and sequesters IFN-α and IFN-β (Symons *et al.* 1995, Cell, Colamonici *et al.* 1995, Journal of Biological Chemistry). Co-infection of IFN-stimulated or IFN–expressing cells with VacV and Vesicular Stomatitis Virus (VSVΔ51), an RNA Rhabdovirus that is very

sensitive to interferon, leads to the replication of both viruses in cell culture (Whitaker-Dowling and Youngner 1983, Virology). This ability of VSVΔ51 to replicate was dependent on the expression of B19 and the transfer of B19-containing cell supernatants to VSVΔ51-infected cells (Le Boeuf *et al* 2010, Molecular Therapy). B19 is released into the extracellular space and can bind to the surface of infected and uninfected cells, fostering a pro-viral niche for infection (Alcami *et al.* 2000, Journal of Virology, Montanuy *et al.* 2011, FASEB Journal). If IFN-β binds to its IFN receptor, it activates the Janus Kinase (JAK) Family kinases to phosphorylate Stat1 and Stat2, leading to their dimerization and entry into the nucleus to induce the expression of ISGs. VacV H1 is a phosphatase that has been implicated in the dephosphorylation of Stat1 and Stat2, blocking their dimerization and translocation into the nucleus (Mann *et al.* 2008, Journal of Interferon and Cytokine Research). Another VacV protein, C6, binds to the Stat1-Stat2 complex once inside the nucleus, and can block the complex's transcription factor activity (Stuart *et al.* 2016, PLoS Pathogens).

Apoptotic cell death is one of the cell's main weapons against viral infection. Apoptosis can be initiated by the host cell in several ways and encompasses both intrinsic and extrinsic apoptosis. Intrinsic apoptosis is initiated at the mitochondria and relies on the activation of Apoptosis Regulator Bax (Bax) and BCL2 Antagonist/Killer 1 (Bak). Upon activation, Bak and Bax oligomerize and form pores in the mitochondrial membrane that allow the efflux of cytochrome C into the cytoplasm (Wei *et al.* 2001, Science). This activates the caspase cascade and results in activational cleavage of the Caspase-3 and Caspase-7 executioners (Brentnall *et al.* 2013, BMC Cell Biology). Many cellular stress

signals can activate intrinsic apoptosis, including ER stress which initiates the unfolded protein response, resulting in Bax/Bak activation (Hetz *et al.* 2006, Science). VacV can inhibit intrinsic apoptosis in several ways. VacV N1 and F1 block the activation of Bak/Bax, E3 and K3 block PKR (a major player in the unfolded protein response), and F1, M1, and B13 block the caspase signalling cascade (Wasilenko *et al.* 2003, PNAS, Maluquer de Motes *et al.* 2011, PLoS Pathogen, Beattie *et al.* 1991, Virology, Lee and Esteban 1993, Virology, Veyer *et al.* 2014, Journal of General Virology). Extrinsic apoptosis is mediated by the binding of death receptor ligands to death receptors on the cell surface, including the Fas Cell Surface Death Receptor (Fas) and Tumour Necrosis Factor Receptor (TNFR) superfamily proteins. (Zhou *et al.* 2017, Viruses). This receptor-ligand binding initiates the recruitment of intracellular death receptor adaptors and the formation of the death-induced signalling complex, which forms a scaffold for pro-caspase-8 cleavage, and results in the activation of the Caspase-3 and Caspase-7 apoptosis executioners (Logue and Martin 2008, Biochem Soc Trans). B13 and C12 are the only two VacV proteins that are known to inhibit extrinsic apoptosis (Macen *et al.* 1996, PNAS).

The delay or inhibition of apoptosis enables VacV to complete its full replication cycle within the host cell, but eventually the cell will die by apoptosis, pyroptosis, or necroptosis (Veyer *et al.* 2017, Immunology Letters). Pyroptosis is a form of inflammatory cell death that can be induced upon inflammasome activation, but it is dependent on the activation of caspase-1 and –11 (Miao *et al.* 2011, Immunology Reviews). Caspase-mediated cleavage of the cell death effector gasdermin-D results in its localization to the cell membrane and the formation of pores for cytoplasmic leakage (Gutierrez *et al.* 2017, Journal

of Immunology, Shi *et al.* 2015, Nature). This cytoplasmic leakage results in the release of PAMPs and active pro-inflammatory cytokines such as IL-1β, IL-18, and IL-33. VacV F1 and B13 block the caspase-mediated activation of pyroptosis (Veyer *et al.* 2017, Immunology Letters). Necroptosis is a form of programmed necrosis that is induced by death receptor or TLR signalling when the caspase cascade is inhibited (Ming and Beg 2000, Journal of Virology). It is characterized by membrane rupture, leading to cytosolic leakage (Cho *et al.* 2009, Cell, Goldstein and Kroemer 2007). Upon caspase inhibition, the Mixed Lineage Kinase Domain-like Protein (MLKL) can become activated and form the cell membrane pores that induce necroptosis (Cho *et al.* 2009, Cell, Goldstein and Kroemer 2007). MLKL activation also triggers the assembly of the inflammasome, resulting in bio-active IL-1β which is then released through the MLKL pores (Gutierrez *et al.* 2017, Journal of Immunology). Pyroptosis and necroptosis are pathways of inflammatory cell death that hinder viral spread; therefore, they are thought to be mechanisms by which cells cope with viral infection (Hitomi *et al.* 2008, Cell, Li and Beg 2000, Journal of Virology).

Inflammatory cell death can result in potent antiviral innate and adaptive immune responses. The mediators of this immune response depend on the viral strain used and the mode of infection. There are three common models for VacV inoculation: intradermal, intranasal, and intraperitoneal. The intradermal model involves the inoculation of VacV into the dermal layer of the mouse ear pinnae and results in a localized pock lesion, similar to those that develop upon vaccination of humans (Tscharke and Smith 1999, Journal of General Virology). The intradermal inoculation results in the infiltration of neutrophils, Natural Killer (NK) cells, and T lymphocytes that keep the viral replication restricted to the

pock lesion (Jacobs *et al.* 2006, Journal of General Virology, Reading and Smith 2003, Journal of General Virology, Pilato *et al.* 2015, PNAS, Kawakami *et al.* 2009, J Exp Med). Intradermal vaccination results in circulating neutralizing antibodies and peripheral blood leukocytes that can control secondary orthopoxvirus infections (Perrin *et al.* 1977, J Exp Med, Belyakov *et al.* 2003, PNAS).

The second *in vivo* model uses the intranasal route of infection, where the virus infects lung epithelial cells and several lung immune cell subsets (Turner 1967, Journal of General Virology, Williamson *et al.* 1990, Journal of General Virology). This leads to inflammation and alveolar damage that results in the dissemination of VacV into the bloodstream, mimicking the secondary viremia seen with respiratory orthopoxvirus infection of humans (Williamson *et al.* 1990, Journal of General Virology). In this model, resident alveolar macrophages and dendritic cells are crucial for controlling viral loads at early time points (Rivera *et al.* 2007, Virology, Bonduelle *et al.* 2012, Journal of Immunology). Resident-lung dendritic cells (DCs) are activated and travel to the raining lymph node to prime CD8+ T cells against VacV epitopes; most importantly VacV envelope proteins such as B5 (Beauchamp *et al.* 2010, Journal of Virology). This priming, along with the production of chemokines at the site of infection, is critical for the recruitment of CD8+ T cells to the lungs (Reading and Smith 2003, Journal of General Virology, Beauchamp *et al.* 2010, Journal of Virology). Additionally, there is a rapid increase in active, IFN-γ-producing NK cells at the site of infection (Abboud *et al.* 2016, Journal of Virology). These NK cells are required to control lung viral loads and, as the major early-releasers of IFN-$\boldsymbol{\gamma}$, they can activate lung-infiltrating T cells that protect the mice from viral dissemination (Abboud *et al.* 2016,

Journal of Virology). The early innate immune response culminates in the mounting of the antigen-specific CD8+ T cell response against VacV-infected lung epidermal cells (Goulding *et al.* 2012, Journal of Immunology). This response is sufficient to control primary VacV respiratory infections and prevent secondary viremia (Goulding *et al.* 2012, Journal of Immunology).

The intraperitoneal model of VacV infection mimics secondary viremia, with VacV circulating through the bloodstream and spreading to the visceral organs and brain (Kretzschmar *et al.* 2006, PLoS Medicine). Once secondary viremia has begun, the most important immune response is the CD4+ T cell-mediated activation of the humoural response carried out by the neutralizing antibody-producing B cells (Xu *et al.* 2004, Journal of Immunology, Panchanathan *et al.* 2006).

Wildtype VacV strains can evade these host immune responses in several ways. First, VacV can infect a variety of host immune cells, including macrophages and DCs, and block the ability of these cells to create an inflammatory response (Sanchez-Puig *et al.* 2004, Journal of Virology). Second, VacV encodes many proteins (as described above) that block the recognition of PAMPs and their downstream signalling pathways that would otherwise lead to an inflammatory, immunostimulatory site of infection. Third, VacV produces several proteins that sequester the cytokines and chemokines that directly stimulate host immune cells. For example, VacV's B19 decoy receptor sequesters IFN-α so that immune cell activation is reduced (Symons *et al.* 1995, Cell). Similarly, VacV encodes B8, an IFN-γ decoy receptor, that is released from the cell and reduces the IFN-γ-mediated activation of T lymphocytes (Alcami and Smith 1996, Comparative Immunology). The study of B8 *in vivo*

has been difficult, as it does not bind to mouse IFN-γ (Symons *et al.* 2002, Journal of General Virology). Extracellular IL-1β is sequestered by VacV B15, reducing inflammasome activation (Alcami and Smith 1992, Cell). Fourth, VacV encodes proteins that directly inhibit innate immune cells. For example, VacV has an NK cell immune escape strategy in which VacV A56 on the cell surface can inhibit NK cell activation (Jarahian *et al.* 2011, PLoS Pathogens). Finally, VacV can directly inhibit the complement cascade, which plays an important role in virus-infected cell phagocytosis and inflammation, in two ways: (1) VacV incorporates several host-derived complement control proteins in its EEV envelope, and (2) VacV-derived C3 protein binds complement cascade proteins, promoting their cleavage (Mackenzie *et al.* 1992, Smith *et al.* 2013, Journal of General Virology, Hollinhead *et al.* 2002, Journal of General Virology).

1.1.7 Vaccinia virus as an oncolytic virus

Oncolytic viruses are an exciting anticancer platform that is uniquely targeted to infect and lyse cancer cells (Russell *et al.* 2012, Nature Biotechnology). Oncolytic viruses are engineered to preferentially infect neoplastic cells, which contain defects in innate antiviral signalling. Upon cancer cell lysis, tumour-associated antigens are released and can induce an adaptive immune response against the cancer cells that express these antigens. This multi-mechanistic approach has shown great promise in Phase I, II, and III clinical trials over the past decade (Rowan *et al.* 2010, J Natl Canc Inst). For example, in 2015, T-Vec, an oncolytic herpesvirus, became FDA-approved for the treatment of advance melanoma (Conry *et al.* 2018, Human Vaccine Immunotherapy).

Multiple oncolytic VacV strains have been genetically modified to preferentially infect and replicate in cancerous cells. This has been accomplished by deleting VacV genes involved in the inhibition of apoptosis, including B13R, and the modulation of the immune response, including B19R (Torres-Dominguez and McFadden 2019, Expert Opinion on Biological Therapy, Guo *et al.* 2005, Cancer Research). Several therapeutic oncolytic VacVs have shown positive safety profiles in Phase I and II clinical trials (Arien *et al.* 2006, Heo *et al.* 2013). Specifically, SillaJen's PexaVec, a modified version of the VacV Wyeth strain, was tolerable in both Phase I and II trials. (Heo *et al.* 2013, NCT:00429312, NCT01394939). GeneLux is currently recruiting for their Phase II clinical trial with GL-ONC1, a modified Lister strain oncolytic VacV, for the treatment of Ovarian Cancer (NCT02759588).

VacV is an attractive oncolytic virus because it has a well-characterized safety profile, its large genome can host a variety of transgenes, its innate immunogenicity can help to recruit immune cells to the tumour, and its cytoplasmic replication eliminates the risk of viral genes integrating into the host genome (Tores-Dominguez and McFadden 2019, Expert Opinion on Biological Therapy).

1.1.8 Vaccinia Virus as a Next-Generation Vaccine for Infectious Diseases

Several highly attenuated VacVs, including NYVAC and MVA, have been used as vaccine vectors in both preclinical studies and clinical trials (NCT01799954, NCT00301184). These vaccine vectors can be further modified to express a variety of antigens and can therefore create a robust adaptive immune response against a variety of infectious diseases. Their selective attenuation resulted in the deletion of many of VacV's

immunomodulatory genes. Therefore, they stimulate robust immune responses and are a promising candidate vaccine vector. MVA85A, an MVA-based tuberculosis vaccine was both well-tolerated and immunogenic in Phase I and II clinical trials (Ndiaye *et al.* 2015, Lancet Resp. Med.). NYVAC-Pf7, a NYVAC-based multiantigen malaria vaccine, was well-tolerated, immunogenic in 90% of patients, and had some protective effects in a Phase I/IIa trial (Ockenhouse *et al.* 1998, Journal of Infectious Disease). Many other VacV-based vaccines have been investigated or are currently being investigated in clinical trials, including for viral infections such as HIV (NCT00301184) and Ebola (NCT02661464), the bacterial infection Tuberculosis (NCT00731471), and parasitic diseases such as malaria (NCT00890760).

1.1.9 The Importance of Studying Vaccinia Viruses

Though VacV gained the spotlight because of its use as the smallpox vaccine, the virology community's sustained interest in VacV genetics and immunology over the last four decades is due to its potential use in protection against a variety of emerging diseases, as well as in fighting cancers. Even with this consistent interest in studying VacV, there is still much to discover about the biology of this virus. VacV is a complex virus that encodes many immunomodulatory and anti-apoptotic genes. For oncolytic VacV, the hope is to modify these genes for sustained infection of the tumour niche and the enhanced recruitment of anti-tumour immune cells, all while maintaining its relatively low adverse effects. For VacV-based vaccines, these gene modifications are done to enable a potent immune response while

reducing VacV replication and potential toxicities. The continued study of VacV is important in order to create the most effective VacV-based therapies.

1.2 Extracellular Vesicles and Virus Infections

The term "extracellular vesicles" (EV) encompasses a variety of nanoscale membrane-bound vesicles that are released from the cell. EVs facilitate intercellular communication through the transfer of proteins, lipids, polysaccharides, and nucleic acids to other cells (Heijnen *et al.* 1999, Blood). This EV-mediated intercellular crosstalk is essential for normal cellular processes, including growth, immune modulation, and the inhibition of tumorigenesis. Therefore, the release, contents, and uptake of EVs have important implications for human disease.

1.2.1 Extracellular Vesicles: Exosomes, Microvesicles, and Apoptotic Bodies

There are three subpopulations of EVs: exosomes, microvesicles, and apoptotic bodies, which have been categorized based on their cellular origin and biogenesis processes.

Exosomes are 30-160 nm vesicles of endosomal-origin released from the cell upon fusion of a multivesicular body (MVB) membrane with the plasma membrane (Stoorvogel *et al.* 2002, Traffic). Exosomes are produced by every cell type and their release can be induced by a variety of stimuli, including stress, hypoxia, cell death, and infection (Park *et al.* 2010, Mol Cell Proteomics, Gutwein *et al.* 2005, Clinical Cancer Research, Lancaster *et al.* 2005, Journal of Biological Chemistry). Exosomes released from any given cell represent a heterogeneous population that can have starkly different effects on recipient cells. In fact,

several researchers have reported the isolation of distinct exosome subpopulations of different sizes, and with different markers, cargo, and functions (Vyas *et al.* 2015, Scientific Reports, Chevillet *et al.* 2014, PNAS, Willms *et al.* 2016, Scientific Reports, Crescitelli *et al.* 2013, Journal of Extracellular Vesicles).

Classical **microvesicles** (also known as microparticles) are 100nm-1μm vesicles released from the cell by shedding of the plasma membrane (Jeppesen *et al.* 2019, Cell). Cancer cells can also secrete larger microvesicles (>1 μm) called oncosomes, which only differ from classical microvesicles in regard to their size. Like exosomes, microvesicle release can be induced by stress and viral infection, and their contents are heterogeneous (Del Conde *et al.* 2005, Blood, Bianco *et al.* 2005, Journal of Immunology, Kobayashi *et al.* 1984, Biochimica et Biophvsica Acta, Meckes *et al.* 2011, Journal of Virology). But unlike exosomes, they have very few known markers (Jeppesen *et al.* 2019, Cell). Microvesicle biogenesis is dependent on cytoskeleton organization; therefore, cytoskeleton proteins including actin are commonly found in microvesicles (Jeppesen *et al.* 2019, Cell). The outer layer of microvesicles contains both Annexin A1 and phosphatydilserine, which could be used to distinguish them from exosomes (Jeppesen *et al.* 2019, Cell).

Apoptotic bodies are large EVs that are released from apoptotic cells by blebbing and range in size from 200 nm to 5 μm (Crescitelli *et al.* 2013, Journal of Extracellular Vesicles). These phosphatidylserine- and Annexin V-coated EVs contain cytoplasmic contents from the dying cell (Jeppesen *et al.* 2019, Cell). They are engulfed by phagocytes, in order to inhibit any potential inflammatory response to the cell death (Henson *et al.* 2001, Cell).

Traditionally, EVs that pelleted at 100,000g were referred to as exosomes, but in fact this pellet contains a combination of microvesicles and exosomes (Jeppesen *et al.* 2019, Cell). Though their biogenesis pathways are distinct, exosomes and microvesicles have many similarities and are difficult to distinguish from one another once released from the cell. Recently, the International Society for Extracellular Vesicles suggested the term Small EVs (sEVs) should be used for particles less than 200nm in size, while the term Large EVs (lEVs) should be used for particles greater than 200 nm (Thery *et al.* 2018, Journal of Extracellular Vesicles). The exact effect that each EV has on the host cell is difficult to study due to their co-pelleting, but it is believed that they can affect recipient cells through similar mechanisms (Mateescu *et al.* 2017, Journal of Extracellular Vesicles).

1.2.2 sEV Biogenesis Pathways

Exosomes are intraluminal vesicles (ILVs) that have been released upon the binding of a multivesicular body with the plasma membrane (Fig. 2). The two major steps in exosome biogenesis are the creation of ILVs and the release of exosomes. ILVs form by reverse budding of the endosomal membrane, engulfing cargo that are selectively brought to the endosomal membrane or passively engulfing cytoplasmic contents in its vicinity (Noltet Hoen *et al.* 2012, Nucleic Acids Research, Skog *et al.* 2008, Nature Cell Biology, Villarroya *et al.* 2015, Seminars in Cancer Biology, De Jong *et al.* 2012, Journal of Extracellular Vesicles). Several proteins are pertinent for the creation of ILVs in multivesicular bodies: the Endosomal Sorting Complex Required For Transport (ESCRT) proteins and their interactors including Tumour Susceptibility Gene 101 (Tsg101) and Programmed Cell Death 6

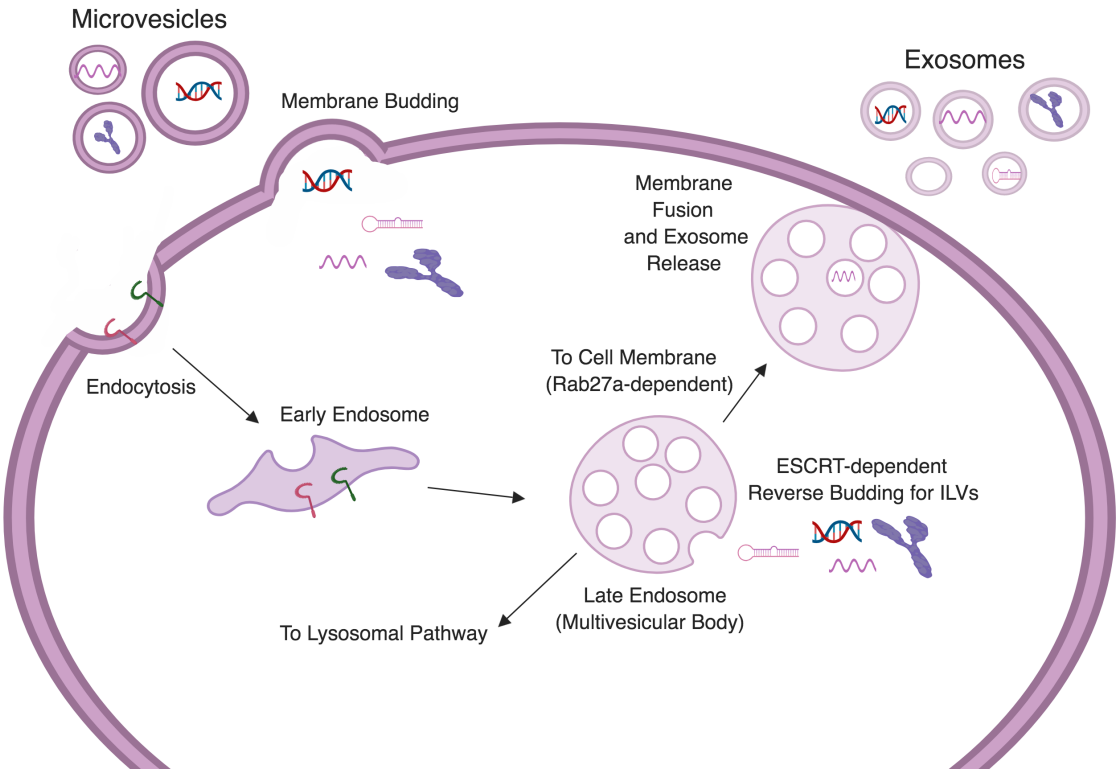

Figure 2. Small Extracellular Vesicle Biogenesis Pathways. Exosomes are a byproduct of the endosomal pathway, that are released upon fusion of the late endosome (or multi vesicular body) with the plasma membrane. Briefly, the late endosome is a membrane-enclosed vesicle that contains a large number of intraluminal vesicles (ILVs), formed by the reverse-budding of the late endosomal membrane. This process is ESCRT-dependent and leads to the uptake of various cargo into the ILVs. The late endosome can either travel to the cell membrane in a Rab27a-dependent manner and fuse with the plasma membrane or it can enter the lysosomal pathway for recycling of the ILV cargo. Upon fusion of the late endosome with the cell membrane, the ILVs are released. These released ILVs are called exosomes. Microvesicles are created through cell membrane budding (or membrane shedding), leading to the release of sEVs containing cell-membrane-associated cargo. Created with biorender.com © Hayley Elizabeth McKay 2019.

Interacting Protein (commonly known as Alix), as well as the tetraspanins CD81, CD63, and CD9 (Williams and Urbe 2007, Nature Reviews Molecular Cell Biology). The tetraspanins, Tsg101, and Alix are considered strong exosomal markers (Jeppesen *et al.* 2019, Cell). Once the MVB has formed, it can bind to the lysosome where its cargo is degraded, or it can fuse with the cell membrane and release the ILVs as exosomes.

MVB fate depends on the Ras-Related Proteins in Brain (RAB) GTPases, key proteins involved in the regulation of intracellular transport (Zerial and McBride 2001, Nat Rev Mol Cell Bio). Specifically, Rab27a and Rab27b are required for MVB transport to the plasma membrane and silencing of either Rab27a or Rab27b results in reduced exosome production (Ostrowsji *et al.* 2010, Nature Cell Biology).

Much less is known about the formation of microvesicles. Microvesicle budding occurs at cholesterol-rich regions of the plasma membrane, called lipid rafts (Coccuci *et al.* 2009, Trends in Cell Biology). Cytoplasmic protrusions form at these lipid rafts at low levels in resting cells, and more frequently upon stimulation with chemical agents or upon intracellular stimulation, such as by Ca++-dependent ATP in dendritic and glial cells (Del Conde *et al.* 2005, Blood, Bianco *et al.* 2005, Journal of Immunology, Kobayashi *et al.* 1984, Biochimica et Biophvsica Acta). These cytoplasmic protrusions are then released upon fission, with the plasma membrane and its associated proteins making up the sEV membrane (Coccuci *et al.* 2009, Trends in Cell Biology).

1.2.3 The Sorting of Cargo into sEVs

sEV-associated RNAs include miRNAs, lncRNAs, mRNAs, and rRNAs, among others (Ekstrom *et al.* 2012, Journal of Extracellular Vesicles). The sorting of RNAs into sEVs can be specific or expression-dependent (Squadrito *et al.* 2014, Cell Reports, De Jong *et al.* 2012, Journal of Extracellular Vesicles). Several RNA motifs have been identified that actively enrich miRNAs or mRNAs in sEVs, through the direct binding of RNA-binding proteins (RBP) to these motifs or by RBP binding to loop-based secondary structures that are dependent on these sequences (Villarroya-Beltri *et al.* 2013, Nature Communications, Szostak *et al.* 2014, RNA Biology, Shurtleff *et al.* 2016, eLIFE, Batagov *et al.* 2011, BMC Genomics). Bound RBP-RNA complexes can be shuttled to the MVB or to the cell membrane via microtubules (Hessvik and Llorente 2018, Cell Mol Life Sci). At the MVB, the RNA-RBP complex can be internalized into the MVB, becoming ILV cargo (Hessvik and Llorente 2018, Cell Mol Life Sci). Alternatively, the RNA can bind to membrane-bound RBPs, such as ESCRT-II, and be internalized in ILVs without the RBP that shuttled it there (Mukherjee *et al*. 2016, EMBO Reports). It is also at the MVB that passive RNA loading occurs with increased loading of more highly expressed RNAs (Squadrito *et al.* 2014, Cell Reports).

There is some debate regarding the sorting of cellular contents into budding microvesicles. But generally, it thought to be a less specific process than exosomal sorting (Hessvik and Llorente 2018, Cell Mol Life Sci). Still, it is probable that some RNA species are specifically enriched in microvesicles (Crescitelli *et al.* 2013, Journal of Extracellular Vesicles).

Several groups of proteins are found to be associated with sEVs. First, there are many proteins involved in exosome biogenesis that form part of the exosome membrane or interior exosomal contents upon release, including the exosomal markers, structural proteins such as Flotillin-1, and some RAB GTPases (Thery *et al.* 2001, Journal of Immunology). Other proteins are taken up into exosomes based on their post-translational modifications, including ubiquination (Reggiori and Pelham 2001, EMBO). Proteins involved in the budding of the plasma membrane are detected in microvesicles, including Actin and ARF6 (Jeppesen *et al.* 2019, Cell). Additionally, microvesicles contain lipid raft proteins and other plasma membrane proteins present at sites of membrane shedding (Jeppesen *et al.* 2019, Cell).

1.2.4 sEV Uptake into Recipient Cells

Upon sEV binding to the recipient cell, there are several possible outcomes. First, the binding of sEV membrane proteins to cellular receptors can result in: (1) blocking these receptors from binding cell-free proteins; (2) initiating an intracellular signalling cascade; or (3) transferring EV proteins to the plasma membrane (Mack *et al.* 2000, Nature Medicine). Alternatively, the EV-receptor binding can result in uptake of the EV by phagocytosis, macropinocytosis, fusion, clathrin-independent endocytosis, or clathirin-dependent endocytosis (Mulcahy *et al.* 2014, Journal of Extracellular Vesicles, Feng *et al.* 2010, Traffic, French *et al.* 2017, Semin Cell Dev Biol, Escrevente *et al.* 2011, BMC Cancer). sEV contents can be directly released into the cytoplasm upon fusion with the plasma membrane or endosomal membrane, or sEVs can be transported in endosomes to the endoplasmic

reticulum or lysosome (Escrevente *et al.* 2011, BMC Cancer, Morelli *et al.* 2004, Blood). Therefore, EV-RNAs can be biologically active, recognized as PAMPs, or degraded, upon recipient cell entry (Lai *et al.* 2015, Nature Communications). sEV-miRNAs that are delivered directly into the cytoplasm require the presence of bound RBPs, like Argonaute 1-4, in order to avoid rapid degradation (Winter and Diederichs 2011, RNA Biology). Low amounts of Argonaute localize to sEVs; therefore, it is thought that sEV-miRNAs bind to Argonaute 1-4 in the ER, where a large proportion of the miRNA-mediated inhibition of host gene expression occurs through the blocking of mRNA transcription (Arroyo *et al.* 2011, PNAS). Once released into the cytoplasm, sEV-associated mRNA can be translated within 30 minutes of uptake (Lai *et al.* 2015, Nature Communications, Ratajczak *et al.* 2006, Leukemia, Valadi *et al.* 2007, Nature Cell Biology).

1.2.5 sEV Biodistribution

The biodistribution of sEVs is dependent on their specific characteristics and differs based on cell type. sEVs can be uptaken by neighbouring cells or they can be disseminated throughout an organism through either the lymphatic system or bloodstream (Pucci *et al.* 2016, Science, Ridder *et al.* 2014, PLoS Biology). Consequently, sEVs have been identified in a variety of biological fluids, including urine, plasma, breast milk, and saliva (Conde-Vancells *et al.* 2010, Proteomics Clin. Appl., Orozco *et al.* 2009, Placenta, Admyre *et al*. 2007, Journal of Immunology, Michael *et al.* 2010, Oral Disease). Additionally, the presence of sEVs within the tumour microenvironment has been well-established (Ridder *et al.* 2015, OncoImmunology). The uptake of tumour-derived sEV-RNA by a variety of different cell

types in the tumour microenvironment, including tumour-infiltrating leukocytes and macrophages, has been reported (Ridder *et al.* 2015, OncoImmunology).

1.2.6 sEVs in Health and Disease

Many disease states, including cancer, autoimmune disease, renal disease, and infection, are characterized by altered sEV miRNA, mRNA, and protein profiles (Skog *et al.* 2008, Nature Cell Biology, Conley *et al.* 2017, RNA Biology, Camussi *et al.* 2010, Kidney International, Choi *et al.* 2007, Journal of Proteomic Research). These altered sEVs can affect disease progression and can also be used in diagnostics. For example, the distribution of sEVs within the tumour microenvironment can have important implications for tumour progression and anti-tumour immunity, while the presence of specific RNA profiles in circulating sEVs could be used for cancer diagnosis (Ridder *et al.* 2015, OncoImmunology).

Due to the widespread biodistribution of sEVs, they could be used as a delivery vehicle for therapeutic RNAs and proteins. The therapeutic cargo of interest can be selectively enriched in sEVs using several different methods. Simply transfecting plasmids encoding miRNAs or mRNAs with sEV-targeting motifs has been shown to be effective in enriching specific cargo in their sEV populations (Balukbasi *et al.* 2012, Molecular Therapy Nucleic Acids, Villarroya-Beltri *et al.* 2013, Nature Communications, Batagov *et al.* 2011, BMV Genomics). Donor cell choice depends on the target organ, as sEV donor cells can have an impact on both sEV biodistribution and recipient cell uptake (Horibe *et al.* 2018, BMC Cancer, Sanchero-Albero *et al.* 2019, Journal of Nanobiotechnology). More complex platforms have been developed using sEV protein-RBP complexes in conjunction with RNAs

tagged with RBP-specific binding motifs, but so far these methods have resulted in the enriched RNA being rapidly degraded once inside the recipient cell (Hung and Leonard *et al.* 2016, Journal of Extracellular Vesicles). To target proteins to sEVs, there are several commercially-available protein tags that embed within endosomal or plasma membranes and force uptake of the tagged proteins (Shen *et al.* 2011, J Biol Chem).

1.2.7 Immunostimulatory and Immunomodulatory sEVs

sEVs are an important component of the host immune response to infection. sEV-mediated crosstalk regulates the activation of key immune cells, including B cells, T cells, and DCs. sEVs can directly activate B cells, T cells, and DCs through the transfer of antigens (Skokos *et al.* 2003, Journal of Immunology). The major histocompatability complex II (MHC II), a key component in the presentation of antigens to prime T cell responses, has been identified on the surface of B cell sEVs and facilitates the priming of antigen-specific T cells (Raposo *et al.* 1996, Journal of Experimental Medicine). These MHC II molecules can also be taken up by DCs to efficiently stimulate T cell responses (Vincent-Schneider *et al.* 2002, International Immunology). DCs can take up sEVs and display sEV-associated antigens to prime the immune system (Morelli *et al.* 2004, Blood, Thery *et al.* 2002, Nature Immunology). Additionally, DCs release sEVs containing a variety of immune-activating cargo. Montecalvo and colleagues (2012) found that immature and mature dendritic cells differ in their miRNA profiles (Montecalvo *et al*. 2012, Blood). Specifically, miRNAs enriched in mature dendritic cell-derived sEVs downregulated pro-inflammatory transcripts and could be an important negative feedback loop to regulate the immune response

(Montecalvo *et al.* 2012, Blood). T cells and B cells also produce sEVs containing miRNAs, which are thought to be a host-specific mechanism of regulating the immune response (Mittelbrunn *et al.* 2011, Nature Communications). Recently, genomic and mitochondrial DNA were found to be released in T cell-derived sEVs upon stimulation by DCs (Torralba *et al.* 2018, Nature Communications). These sEVs were then taken up by the DCs and the DNA cargo was recognized by DNA sensor cGAS, resulting in an antiviral state. (Torralba *et al.* 2018, Nature Communications). Other antiviral sEVs have been identified in the context of hepatitis B infection and rabies virus infection (Wang *et al.* 2019, International Journal of Molecular Sciences, Li *et al.* 2013, Nature Immunology). Tumour cells can also release a variety of cargo in sEVs that alter the activity of various immune cells within the tumour microenvironment (Fanini and Fabbri 2017, Semin Cell Dev Biol). Therefore, both immunostimulatory and immunomodulatory sEVs have important implications in cancer progression and viral infection.

1.2.8 Viruses Hijack sEVs

sEVs and enveloped viruses share many similarities in their assembly, exit, entry, and structure. In fact, many viruses rely on sEV loading and biogenesis components for their assembly and egress (Meckes and Raab-Traub 2011, Journal of Virology). Human herpesvirus-6 (HHV-6) directly uses vesicularization at the multivesicular body for assembly and egress (Mori *et al.* 2008, Traffic). Some viruses, including HIV-1, HTLV-1, hepatitis A virus, and hepatitis B virus (HBV), recruit the ESCRT proteins to the plasma membrane to induce budding (Martin-Serrano *et al.* 2003, PNAS, Chen and Lamb 2008, Virology, Feng *et*

al. 2013, Nature). Other viruses, such as sendai virus, epstein-barr virus (EBV), and marburg virus, encode proteins that bind to ESCRT proteins but their reliance on this pathway is unclear or disputed (Neumann *et al.* 2005, Journal of Virology, Chen and Lamb 2008, Virology). Several viruses rely on tetraspanins in plasma membrane microdomains, including CD81, CD82, and CD63, for virion formation (Grigorov *et al.* 2009, Retrovirology, Mazurov *et al.* 2006, Virology).

Due to the similarities between viral assembly and sEV formation, as well as between viral egress and sEV release, it is not surprising that many viruses alter sEV cargo upon infection. HIV-1 can alter sEVs in several ways. In order to increase viral entry, both of HIV-1's receptors can be transferred to uninfected cells through sEVs from infected cells (Mack *et al.* 2000, Nature Medicine, Rozmyslowicz *et al.* 2003, AIDS). HIV-encoded proteins have been identified in sEVs upon infection, including Negative Regulatory Factor (Nef), which can induce apoptosis of CD4+ Helper T cells (Lenassi *et al.* 2010, Traffic). Additionally, Nef induces increased vesicle secretion from infected cells, as well as from uninfected cells through the transfer of Nef protein in sEVs (Ali *et al.* 2010, AIDS, Muratori *et al.* 2009, Cell Host Microbe). EBV also hijacks host sEVs. EBV's major oncoprotein is released in sEVs from B cells and epithelial cells upon infection, leading to the inhibition of T cell proliferation (Ceccarelli *et al.* 2007, International Journal of Cancer, Dukers *et al.* 2000, Journal of Immunology). Additionally, sEV-associated galectin9 and Basic Fibroblast Growth Factor (FGF2) can increase EBV immunosuppressive and oncogeneic effects in the context of EBV cancers (Klibi *et al.* 2009, Blood, Ceccarelli *et al.* 2007, International Journal of Cancer). Several viruses, including EBV and Kaposi's sarcoma-associated

herpesvirus (KSHV), encode their own miRNAs that are released in sEVs upon infection and regulate antiviral gene expression in recipient cells (Pegtel *et al.* 2010, PNAS, Yogev *et al.* 2017). Other viruses, including enterovirus 71 (EV71), alter which cell-derived miRNAs are enriched in sEVs from infected cells (Cocucci *et al.* 2009, Trends in Cell Biology). EV71 sEVs are enriched for miR-146a, which targets Type I IFN and primes uninfected cells to be infected (Fu *et al.* 2017, Trends in Cell Biology). Some viruses have been found to release sEVs that mimic virions. HBV infection leads to an increased release of sEVs containing viral surface antigens, which are thought to distract the host's immune system from neutralizing HBV virions (Chai *et al.* 2008, Journal of Virology). Hepatitis C virus (HCV) releases both its RNA genome as well as structural proteins into sEVs, and these sEVs can be isolated from the plasma of infected individuals (Cosset and Dreux 2014, Masciopinto 2004, European Journal of Immunology). Some of these sEVs have been found to be infectious but were structurally distinct from HCV virions, perhaps as a viral strategy to avoid neutralization (Ramakrishnaiah *et al.* 2013, PNAS).

1.2.9 sEVs and VacV

Not much is known about the association between VacV and sEVs. One VacV protein, F13, contains a binding site for Tsg101 and Alix (Honeychurch *et al.* 2007, Journal of Virology). Interestingly, when this binding domain is deleted, or alternatively when Alix or Tsg101 are knocked down, the production of EEV is diminished (Honeychurch *et al.* 2007, Journal of Virology). During wrapping of the VacV IMV particle, F13 localizes to the

MVB where it most likely uses sEV loading machinery for assembly of the IEV membranes (Chen *et al.* 2009, Virology Journal).

Spehner and Drillien investigated the production of extracellular vesicles from MVA-infected cells (2008, Virus Research). They found that sEVs containing the VacV membrane protein B5 and an inserted transgene (CD40 ligand) were released upon infection with MVA, as well as upon infection with VacV-IHJ or VacV-Cop. They also identified VacV B5 within the MVB and on the cell surface; therefore, the origin of these sEVs remains unclear. Another research group created a recombinant MVA strain that released the prostate-specific antigen (PSA) into sEVs upon infection, in order to stimulate a more potent anti-tumour immune response (Rountree *et al.* 2011, Cancer Research).

It is evident that the effects of VacV infection on sEV production and cargo are not well understood and should be further explored.

1.3 Study Rationale and Hypothesis

Vaccinia virus is a complex virus that encodes a variety of immunomodulatory gene products. Based on VacV's close association with MVBs and its possible reliance on exosome biogenesis- and loading-related proteins, it is probable that some VacV gene products are released in VacV-infected cell sEVs.

We hypothesize that VacV-derived RNAs are present in sEVs following VacV infection and that these sEVs prime uninfected cells to become infected.

We set out to:

1. Characterize sEVs following VacV infection

2. Identify which VacV mRNA molecules (if any) are present in sEVs

3. Characterize how sEV-associated mRNAs may affect the cellular antiviral response.

Materials and Methods

2.1 Cells

All cell lines were purchased from ATCC (American Type Culture Collection): 786-O (ATCC CRL-1932), U2OS (ATCC HTB-96), 293T (CRL-3216), MiaPACA-2 (CRL-1420), and Vero (ATCC CRL-1587). A 786-O CRISPR-Cas9-mediated Rab27a knockout monoclonal cell line was generated using lentiCRISPRv2 protocol described below (Section 2.19, 2.20). Cells were incubated at 37°C and 5% CO2 in Dulbecco's Modified Eagle medium (DMEM) with 10% Fetal Bovine Serum.

2.2 Viruses

VacV Wildtype Copenhagen Strain (VacV-Cop) was provided by Dr. Grant McFadden (Arizona State University). Recombinant VacV Copenhagen ΔB19R-mCherry was provided by Dr. John Bell (Dr. Brian Keller 2017, Functional genomic studies of vaccinia virus provide fundamental insights into virus-host interactions, University of Ottawa PhD Thesis). VSVΔ51-GFP was provided by Dr. John Bell (Stojdl *et al.* 2003, Cancer Cell).

2.3 Poxvirus Amplification

1e7 U2OS cells were seeded in 850 cm2 roller bottles and incubated at 37°C and 5% CO2 in 150 mL Dulbecco's Modified Eagle medium (DMEM) with 10% Fetal Bovine Serum (FBS) and 25mM Hepes at 0.1 rpm for 48 hours. When U2OS were 95% confluent, they were infected with Vaccinia Virus at a multiplicity of infection (MOI) of 0.1 for 48-72 hours. When almost all cells had rounded, cells were resuspended in the media, collected in conical tubes, and centrifuged at 1200 rpm for 10 minutes. Cell pellets were resuspended in 40 mL 1mM Tris pH 9.0 and freeze-thawed at -80°C/37°C three times. Cells were then spun at 3000 rpm for 10 min to pellet cell debris. 20 mL of the cleared lysate (supernatant) was then overlaid on 10 mL 36% sucrose in a 30 mL Oakridge centrifuge tube. To pellet VacV, tubes were spun in a swing-bucket rotor at 11,500 rpm for 1h30 minutes at 4°C. Viral pellets were resuspended and pooled in 1 mL 1 mM Tris pH 9.0 and stored at -80°C. An aliquot was used for a plaque assay to determine viral titers (2.5).

2.4 Rhabdovirus Amplification

1e7 Vero cells were seeded in 850 cm2 roller bottles and incubated at 37°C and 5% CO2 in 150 mL DMEM with 10% FBS and 25mM Hepes at 0.1 rpm for 48 hours. When Vero cells were 90% confluent, they were infected with VSVΔ51-GFP at a MOI of 0.05. When cytopathic effect was evident (roughly 50% cell detachment), supernatant was harvested and cell debris was removed by centrifugation at 1500 rpm for 10 min. Supernatant was filtered through a 0.22 um filter and the virus was pelleted at 14,000 rpm for 1h30

minutes at 4°C. Pellets were resuspended in PBS, aliquoted, and stored at -80°C. An aliquot was used for a plaque assay (2.6).

2.5 Poxvirus Plaque Assay

To quantify plaque forming units per mL (pfu/mL) of VacV samples, plaque assays were performed. For this assay, 50-100 uL viral aliquots were serially-diluted (1 in 10) in serum-free DMEM and confluent U2OS 12-well plates were infected with 800uL of dilutions 10e-3 to 10e-8. Infections were incubated at 37°C and 5% CO2 for 2 hours, then media was replaced with overlay consisting of one-part 3% CMC to one-part 2x DMEM with 20% FBS. Cells were stained with crystal violet (CV) 48 hours post-infection and plaques were counted to determine pfu/mL.

2.6 Rhabdovirus Plaque Assay

For VSVΔ51 plaque assays, 100 uL viral aliquots were serially-diluted (1 in 10) in serum-free DMEM and confluent Vero 12-well plates were infected with 800uL dilutions of 10e-2 to 10e-7. Infections were incubated at 37°C and 5% CO2 for 1 hour, then media was replaced with overlay (one-part 6% CMC to one-part 2x DMEM with 20% FBS). Cells were stained with CV 48 hours post-infection and plaques were counted to determine pfu/mL.

2.7 Small EV Isolation from VacV-Infected and Mock Cells

Mock and infected-cell conditioned media was collected and spun at 1200 g for 15 min to pellet cell debris and large apoptotic bodies. The resulting supernatant was moved to a

38mL Oakridge centrifuge tube and spun at 12,000 g for 35 min at 4°C in an Avanti J-E High Speed Centrifuge (Beckman Coulter, Indianapolis, IN, USA) to pellet large extracellular vesicles. The resulting supernatants were filtered through 0.22 μm filters to remove cell-free VacV virions (360 × 270 × 250 nm). The filtered supernatant was then spun at 120,000 g for 3 hours at 4°C in Ultra-Clear Centrifuge Tubes (Beckman Coulter, Indianapolis, IN, USA) in an Optima-XPN or Optima L-100 Ultracentrifuge (Beckman Coulter, Indianapolis, IN, USA) to pellet the small extracellular vesicles. Supernatant was aspirated and the small EV pellet was resuspended in 200 uL PBS for sEV treatments, Nanoparticle Tracking Analysis, or RNA extractions, and 150 uL NP-40 lysis buffer (1% NP-40, 150 mM NaCl, 2 mM EDTA, 50 mM Tris, pH 7.4) for western blot analysis of exosomal markers.

2.8 Nanoparticle Tracking Analysis (NTA)

Quantity and size distributions of small extracellular vesicles were assessed using the ZetaView PMX110 Multiple Parameter Particle Tracking Analyzer (Particle Metrix, Meerbusch, Germany). The ZetaView system was calibrated using 90 nm beads. For quantification and sizing of EVs from Mock and VacV-infected cells, 100uL of small EVs were diluted in 1 mL PBS and loaded into the ZetaView. For EV quantification for RNA extractions, a 20uL sEV aliquot was diluted in 1 mL PBS and loaded into the ZetaView.

2.9 Nanoscale Flow Cytometry (NFC)

Nanoscale Flow Cytometry was performed on a special-order research product (SORP) BD LSR Fortessa flow cytometer (BD Biosciences, San Jose, CA, USA). All four

100 uL samples (VacV and Mock 786-O exosomes - 0.45 um or 0.22 um filtered) of small EVs were incubated with 200 uM CellTrace CFSE Stain (ThermoFisher Scientific, Waltham, Massachusetts, USA) for 1 hour at 37°C in the dark, then diluted in 1 mL PBS. NFC was performed by Vera A. Tang and NFC settings were previously optimized (Tang et al. 2017, Scientific Reports).

2.10 Western Blotting of Small EV Lysates

First, 15 uL of DTT-containing gel loading buffer was added to 75uL of each sEV sample and samples were incubated at 95°C for 5 minutes. Samples were loaded into a 4-15% Mini-PROTEAN TGX Stain-Free Precast Protein Gel (Bio-Rad, Hercules, California, USA), along with the Precision Plus Protein™ All Blue Prestained Protein Standard (Bio-Rad, Hercules, California, USA). Gel was run for 45 minutes at 150V in a Mini-PROTEAN® Tetra Vertical Electrophoresis Cell (Bio-Rad, Hercules, California, USA) in 1X Tris/Glycine/SDS Running Buffer (Bio-Rad, Hercules, California, USA). Gels were photo-activated for total protein visualization with a 90s UV exposure in the ChemiDoc Imaging System (Bio-Rad, Hercules, California, USA). Proteins were transferred to pre-activated (5 minutes in 100% ethanol) PVDF membranes in a TransBlot Turbo Transfer System (Bio-Rad, Hercules, California, USA) using the Mixed MW Protocol (7 minutes at 2.5 A constant, up to 25 V). PVDF membrane, transfer stacks, and transfer buffers were used from the Trans-Blot® Turbo™ RTA Mini PVDF Transfer Kit (Bio-Rad, Hercules, California, USA). Following transfer, samples were blocked in 5% milk in TBS-T (0.1% Tween-20, Sigma-Aldrich, St. Louis, MO, USA) for 1 hour at room temperature on a rocker, then immunoblotted overnight at 4°C on a rocker with one of the following primary antibodies:

Flotillin-1 (1:1000, #610821, BD BioSciences, San Jose, CA, USA) or Lamp2 (1:1000, in 5% milk-TBS-T, #ab25631, Abcam, Cambridge, UK). Membranes were washed three times for 10-15 minutes each in TBS-T at room temperature on a rocker, then immunoblotted with anti-mouse IgG HRP-linked secondary antibody (1:5000, in 5% milk-TBS-T, #7076S, Cell Signaling Technology, Danvers, MA, USA) at room temperature for 1 hour on a rocker. Membranes were washed three times for 10-15 minutes each in TBS-T at room temperature on a rocker. Membranes were incubated in Clarity Max Western ECL Substrate (Bio-Rad, Hercules, California, USA) for 2 minutes, and exposed in a ChemiDoc Imaging System (Bio-Rad, Hercules, California, USA).

2.11 Western Blotting of Whole Cell Lysates

Samples were harvested in NP-40 lysis buffer containing CompleteTM EDTA-free Protease Inhibitors (Roche, Basel, Switzerland). Protein concentrations were calculated using the Pierce BCA Protein Assay Kit (ThermoFisher Scientific, Waltham, Massachusetts, USA). 20 ug samples were run on NuPAGE Bis-Tris Gels (Invitrogen, Carlsbad, CAL, USA) for 1.5 h at 150V in the NuPAGE Bis-Tris Electrophoresis System (Invitrogen, Carlsbad, California, USA) in 1X MOPS Buffer. Gels were transferred to pre-activated (30 seconds in 100% methanol) PVDF membranes (Immobilon-P, Burlington, Massachusetts, USA) for 1 hour at 90V in 4°C cold room in a Mini Trans Blot Cell (Bio-Rad, Hercules, California, USA). Membranes were blocked in 5% milk in TBS-T for 1 hour at room temperature on a rocker. Membranes were then immunoblotted with anti-RAB27a primary antibody (1:500, in 5% milk-TBS-T, #ab55667, Abcam, Cambridge, UK) or Beta-Tubulin (1:1000, in 5% milk-TBS-

T, #2118, Cell signaling Technology, Danvers, MA, USA) overnight at 4°C on a rocker. Subsequent wash and secondary antibody steps were carried out as described above (2.10). Membranes were incubated in Clarity Western ECL Substrate (Bio-Rad, Hercules, California, USA) for 2 minutes, followed by exposure to X-Ray film (Fuji Photo Film Co, LTD).

2.12 Crystal Violet Staining and Quantification for Cell Viability

For a 96-well plate, cells were washed with 100 uL of 1X PBS and stained with 100 uL of 0.5% Crystal Violet Staining Solution (20% methanol) for 15 minutes on a rocker. Crystal Violet was removed and stained/fixed cells were washed twice with ddH2O and dried overnight. For quantification of crystal violet stain, 100uL of 100% molecular biology-grade methanol was added per well and cells were incubated on a rocker at room temperature for 15-30 minutes. Once stain had completely lifted, quantification of stain was performed in a Multiskan Ascent 96/384 Plate Reader (Bradenton, FL, USA) at 570nm.

2.13 Small RNA-Sequencing

sEVs were harvested from VacV- and Mock-infected cells 48 hours after infection at MOI of 0.1. Total RNA was extracted using the miRVana miRNA Isolation Kit (ThermoFisher Scientific, Waltham, Massachusetts, USA). Size Selection, Quality Control, Library Prep, and Small RNA Sequencing was carried out by Fasteris AS (Geneva, Switzerland), based on the Illumina TruSeq Small RNA Library Prep Kit (Illumina, San Diego, CA, USA). QuBIT 4 Fluorometer (ThermoFisher Scientific, Waltham, Massachusetts, USA) was used to assess RNA quantity and Bioanalyzer Fragment Analyzer (Agilent, Santa

Clara, CA, USA) was used to assess RNA quality and size distribution. Total RNA was run on a polyacrylamide gel and size-selected for 15-30 nucleotides. Adapters were ligated to RNA ends and cDNA was synthesized. Sequencing was performed on an Illumina HiSeq 2500 system (Illumina, San Diego, CA, USA) with 50 bp single-end reads. For sequencing analysis, Trimmomatic was used to trim illumina adapters. bbmap was used to map reads to the Vaccinia Virus Copenhagen strain genome (GenBank M35027). Finally, bedtools was used to generate coverage tables from mapped files.

2.14 Quantitative Real-Time PCR of Small EV RNA

For relative expression qPCR experiments, Total RNA was extracted from whole EV samples and whole cell samples (for both Mock and VacV-infected EVs) using TRIzol Reagent (ThermoFisher Scientific, Waltham, Massachusetts, USA). For TriZOL RNA extractions, cells were lysed and homogenized in 500 uL TriZOL. 200uL of chloroform was added for phase-separation with a spin at 12,000 g for 15 minutes. RNA was precipitated from the aqueous phase with 500 uL of 100% isopropanol, followed by centrifugation at 12,000g for 10 minutes. RNA pellet was washed with 75% ethanol, re-centrifuged at 7,500 g for 5 minutes, and then air dried at room temperature for 10 minutes. Pellets were resuspended in 20 uL DEPC-treated nuclease-free water and RNA concentrations were estimated using a NanoDrop 2000 or NanoDrop One Microvolume UV-Vis Spectrophotometer (ThermoFisher Scientific, Waltham, Massachusetts, USA). 500 ng to 1 ug RNA was used to synthesize cDNA with the iScript gDNA Clear cDNA Synthesis Kit (Bio-Rad, Hercules, California, USA) as per their protocol. Quantitative Real-Time PCR reactions

were performed with QuantiTect SYBR Green (Qiagen, Hilden, Germany) according to their protocol, carried out on an ABI 7500 Fast Real-Time PCR System (ThermoFisher Scientific, Waltham, Massachusetts, USA) with the following cycling conditions: 15 min at 95°C followed by 40 cycles of (1) 15s at 94°C (2) 30s at 55°C (3) 30s at 72°C, with detection at the end of each cycle. Fold changes were calculated using the ΔΔCT method, with normalization to 18S RNA.

For absolute quantification qPCR experiments, sEVs/sample were quantified by NTA and equal sEV quantities were used for total RNA Extraction. Total RNA was extracted with NucleoZOL (Macherey-Nagel, Duren, Germany). Equal volumes (and therefore equal original EV quantities) of RNA (up to 1 ug total) were used for cDNA synthesis with the iScript gDNA Clear cDNA Synthesis Kit (Bio-Rad, Hercules, California, USA). A standard curve for B19R was created using pcDNA3.1-B18R, provided by John Bell, to calculate the absolute number of copies of B19R RNA per reaction. A standard curve for C12L was prepared by PCR of the entire coding region of C12L, and gel extraction of the resulting amplicon. cDNA and qPCR reactions were prepared as described above. B19R or C12L pg per reaction was quantified using the following equation: exp((Ct value – y-intercept of Standard Curve)/(slope of standard curve). This number was then divided by (340*1062) to obtain pmol/rxn. Molecules/rxn was calculated using the following equation: (pmol/rxn)* (6.02e23/10^12). Finally, number of molecules per EV was calculated by dividing molecules/rxn by EVs/reaction.

2.15 Assay 1: sEV Treatment Prior to VSVΔ51 Infection

90% confluent 786-O Cas9 and 786-O ΔRab27a cells were infected with VacV-WT or VacV-ΔB19R at an MOI of 1 in serum-free DMEM. 1.5 hours post-infection, media was changed to 5% EV-depleted FBS-containing DMEM. One day prior to sEV treatment, 1e4 786-O cells were seeded per 96 well. Cells were treated with roughly 2e7 small EVs per well in EV-depleted FBS-containing DMEM for 9 hours. Pre-treated cells were then infected at various MOIs (3, 0.5, 0.1, 0.05) for 1 hour in serum-free DMEM. Media was replaced with DMEM (5% FBS). 24 hours post-infection, VSVΔ51-GFP replication was assessed by both plaque assay and fluorescence microscopy, while VSVΔ51-GFP cytotoxicity was assessed by crystal violet staining and quantification.

2.16 Assay 2: sEV Treatment Following VSVΔ51 Infection

One day before EV treatment, 1e4 786-O cells were seeded per 96 well. When confluent, cells were infected with VSVΔ51-GFP at various MOIs (3, 0.5, 0.1, 0.05) for 1 hour in serum-free DMEM. Following infection, roughly 2e7 small EVs were added per well in 5% EV-depleted FBS-containing DMEM. 24 hours post-infection, VSVΔ51-GFP replication was assessed by both plaque assay and fluorescence microscopy, while VSVΔ51-GFP cytotoxicity was assessed by crystal violet staining and quantification.

2.17 Assay 3: EV Treatment Without VSVΔ51 Infection

One day before sEV treatment, 1e4 786-O cells were seeded per 96 well. When 80% confluent, cells were treated with roughly 2e7 small sEVs per well in 5% EV-depleted FBS-

containing DMEM. 24- and 48-hours post-treatment, sEV cytotoxicity was assessed by crystal violet staining and quantification.

2.18 CRISPR-Cas9 mediated Rab27a Knockout

Rab27a gRNA spacer sequence region was chosen from the GeCKO Lentiviral sgRNA v2 libraries (Human GeCKOv2 CRISPR knockout pooled library, Sanjana et al. 2014, Nature Methods). LentiCRISPRv2 plasmid was digested with BbsI (NEB, Ipswich, MA, USA) and gel purified using the QIAquick Gel Extraction Kit (Qiagen, Hilden, Germany). gRNA ssOligos complementary to the target region and containing stick-end BbsI cut sites were phosphorylated with Polynucleotide Kinase (NEB, Ipswich, MA, USA) and annealed in 1X Annealing Buffer (10 mM Tris, 50 nM NaCl, 1 mM EDTA). lentiCRISPR v2 was a gift from Feng Zhang (Addgene plasmid # 52961; http://n2t.net/addgene:52961; RRID:Addgene_52961). Annealed ds-oligos were diluted 1:200 and ligated into the cut LentiCRISPRv2 with Quick Ligase (NEB, Ipswich, MA, USA) at room temperature and transformed in Stbl3 competent E. coli (Invitrogen, Carlsbad, California, USA) according to their recommended protocol. Plasmids were extracted from transformants using the Qiagen Miniprep Kit (Qiagen, Hilden, Germany) at correct plasmids were confirmed by Sanger Sequencing (OHRI StemCore Laboraties, Ottawa, ON, Canada). Lentivirus was produced by lipofectamine transfection of the third-generation packaging plasmids (pMD2.G and psPAX2) and the cloned Rab27a-targeting lentiCRISPRv2 plasmid into 60% confluent 293T

cells. pMD2.G was a gift from Didier Trono (Addgene plasmid # 12259; http://n2t.net/addgene:12259 ; RRID:Addgene_12259) and psPAX2 was a gift from Didier Trono (Addgene plasmid # 12260 ; http://n2t.net/addgene:12260 ; RRID:Addgene_12260). For three consecutive days post-transfection, lentiviral supernatants were collected. 786-O cells were transduced with 1mL of lentivirus or mock-transduced (negative control) when 70% confluent. After 18 hours, cells were selected with 3.5 ug/mL puromycin. Puromycin selection was complete when all cells in the mock-transduced well were dead.

2.19 Isolation and Confirmation of a 786-O ΔRab27a Monoclonal Cell Line

Monoclonal cell lines were created by limiting dilutions of the Rab27a-CRISPR-targeted 786-O bulk population in 96-well plates. Three days post-plating, wells containing single colonies were identified by brightfield microscopy (EVOS). These monoclonal cell lines were expanded to 24-well, 12-well, and then 6-well plates. Protein lysates were harvested to confirm Rab27 deletion (section 2.12), small EVs were harvested for NTA (section 2.9) and western blotting (section 2.11), and DNA was harvested for Sanger sequencing (OHRI StemCore Laboraties, Ottawa, ON, Canada).

2.20 Statistical Analyses

All statistical analyses were performed using Prism GraphPad 7.0 and are described in figure legends. Error bars represent SEM. * denotes $p<0.05$, ** denotes $p<0.01$, *** denotes $p<0.001$. Statistics were reported for all experiments with at least three biological replicates.

3. RESULTS

3.1 VacV-infected cells release more small extracellular vesicles than uninfected cell.

Several viruses have been reported to increase sEV production upon infection (Muratori *et al.* 2009, Cell Host Microbe, Chai et al. 2008, Journal of Virology). Here, we investigated the impact of VacV infection on sEV populations.

To characterize sEV populations following VacV infection, we used Nanoparticle Tracking Analysis (NTA) to quantify sEVs and estimate sEV size distributions following VacV infection compared to mock-infected controls (Fig. 3). 786-O cells were infected with VacV for 2 hours and sEVs were harvested 48 hours later by ultracentrifugation, including filtration through a 0.22 μm filter to exclude VacV virions (360 × 270 × 250 nm). sEVs were detected between 30 and 170nm, with clearly significant differences in the size distribution upon VacV infection (Fig 3A). Overall, VacV-infected 786-O cells released significantly more sEVs than uninfected cells ($p = 0.03$, $T=2.952$, $df=3$) (Fig. 3B). Interestingly, we noticed a shift in peak sEV size between VacV and Mock samples. Median sEV size was significantly decreased in VacV-infected sEV samples compared to controls ($p=0.0261$, $t=3.127$, $df=3$) (Fig. 3C).

Next, we used Nanoscale Flow Cytometry (NFC) to independently investigate the differences in sEV counts and sizes between VacV and control samples. For this experiment, sEVs were stained with CFSE, and diluted 1/1000 for NFC Analysis. Consistent with our NTA data, we found that sEV counts in VacV-infected samples were greater and based on the side scatter (SSC) in these NFC plots, there was a larger increase in the smaller sEVs (Fig. 3D).

To corroborate this data, we performed NTA on sEV samples harvested from VacV-infected 293T (Fig. 3E) and MiaPACA-2 cells (Fig. 3F). Again, we observed an increase in sEV quantities and decrease in sEV size upon VacV infection (Fig. 3E-F). Taken together, VacV infection resulted in an increase in sEVs with a simultaneous decrease in the size of sEVs in several independent cell lines.

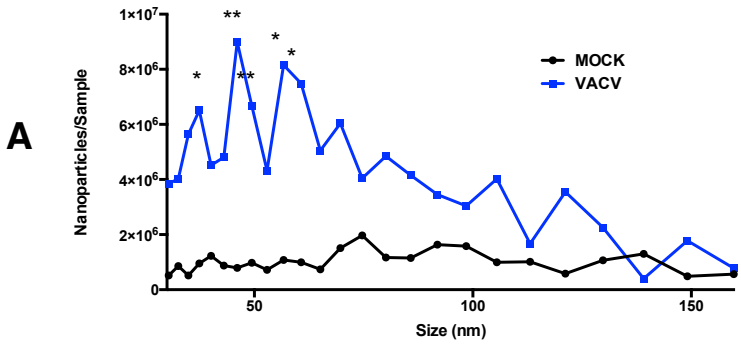
A
Nanoparticles/Sample
1×10^7
8×10^6
6×10^6
4×10^6
2×10^6
0
50
100
150
Size (nm)
MOCK
VACV
*
**
*
**
*
*

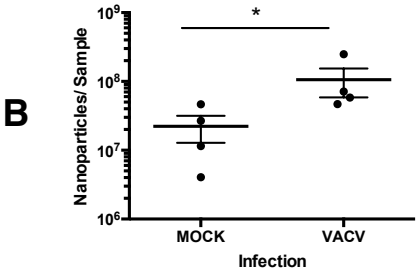
B
Nanoparticles/ Sample
10^9
10^8
10^7
10^6
MOCK
VACV
Infection
*

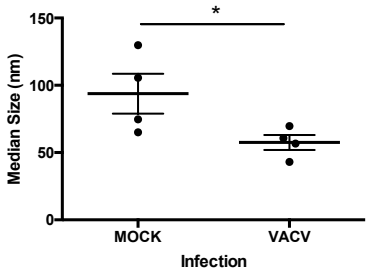
C
Median Size (nm)
150
100
50
0
MOCK
VACV
Infection
*

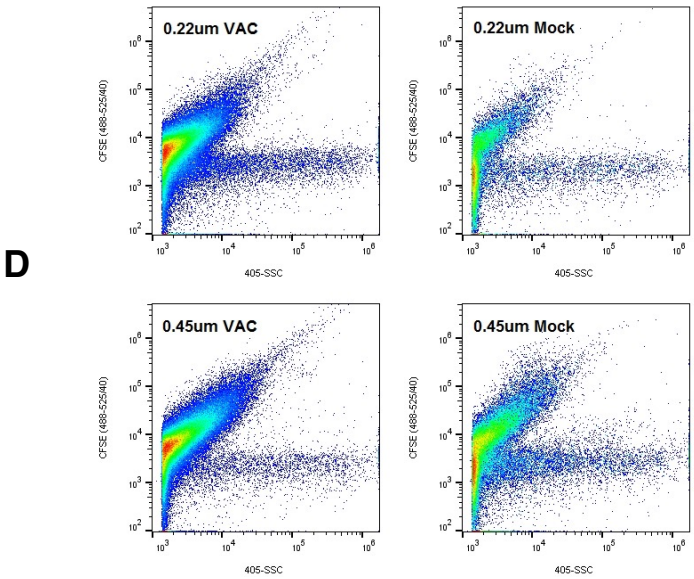
D
0.22um VAC
0.22um Mock
0.45um VAC
0.45um Mock
CFSE (488-525/40)
405-SSC

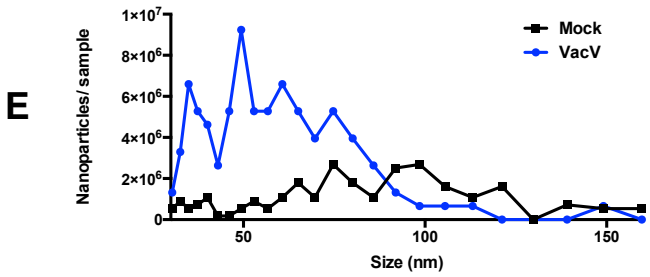
E
Nanoparticles/ sample
1×10^7
8×10^6
6×10^6
4×10^6
2×10^6
0
50
100
150
Size (nm)
Mock
VacV

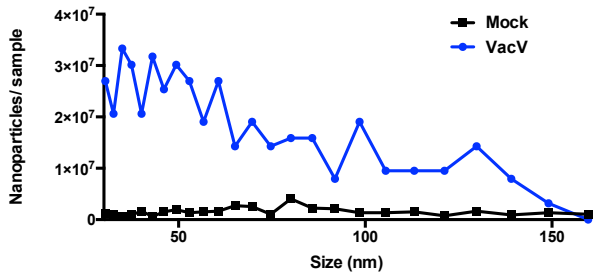
F
Nanoparticles/ sample
4×10^7
3×10^7
2×10^7
1×10^7
0
50
100
150
Size (nm)
Mock
VacV

Figure 3. Characterization of sEVs following VacV infection. (A-C) Four independent biological replicates were used to investigate 786-O sEV counts and size distributions following VacV infection compared to mock-infected control. (A) The number of sEVs was determined as a function of particle size (n=4). Unpaired t-tests were performed at each size point. * $p<0.05$, ** $p<0.01$. (B) Total nanoparticle counts of VacV and Mock-infected 786-O sEVs (n=4) were compared using a one-tailed ratio paired t-test. (C) Median size of 786-O VacV and Mock sEVs (n=4) was assessed using a one-tailed paired t-test. (D) An independent 786-O sEV sample was assessed by NFC and plotted on CFSE fluorescence and SSC (n=1). (E and F) Size distributions of sEVs harvested from VacV-infected and Mock-infected 293T (E) and MiaPACA-2 (F) were assessed by NTA (each n=1).

3.2 B19R and C12L RNAs are present in small extracellular vesicles following infection with Vaccinia Virus Copenhagen Strain

Then, we sought to determine if VacV-derived RNAs could be detected in sEVs following infection. We analyzed previously-obtained Small RNA-Seq raw data (Wedge and Ilkow, unpublished data). For this experiment, sEV and cellular reads from VacV-infected MiaPACA-2 cells were aligned to the entire VacV Copenhagen Strain genome (Fig. 4A). Hits were distributed throughout the VacV genome, but two VacV genes, B19R and C12L, contained an enrichment of hits in sEVs compared to cells, while other VacV genes (e.g. A11R) had fewer relative hits in sEVs than in cells (Fig. 4B-E). B19R and C12L sequences in both cellular and sEV Small RNA-Seq data were distributed across the coding regions of B19R and C12L (Fig. 4B-E).

To confirm the presence of B19R and C12L in VacV-infected cell-derived sEVs, 786-O sEVs and cells were harvested 48 hours post VacV or Mock infection. Quantitative Real-Time PCR analysis of sEV and cellular samples revealed the presence of B19R and C12L in sEVs (Fig. 5A). There was a significant difference in relative expression across B19R, C12L, and A11R ($p=0.0034$, $F=16.87$, $df=2$, $R2=0.849$). The relative expressions of B19R and C12L in sEVs versus cells were significantly greater than that of A11R (B19R v. A11R: $p=0.0031$, $t=5.940$, $df=4.692$; C12L v. A11R: $p=0.0226$, $t=5.578$, $df=2.248$). Total B19R and C12L molecules per 1000 sEVs (defined by 30-160nm) was quantified by comparing absolute qRT-PCR values with NTA counts/reaction, revealing that an average of 12.253 ± 6.043 molecules of B19R and 5.960 ± 4.540 molecules of C12L were present per 1000 sEVs (Fig. 5B).

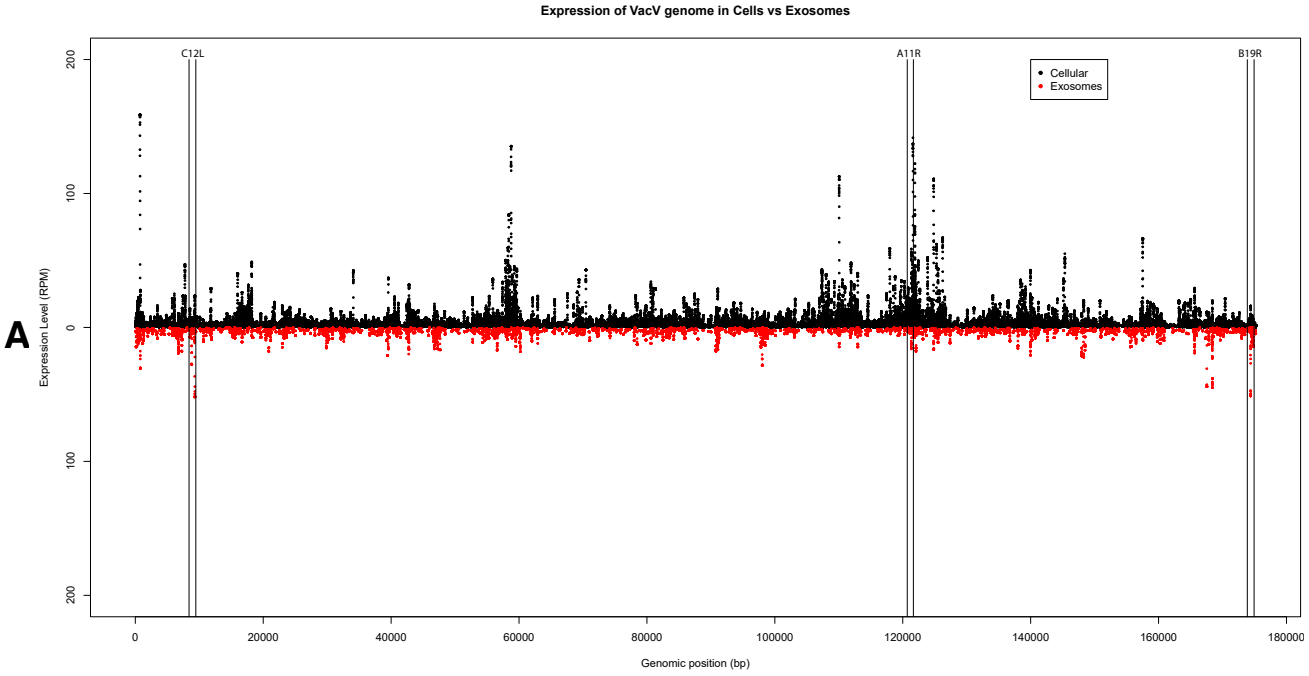
A
Expression of VacV genome in Cells vs Exosomes
C12L
A11R
B19R
Cellular
Exosomes
Expression Level (RPM)
Genomic position (bp)

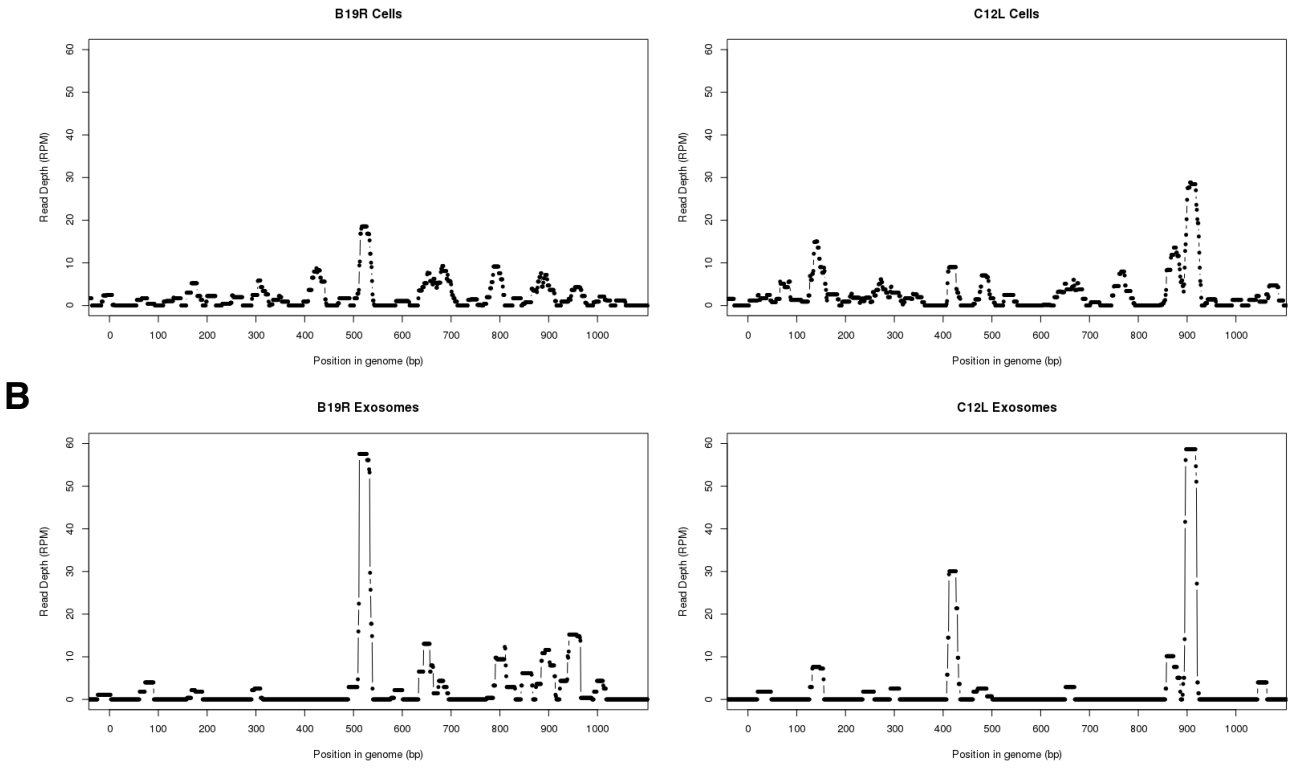
B
B19R Cells
C12L Cells
B19R Exosomes
C12L Exosomes
Read Depth (RPM)
Position in genome (bp)

Figure 4. Small RNA-Seq experiment reveals B19R and C12L RNA are present in VacV-infected cell sEVs. (A) Small RNA reads from VacV-infected MiaPACA-2 sEV and cellular RNA samples were aligned to Vaccinia Virus Copenhagen Strain genome. B19R and C12L were identified with enriched hits in the sEV portion, while other VacV genes (including A11R) had comparatively fewer hits in their sEV portions. (B) When B19R and C12L were assessed individually, they both had reads distributed throughout their coding regions. Experiment performed by M-E. Wedge and bioinformatic analysis performed by A. Pelin.

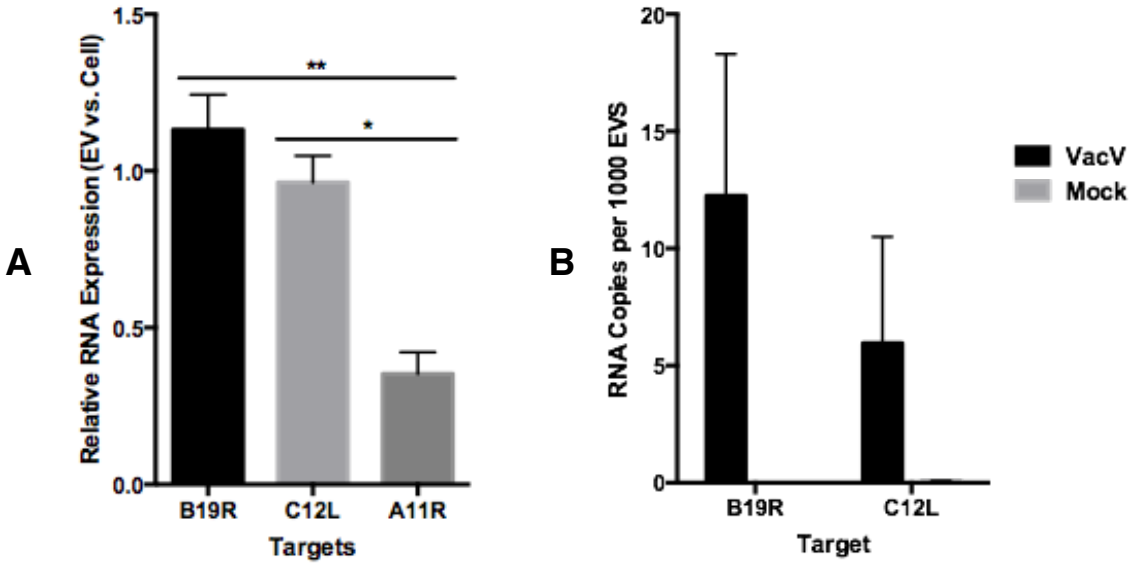

Figure 5. B19R and C12L RNA detection in VacV-infected cell-derived sEVs by Quantitative Real-Time PCR. (A) 48 hours post-infection with VacV wildtype, 786-O sEVs and cells were harvested and RNA was extracted. cDNA was synthesized from equal quantities of RNA, and qRT-PCR was performed to assess the relative expression of B19R, C12L, and A11R in sEV RNA as compared to cellular RNA, with normalization to 18S RNA. Mean fold changes in sEV samples compared to cellular samples were assessed (B19R: n=4, C12L: n=2, A11R: n=3) by one-way ANOVA, followed by Tukey's post-test. (B) Total number of B19R and C12L molecules per 1000 sEVs (30 to 160nm) was quantified. For mock samples, B19R and C12L had undetermined raw Ct values or Ct values were >35 and outside the C12L standard curve, thus these values were not represented in the graph.

3.3 CRISPR-Cas9-mediated targeting of Rab27a in 786-O cells

CRISPR-Cas9-mediated targeting of Rab27a in 786-O parental cells was performed by N. Crawford in our laboratory, to create exosome-deficient cells. We used these cells to further test the hypothesis that B19R RNA was present in the exosomal component of sEVs. Once cells were transduced with the Rab27a-targeting CRISPR-Cas9 lentivirus (Fig. 6A, Table 2), monoclonal cell lines were separated from the bulk population and one cell line was found to have at least a partial Rab27a deletion by immunoblotting for Rab27a (Fig. 4B) This monoclonal population production was carried out by Natalie Crawford.

Once the ΔRab27a 786-O monoclonal cell line was chosen, we characterized it further. Upon sanger sequencing analysis of the ΔRab27a 786-O cells, we found that at least one allele contained a 17 bp deletion and several mismatches when compared to our parental 786-O cell line and the most common Rab27a transcript variant using the Clustal_W2 alignment program (NM_004580.4) (Fig. 6C). We then used ExPASY Translate to predict the amino acid sequence of the ΔRab27a 786-O and the parental 786-O cell lines, revealing a probable 92 amino acid truncation in ΔRab27a 786-O line (Fig. 6D). sEVs were harvested from both the ΔRab27a and parental 786-O lines to compare their total sEV and exosome quantities by NTA, total protein visualization, and immunoblotting for an exosomal marker. We found that the ΔRab27a 786-O cells produced less sEVs in the 30-80 nm range (Fig. 7A), that these ΔRab27a sEVs contain less total protein (Fig. 7B), and that they have lower expression of the exosomal marker Flotillin-1 (Fig. 7C).

A

ATGTCTGATGGAGATTATGATTACCTCATCAAGTTTTTAGCTTTGGGAGACTCTGGTGTAGGGAAGACCA
GTGTACTTTACCAATATACAGATGGTAAATTTAACTCCAAATTTATCACAACAGTGGGCATTGATTTCAG
GGAAAAAAGAGTGGTGTACAGAGCCAGTGGGCCGGATGGAGCCACTGGCAGAGGCCAGAGAATCCACCTG
CAGTTATGGGACACAGCAGGGCAGGAGAGGTTTCGTAGCTTAACGACAGCGTTCTTCAGAGATGCTATGG
GTTTTCTTCTACTTTTTGATCTGACAAATGAGCAAAGTTTCCTCAATGTCAGAAACTGGATAAGCCAGCT
ACAGATGCATGCATATTGTGAAAACCCAGATATAGTGCTGTGTGGAAACAAGAGTGATCTGGAGGACCAG
AGAGTAGTGAAAGAGGAGGAAGCCATAGCACTCGCAGAGAAATATGGAATCCCCTACTTTGAAACTAGTG
CTGCCAATGGGACAAACATAAGCCAAGCAATTGAGATGCTTCTGGACCTGATAATGAAGCGAATGGAACG
GTGTGTGGACAAGTCCTGGATTCCTGAAGGAGTGGTGCGATCAAATGGTCATGCCTCTACGGATCAGTTA
AGTGAAGAAAAGGAGAAAGGGGCATGTGGCTGTTGA

B

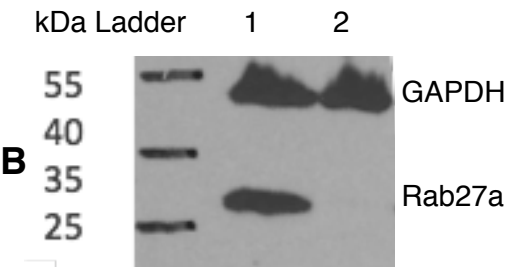

C

```
Wildtype        GGGAAGACCAGTGTACTTTACCAATATACAGATGGTAAATTTAACTCCAAATTTATCACA    120
Rab27a-KO       GGGAAGACCAGTGTACTTTACCAATATACAGATGGTAAATTTAACTCCAAATTTATCACA    120
                ************************************************************

Wildtype        ACAGTGGGCATTGATTTCAGGGAAAAAAGAGTGGTGTACAGAGCCAGTGGGCCGGATGGA    180
Rab27a-KO       ACAGTGGGCATTGATTTCAGGGAAAAAAGAGTGGTGTACAGAGCCAGTGGGCCGGATGGA    180
                ************************************************************

Wildtype        GCCACTGGCAGAGGCCAGAGAATCCACCTGCAGTTATGGGACACAGCAGGGCAGGAGAGG    240
Rab27a-KO       GCCACTGGCAGAGGCCAGAGAATCCACCTGCAGTTATGGGACACAGCAGGGCAGGAGAGG    240
                ************************************************************

Wildtype        TTTCGTAGCTTAACGACAGCGTTCTTCAGAGATGCTATGGGTTTTCTTCTACTTTTTGAT    300
Rab27a-KO       TTTCGTAGCTTAACGACAGCGTTCTTCAGAGATGCTATGGGTTTTCTTCTACTTTTTGAT    300
                ************************************************************

Wildtype        CTGACAAATGAGCAAAGTTTCCTCAATGTCAGAAACTGGATAAGCCAGCTACAGATGCAT    360
Rab27a-KO       CTGACAAATGAGCAAAGTTTCCTCAATGTCAGAAACTGGATAAGCCAGCTACAGATGCAT    360
                ************************************************************

Wildtype        GCATATTGTGAAAACCCAGATATAGTGCTGTGTGGAAACAAGAGTGATCTGGAGGACCAG    420
Rab27a-KO       GGATATAGT----------------GCTGTGTGGAAACAAGAGTGATCTGGAGGACCAG    403
                * **** **                  ***********************************

Wildtype        AGAGTAGTGAAAGAGGAGGAAGCCATAGCACTCGCAGAGAAATATGGGTGA-GTATTTT-    478
Rab27a-KO       AGAGTAGTGAAAGAGGAGGAAGCCAAGTGAATGGGAAGAAAAATTATGGGGAGAAATTTT    463
                *************************    * * * *   ***  *  * *  * * ***

Wildtype        ------------------TGTGGAGAAGTCTAGAGAAAACATTTTCAATATAAACATTA    519
Rab27a-KO       GAGAAAAAATCTTCAACCTTAAGTTTTGGGGGATATTGAATGTGGCCAATATAAACATTA    523
                                 *  *     *   * *   **  *   ***************

Wildtype        GCAGGTGAATGGTAATGAAAAAGATAAAAGTGGACAATTAAAGCAAAACCTCAGCCATAG    579
Rab27a-KO       GCAGGTGAATGGTAATGAAAAAGATAAAAGTGGACAATTAAAGCAAAACCTCAGCCATAG    583
                ************************************************************

Wildtype        GCCTTGGGGCATGTTGAATGTGTCCTTTTTATATGATATGATAGTAGGATCCATTGACAA    639
Rab27a-KO       GCCTTGGGGCATGTTGAATGTGTCCTTTTTATATGATATGATAGTAGGATCCATTGACAA    643
                ************************************************************

Wildtype        TGCATGTGGCAAGGGCCTCCTTCAGTGCTTTGGTCCCATTTTCTCAAACTCTTGGACTG    698
Rab27a-KO       TGCATGTGGCAAGGGCCTCCTTCAGTGCTTTGGTCCCATTTTCTCAAACTCTTGGACTG    702
                ************************************************************
```

D

```
NCBI            MSDGDYDYLIKFLALGDSGVGKTSVLYQYTDGKFNSKFITTVGIDFREKRVVYRASGPDG    60
Rab27a          MSDGDYDYLIKFLALGDSGVGKTSVLYQYTDGKFNSKFITTVGIDFREKRVVYRASGPDG    60
                ************************************************************

NCBI            ATGRGQRIHLQLWDTAGQERFRSLTTAFFRDAMGFLLLFDLTNEQSFLNVRNWISQLQMH    120
Rab27a          ATGRGQRIHLQLWDTAGQERFRSLTTAFFRDAMGFLLLFDLTNEQSFLNVRNWISQLQMH    120
                ************************************************************

NCBI            AYCENPDIVLCGNKSDLEDQRVVKEEEAIALAEKYGIPYFETSAANGTNISQAIEMLLDL    180
Rab27a          GYSAVWKQE-----------------------------------------------------    129
                .*.   .

NCBI            IMKRMERCVDKSWIPEGVVRSNGHASTDQLSEEKEKGACGC    221
Rab27a          -------------------------------------------    129
```

Figure 6. Validation of an exosome-deficient ΔRab27a 786-O monoclonal cell line. (A) Complete Rab27a CDS with CRISPR-Cas9 target sequence (red) and antibody binding region (underlined). (B) Rab27a (25 kDa) is undetectable by immunoblotting of ΔRab27a 786-O protein lysates (lane 2) but detectable in Parental 786-O lysates (lane 1). GAPDH (50 kDa) was used as loading control and was detected at comparable levels in both samples. (C) Sanger sequencing of ΔRab27a and parental 786-O cell lines reveals both deletions and mismatches by Clustal_W2 Analysis. (D) ExPASY Translate was used to determine the predicted amino acid sequence of ΔRab27a and Parental 786-O and these sequences were aligned using Clustal_W2. At least one allele of ΔRab27a has a premature stop codon, leading to a 92 amino acid truncation in the second last exon.

A

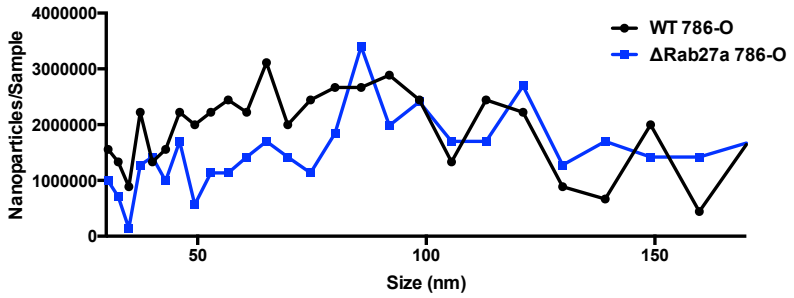
4000000
3000000
2000000
1000000
0
Nanoparticles/Sample
50
100
150
Size (nm)
WT 786-O
ΔRab27a 786-O

B

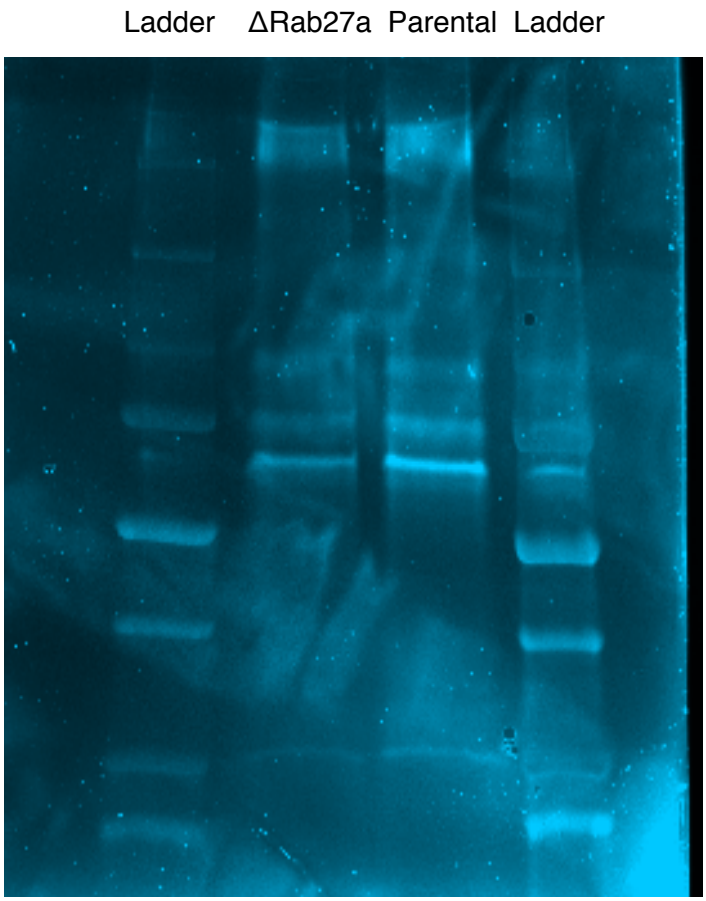
Ladder
ΔRab27a
Parental
Ladder

C

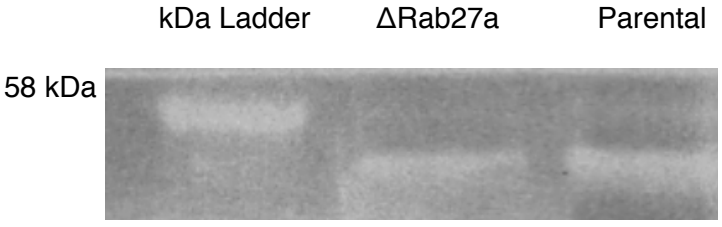
kDa Ladder
ΔRab27a
Parental
58 kDa
Flotillin-1

Figure 7. ΔRab27a 786-O cells produce less sEVs and less exosomes than parental 786-O cells. (A) NTA of ΔRab27a 786-O sEVs reveals a distinct reduction in sEVs in the 30-80 nm range. (B) Total protein visualization of Parental 786-O sEVs (lane 1) versus ΔRab27a 786-O sEVs (lane 2) shows a reduction in total sEV proteins in the ΔRab27a 786-O line. (C) Immunoblotting of ΔRab27a 786-O sEVs (lane 1) demonstrates a reduction in exosomal markers (Flotillin at 55 kDa) compared to Parental 786-O cells (lane 2).

3.4 Small extracellular vesicle-associated B19R RNA augments VSVΔ51-induced cytotoxicity

To study the potential role of sEV-associated B19R RNA (sEV-B19R) in infection, a VSVΔ51-based assay was used to assess sEV-B19R functionality. If sEV-B19R is functional, then treatment of 786-O cells with sEV-B19R should sensitize these cells to VSVΔ51 infection. Briefly, ΔRab27a and Parental 786-O cells were infected with VacV wildtype or VacV ΔB19R and sEVs were harvested 48 hours later (Fig. 8A). These sEVs were then used to treat naïve 786-O cells before (Assay 1) or after (Assay 2) VSVΔ51-GFP infection at an MOI of 0.05. VSVΔ51-GFP cytotoxicity was assessed by crystal violet staining. There was a significant difference in cell viability among the four pre-treatment sEV groups 24 hours after VSVΔ51-GFP infection ($p=0.0213$, $F=9.321$, $R2=0.7565$). Specifically, we found that there was a significant decrease in cell viability when B19R-containing sEVs (EV 1) were used to pre-treat naïve 786-O cells before VSVΔ51-GFP infection, when compared to the ΔRab27a sEV group (EV 3) ($p=0.0081$, $t=4.915$, $df=3$), the ΔB19R control (EV 2) ($p=0.0369$, $t=2.70$, $df=3$), and the ΔRab27a ΔB19R control (EV 4) ($p=0.0052$, $t=5.757$, $df=3$) (Fig. 8B). Therefore, exosomally-transferred B19R RNA is functional in recipient cells.

Next, we performed a similar assay but with VSVΔ51-GFP infection prior to sEV treatment. There was a significant difference in VSVΔ51-GFP cytotoxicity among the four post-treatment sEV groups 24 hours after VSVΔ51-GFP infection at an MOI of 0.05 ($p=0.0043$, $F=59.85$, $R2=0.9677$). Specifically, 786-O cells treated with EV 1 post-infection were significantly more sensitive than the EV 2 treated cells ($p=0.0012$, $t=20.41$, $df=2$), EV 3 treated cells ($p=0.0351$, $t=3.572$, $df=2$), and EV 4 treated cells ($p=0.0086$, $t=7.529$, $df=2$) 24

hours after VSVΔ51-GFP infection (Fig. 8C). Again, this demonstrates that sEV-B19R is functionally present in the exosome fraction of VacV-infected cell sEVs and that these sets may play a role in creating a pro-viral niche for infection.

To ensure that these differences in cytotoxicity were not due to the presence of VacV virions in harvested sEVs, VacV-free sEVs were optimized and were confirmed by plaque assay (Fig. 9A), NFC (Fig. 9B), and NTA (Fig. 9C). Additionally, NTA was used to ensure the differences between EV1 and EV2, as well as EV3 and EV4, were not due to differences in sEVs populations released from VacV WT- and VacV ΔB19R-infected 786-O cells (Fig. 9D).

We attempted to clone a VacV ΔC12L virus using a C12L interruption cassette, but no positive plaques were rescued. Therefore, we decided to focus on B19R in this study.

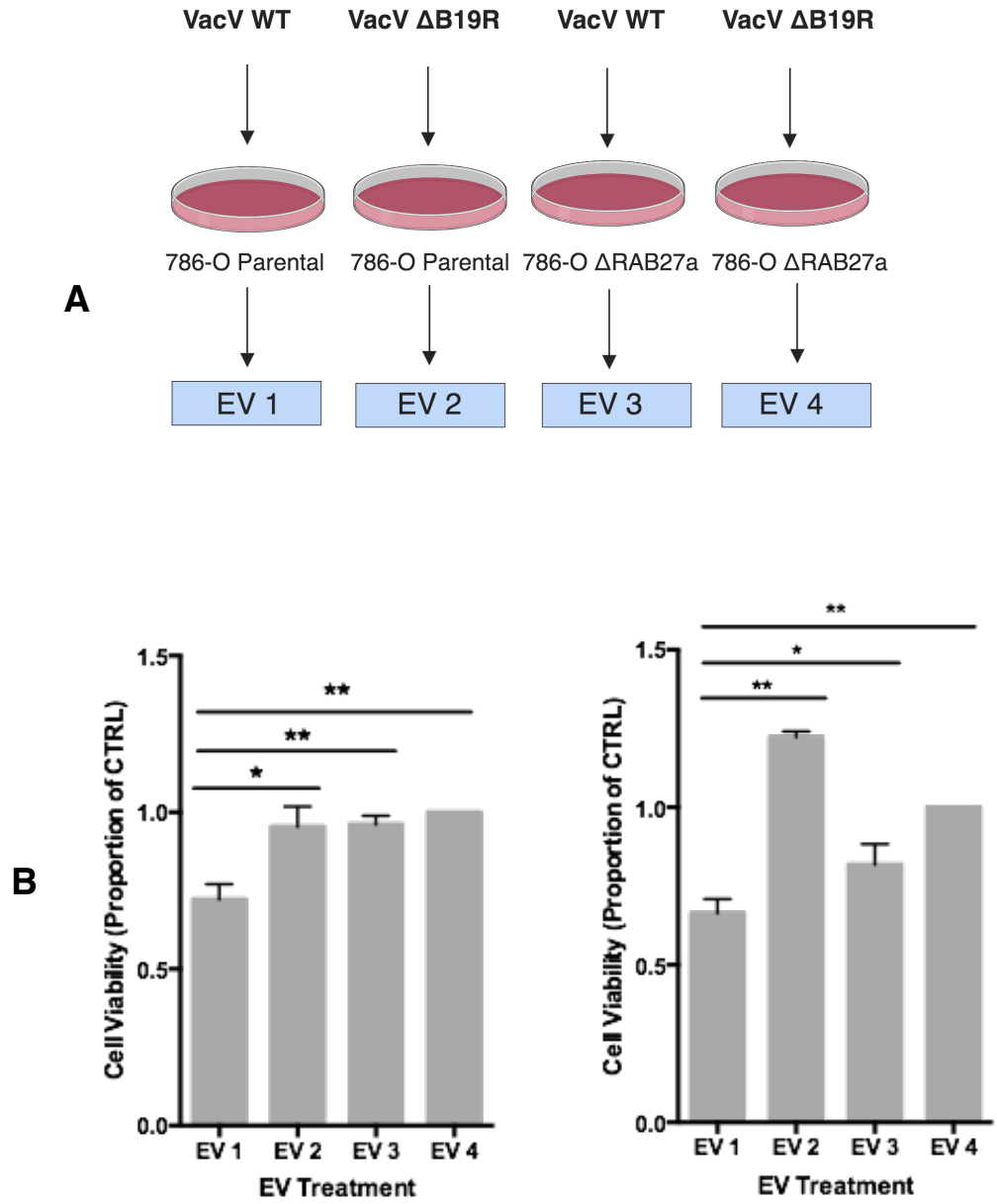

Figure 8. sEV-B19R augments VSVΔ51-dependent cytotoxicity. (A) sEV harvest setup for EV 1-4. (B) Assay 1: 10 Hour sEV Treatment, followed by VSVΔ51-GFP infection (MOI 0.05) and CV staining at 24 hours. (C) Assay 2: VSVΔ51-GFP infection at MOI 0.05 followed by sEV treatment for 24 hours. (B-C) CV quantification represented as average cell viability proportion of EV4 control. Overall change in cell viability was assessed using a Row-Matched, Repeated Measure One-Way ANOVA with Geisser-Greenhouse Correction. Individual differences were assessed using one-tailed paired t-tests.

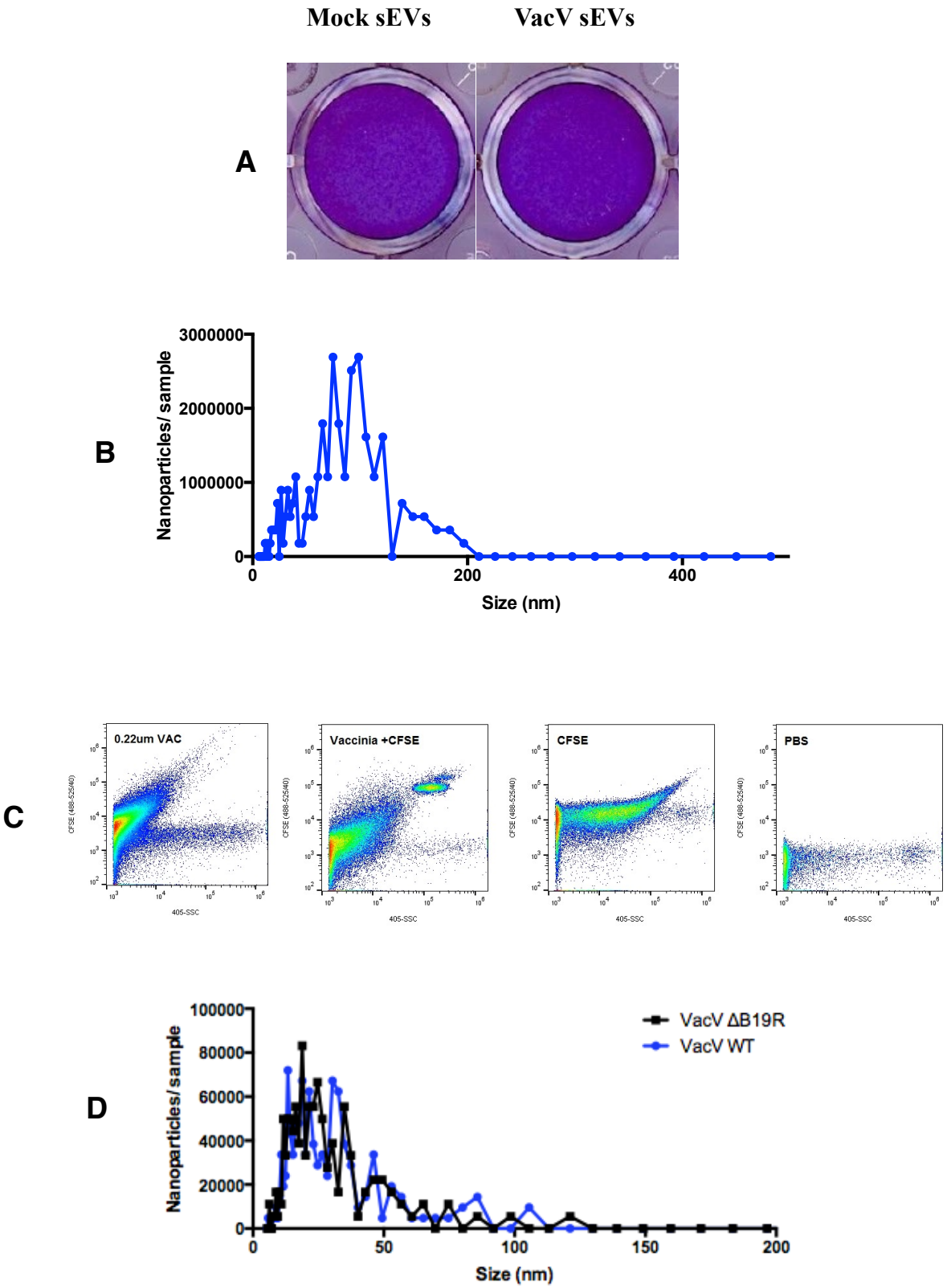
Mock sEVs
VacV sEVs
A
B
Nanoparticles/ sample
3000000
2000000
1000000
0
0
200
400
Size (nm)
C
0.22um VAC
Vaccinia +CFSE
CFSE
PBS
CFSE (488-525/40)
405-SSC
D
Nanoparticles/ sample
100000
80000
60000
40000
20000
0
0
50
100
150
200
Size (nm)
VacV ΔB19R
VacV WT

Figure 9. VacV sEVs are virion-free. (A) Cells were CV stained 48 hours after confluent 786-Os were treated with sEVs from Mock (left) and VacV (right) conditions. (B) NTA on sEV harvests show that sEVs are free of VacV virions, which would be present between 300 nm and 400 nm. (C) NFC on CFSE-stained sEV harvests demonstrates that sEVs are VacV virion-free (panel 1). Panel 2 shows a positive control, where VacV is a distinct population in the upper right quadrant. Panels 3 and 4 are negative controls. (D) sEV quantities and size distributions from VacV WT and ΔB19R are not different, as shown by NTA.

3.5 Small extracellular vesicle-associated B19R RNA does not augment VSVΔ51-GFP replication 24 hours following infection

Prior to crystal violet staining for VSVΔ51-induced cytotoxicity, cell-media samples were collected in technical duplicates from each well of Assays 1 and 2 to test the effect of sEV-B19R on VSVΔ51-GFP replication. These samples were used to perform plaque assays to determine the number of particle forming units per mL of sample at 24 hours post VSVΔ51-GFP infection, as a proxy for the viral replication in each treatment group. Overall, there were no significant differences across groups for either sEV pre-treatment ($p=0.3597$, $F=1.389$, $R2=0.4099$, $df=3$) (Fig. 10A) or sEV post-treatment ($p=0.1228$, $F=4.565$, $R2=0.6954$, $df=3$) (Fig. 10B) at VSVΔ51-GFP MOI of 0.05. Interestingly, there were no significant differences in pairwise comparisons in either Assay 1 (Fig. 10A) or Assay 2 (Fig. 10B), though the comparisons of EV1 to EV2 and EV3 to EV4 in Assay 2 were approaching significance ($0.1>p>0.05$) (Fig. 10B)

3.6 Small extracellular vesicle-associated B19R RNA cytotoxicity is VSVΔ51-dependent

To investigate whether sEV-B19R treatment was cytotoxic in the absence of VSVΔ51-GFP infection, 786-O cells were treated with sEVs and cell viability was assessed at 24- and 48-hour time-points by CV staining and quantification. At 24 hours, there were no significant differences in cell viability across the four treatment groups ($p=0.509$, $F=0.561$, $R2=0.219$) (Fig. 11A). Likewise, there were no significant differences in cell viability across groups at 48 hours ($p=0.559$, $F=0.499$, $R2=0.199$) (Fig. 11B). There were no significant

differences in pairwise comparisons at either the 24- or 48-hour time-point ($p>0.1$ for all pairs).

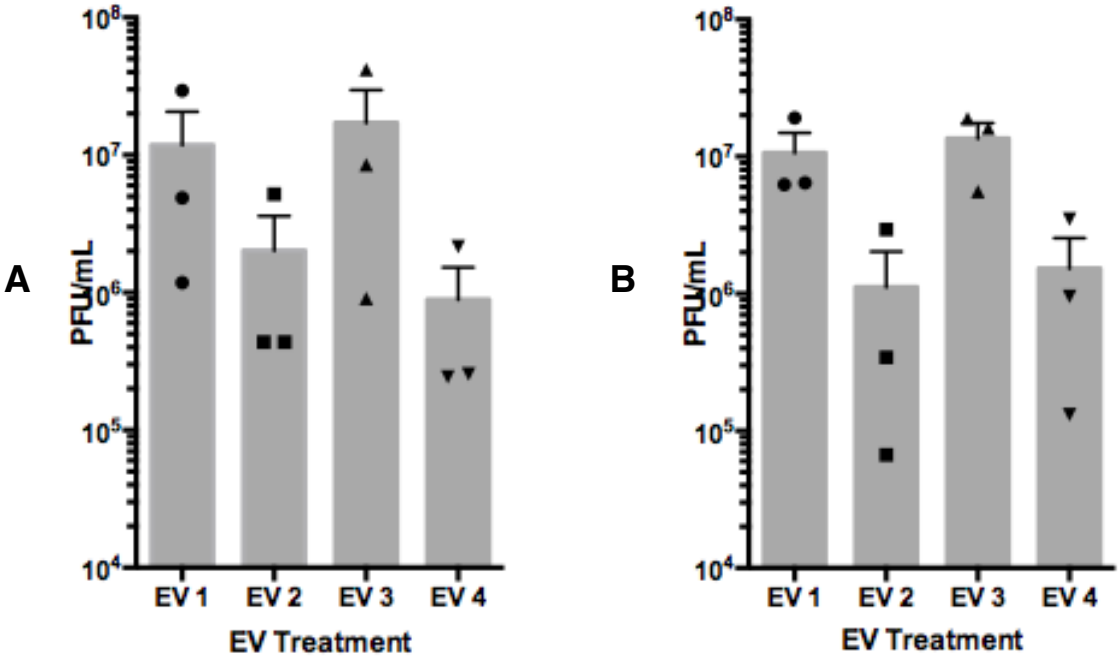

Figure 10. sEV-B19R does not increase VSVΔ51-GFP viral titers at 24 hours post-infection. (A) Assay 1 with pre-treatment (n=3) (B) Assay 2 with post-treatment (n=3). Row-Matched, Repeated Measure One-Way ANOVA with Geisser-Greenhouse Correction was used to assess overall variability between the four treatment groups in each assay. One-tailed paired t-tests were used for pairwise comparisons between the different treatment groups.

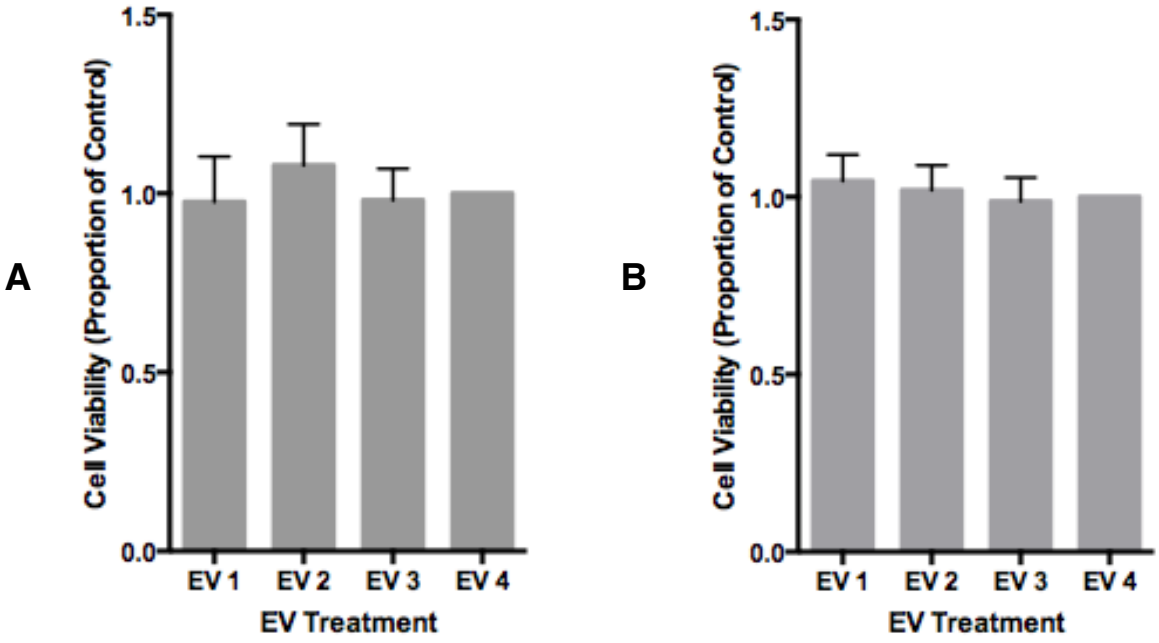

Figure 11. sEV-B19R treatment did not reduce cell viability in the absence of VSVΔ51-GFP infection. (A and B) Cell Viability 24 hours (A) and 48 hours (B) after sEV treatment in the absence of VSVΔ51-GFP infection. Values are representative of proportion of EV 4 treatment group control. Row-Matched, Repeated Measure One-Way ANOVA with Geisser-Greenhouse Correction were used to assess overall variability in cell viability among the four treatment groups at both time points. Two-tailed paired T-tests, assuming a Gaussian distribution and consistent differences between values, were used for pairwise comparisons between the different treatment groups.

4. DISCUSSION

4.1 The Effect of VacV Infection on sEVs

Extracellular vesicles facilitate intracellular crosstalk during periods of normal functioning, as well as during stress. This important host defence system can be co-opted by pathogens, in order to promote their replication and spread. Several viruses, including HIV-1 and HBV, induce an increase in sEV production during infection (Ali *et al*. 2010, AIDS, Muratori *et al*. 2009, Cell Host Microbe, Chai *et al.* 2008, Journal of Virology). Recently, our lab found that infection with the oncolytic rhabdovirus VSVΔ51 led to a 10-fold increase in sEV production (Wedge M-E *et al.* 2019, unpublished data).

In the present study, we compared the quantities and size distributions of sEVs harvested from several cancer cell lines with and without VacV infection. sEV quantities were greater following VacV infection across all three human cell lines tested: 786-O (Fig. 3A), 293T (Fig. 3E), and MiaPACA-2 (Fig. 3F). These three cell lines have different cellular origins, mutational profiles, and gene expression profiles. 786-O is a renal cell cancer line, 293T is a normal human embryonic renal cell line, and MiaPACA-2 is a pancreatic carcinoma cell line of great interest to our lab. Since VacV infection induced an increase in sEV counts across these very distinct cell lines, it is possible that this change in sEV release may be dependent on a VacV-encoded product. F13, which binds to ESCRT proteins and localizes to the MVB during infection, is a candidate which could be explored (Honeychurch *et al.* 2007, Journal of Virology). Alternatively, this increase in sEVs upon VacV infection could be a host stress response to VacV infection. This could occur at early points in the VacV life cycle, including adsorption, entry, uncoating, early gene expression, or early

protein synthesis, or later during replication, intermediate/late gene expression, assembly, or egress. The use of UV- and heat-inactivated VacV could be used to investigate when this would occur, as inactivated VacV enters the cell and expresses early genes, but is DNA replication-deficient (Dai *et al.* 2017, Science Immunology). Finally, this sEV increase could be a universal cellular response to infection, as VacV-Cop is one of several viruses that affects sEV production.

Surprisingly, the size distributions of sEV populations from VacV-infected and uninfected cells were distinct, with a shift towards smaller sEVs upon VacV infection. Since VacV is an enveloped virus, it is possible that this decrease in sEV size is due to a tradeoff between sEV number, sEV size, and virion production. There is a cellular limit to lipid membrane biogenesis, so an increase in sEV production may result in smaller sEVs being produced. This shift is also likely due to an increase in exosome-specific production.

4.2 The Effect of VacV Infection on sEV Cargo

The ability of viruses to modulate sEV RNA cargo has been described previously (Cocucci *et al.* 2009, Trends in Cell Biology). Vaccinia encodes more 200 mRNAs, more than half of which are involved in dampening the host's antiviral response (Gubser *et al.* 2004, Journal of General Virology). Therefore, we set out to determine if any of these mRNAs were present in sEVs. Two VacV loci, B19R and C12L, had an enrichment of aligned reads in small RNA-Seq (Fig. 4A). Because these reads were distributed throughout the B19R and C12L coding regions, it is unlikely that these reads represent VacV-encoded miRNAs (Fig. 4B). RT-qPCR primers amplifying the 5' regions of C12L and B19R, where

there were the fewest aligned reads, were designed to confirm the presence of B19R and C12L RNA in sEVs. Both B19R and C12L were present in sEVs in amounts similar to those in the infected cells, whereas this was not true for another VacV-encoded RNA (Fig. 5A). Additionally, the ability of these primer sets to amplify both B19R and C12L RNA from sEV samples demonstrated that large portions of these RNAs are present in sEVs. Even though only RNA fragments less than 30 nucleotides in length were initially sequenced, it is likely that fragments of B19R and C12L were present in the extracted Total RNA, degraded during processing, and then isolated in the Small RNA portion of the polyacrylamide gel.

The amounts of B19R and C12L per sEV is quantifiable, with roughly 12 molecules of B19R and 6 molecules of C12L per 1000 sEVs (Fig. 5B). These quantities were determined under the assumption that these RNA molecules were homogeneously distributed across all harvested sEVs. Studies which report miRNAs per sEV have shown similar results under this assumption (Chevillet *et al*. 2014, PNAS). This homogeneous distribution of RNA molecules is unlikely. It is more likely that these RNA molecules are present in a fraction of these sEVs, such as the exosomal fraction, or even a subfraction, such as those exosomes produced at a specific time-point during infection. Several researchers have shown that exosomal cargo can be present in a subfraction of exosomes, and still maintain its biological function (Vyas *et al.* 2015, Scientific Reports, Willms et al. 2016, Scientific Reports, Crescitelli et al. 2013, Journal of Extracellular Vesicles). Therefore, B19R and C12L could be present in just a subfraction of sEVs and still be biologically relevant.

B19R and C12L are early VacV genes; transcribed within the VacV core and extruded into the cytoplasm before the formation of the viral factory. Therefore, these RNA molecules

could be accessed by a variety of RBPs within the cytoplasm and shuttled to the MVB early in infection. Due to the close relationship of VacV and the endosomal pathway throughout the VacV life cycle, we hypothesized that B19R and C12L RNA is present in the exosome fraction of sEVs.

4.3 Characterization of a 786-O ΔRab27a Exosome-Deficient Cell Line

Vaccinia virus infection and the release of new virions relies on several components of the secretory pathway. Two VacV EEV membrane proteins, B5 and F13, are localized to the late endosome and MVB upon infection (Lorenzo *et al.* 2000, Husain and Moss 2003, Journal of Virology). B5 is present on the surface of sEVs from MVA-infected cells, while F13 contains binding sites for ESCRT proteins, important components for trafficking of sEV cargo to MVBs (Honeychurch *et al.* 2007, Journal of Virology, Chen *et al.* 2009, Virology Journal, Spehner and Drillien 2008, Virus Research). Therefore, these VacV proteins could influence exosomal cargo loading. VacV virions are also associated with the early endosomal compartment, as the double-wrapping of the IMV to form an IEV relies on lipid membranes derived from the early endosome (Tooze *et al.* 1993, Eur. J. Cell. Biol.). Finally, intracellular vesicular trafficking between endosomes and the trans-golgi network occurs through both the retrograde and anterograde pathways and is critical for VacV infection (Sivan *et al.* 2016, Journal of Virology). VacV's reliance on these various modes of intracellular trafficking throughout its life cycle could influence the packaging of VacV products into ILVs and release in exosomes.

In order to assess the functionality of sEV-associated B19R and C12L in infection, we created an exosome-deficient 786-O cell line by targeting Rab27a using CRISPR-Cas9 technology (Sanjana *et al.* 2014, Nature Methods). After initial screening for Rab27a expression, we identified a ΔRab27a exosome-deficient monoclonal cell line and further analyzed its genomic Rab27a sequence and sEV production. Sequencing revealed a 17 bp deletion at the target site, resulting in a premature stop codon in at least one Rab27a allele (Fig. 6C). The lack of Rab27a detection by immunoblotting could be due to the deletion within the antibody binding site or the inability of the antibody to bind to the truncated protein (Fig. 6B). Additionally, it is possible that Rab27a mRNA is degraded through the nonsense-mediated mRNA decay pathway because the premature stop codon is in its second-last exon. The reduction in sEV particles in the 30-80 nm range produced by our 786-O-ΔRab27a cells demonstrates that these cells produce fewer exosomes (Fig. 7A), as described previously (Ostrowsji *et al.* 2010, Nature Cell Biology). This was corroborated by blotting for the exosomal marker Flotillin-1 (Fig. 7C).

Using these ΔRab27a exosome-deficient 786-O cells, we wanted to investigate whether the B19R and C12L RNA present in sEVs was functional. In order to test this hypothesis, we needed to use VacV ΔB19R and VacV ΔC12L viruses as controls. We already had a VacV ΔB19R, but we needed to clone a VacV ΔC12L. We attempted to create VacV ΔC12L by insertional mutagenesis with a GFP marker, but this virus could not be rescued (data not shown). C12 is the only VacV inhibitor of extrinsic apoptosis encoded by the VacV Copenhagen strain, as this strain does not encode B13R. Therefore, it is likely that the deletion of C12L (B22R in Western Reserve Strain) inhibited VacV replication due to its

inability to inhibit extrinsic apoptosis. It is for this reason that the remainder of this research project is focused on the effects of sEV B19R.

4.4 Potential Effect of sEV-Associated C12L in Infection

Though we were unable to perform assays to assess the functionality of sEV C12L, we have proposed a mechanism for its role in VacV infection. Since C12 inhibits extrinsic apoptosis, sEV C12L could inhibit apoptosis in uninfected recipient cells, thereby improving the chances that the cell would remain viable prior to infection. Infected cells secrete a variety of cell death signals, including FasL and TNF-α, that can induce death upon binding to death receptors (Zhou *et al.* 2017, Viruses). If these cell death signals bind to uninfected cells, they can induce apoptosis, thus reducing the pool of cells that can become infected by VacV (Zhou *et al.* 2017, Viruses). Therefore, we propose that sEV C12L could block this extrinsic apoptotic signalling in recipient uninfected cells, thereby allowing more uninfected cells to remain viable prior to infection with VacV. As mentioned previously, caspase inhibition is an important factor in the induction of necroptosis (Li and Beg 2000, Journal of Virology). Therefore, it is possible that functional C12 in recipient cells could induce necroptosis, creating a more inflammatory and possibly antiviral infection site.

4.5 The Functional Effect of sEV-Associated B19R in Infection

It is well-established that B19 sequesters IFN-α and IFN-β, blocking the downstream production of ISGs (Symons *et al.* 1995, Cell). Several interferon-sensitive viruses, including VSVΔ51, can synergize with B19 because of its ability to dampen the cell's antiviral state

(Le Boeuf *et al.* 2010, Molecular Therapy). In fact, Le Boeuf and colleagues (2010) showed that the treatment of HT29 cells with B19-containing supernatants following VSVΔ51 infection led to increased VSVΔ51 replication and spread. This increased replication and spread was dependent on the presence of B19 in the treatment supernatant. If B19R RNA is functionally present in exosomes, then the treatment of interferon-producing cells with B19R-containing exosomes should have similar effects on VSVΔ51. Therefore, we used VSVΔ51 infection as a proxy for functional B19R RNA, predicting that if exosomal B19R is functional, then it should prime recipient cells to be infected with VSVΔ51.

Pre-treatment of 786-O cells with EV1 resulted in increased cell death upon VSVΔ51 infection when compared to EV2, EV3, and EV4 treatments (Fig. 8B). EV1 contains sEV-associated B19R, while EV2 contains sEVs but no B19R. Therefore, the pretreatment of 786-O cells with sEVs harvested from WT VacV-infected cells improved VSVΔ51-GFP cytotoxicity. It is possible that there was B19 contamination of the EV1 sEV harvest, as B19 is a secreted protein. Therefore, the ΔRab27a 786-O cells were used in this experiment for two reasons: (1) to investigate whether sEV-B19R was functionally present in the exosomes from infected cells, and (2) to determine the extent of B19R protein contamination of sEV samples. EV2 and EV3 pre-treatment resulted in no VSVΔ51-induced cell death at 24 hours, whereas only 70% of cells pre-treated with EV1 were viable at 24 hours post-VSVΔ51-infection. This confirmed that sEV-B19R is in fact present in exosomes and is functional in recipient cells, because the increased cytotoxic effects seen with B19R and VSVΔ51 did not occur when the sEV samples did not contain exosomes.

This pre-treatment model for sEV B19R mimics what could happen in the vicinity of the infection site. As the VacV infection progresses, exosomes containing B19R could be taken up by uninfected cells that may not be reached by secreted B19. This functional B19R mRNA could be translated and secreted from the cell to sequester extracellular interferon. Alternatively, it could possibly function to sequester interferon intracellularly prior to release.

We performed a similar assay but with sEV treatment directly following VSVΔ51 entry (Fig. 8C). In this scenario, the uninfected cells are exposed to a variety of molecules secreted by the VSVΔ51-infected cells, including IFN-β. There was a large difference in cell viability with EV1 post-treatment when compared to EV2 post-treatment. But in this setup, EV3 post-treatment still partially improved VSVΔ51 cytotoxicity, which was most likely due to the presence of contaminating B19 protein in the EV3 sample. Nevertheless, there was still a small but significant difference in cell viability between EV1 and EV3 post-treated cells, which is the result of exosomal B19R. Therefore, even in the presence of secreted B19 protein, exosomal B19R has an additive effect in reducing the cell's antiviral state.

To ensure that the effect of EV1 on VSVΔ51 cytotoxicity was not due to the presence of VacV infectious particles, we confirmed that our sEVs were virion free (Fig. 9A-C). We then investigated whether the absence of B19R in VacV infection had an impact on sEV populations (Fig. 9D). sEV populations from VacV WT- and VacV ΔB19R-infected cells were identical based on our NTA data. Therefore, we concluded that the differences between the EV1 and EV2-4 treatment groups for the pre-treatment experiment and the EV1 and EV3

treatment groups for the post-treatment experiment were due the presence of exosomal B19R.

We predicted that the increase in VSVΔ51 cytotoxicity would be accompanied by an increase in VSVΔ51 replication and spread, but this was not the case as we did not find a difference in VSVΔ51 titers between EV1 and EV3 pre- or post-treatment groups at 24 hours (Fig 10A-B). This could be because the cells primed with exosomal B19R die more quickly or it could be simply due to the shorter time point of 24 hours.

Finally, to ensure that the difference in cell viability in Assay 1 and Assay 2 was VSVΔ51-dependent, and not due to exosomal B19R-induced cell death, we sought to investigate the potential cytotoxic effect of EV1 on 786-O cells. Since there were no differences in cell viability upon EV1 treatment compared to control treatments, we concluded that EV1 cytotoxicity required VSVΔ51 infection. Altogether, our data demonstrates a functional role for exosomal B19R in priming cells for infection.

4.6 Future Directions

We propose several future experiments to continue exploring the role of sEVs in VacV infection. First, there are likely several VacV and host proteins present in VacV-infected cell sEVs that could have functional roles in infection. These proteins could play confounding roles in our functional studies and should be explored. Mass Spectrometry of VacV-infected cell sEVs should be performed, followed by confirmation by western blot analysis. Second, the possible functional role of sEV C12L in infection should be explored. If C12L is present in sEVs following transduction with a C12L-expressing lentivector, then this

method could be used to test the differences in extrinsic apoptosis with and without sEV C12L. Specifically, levels of cleaved Caspase-3, -7, and -8 could be investigated as downstream effectors in extrinsic apoptosis following C12L sEV treatment with and without infection. Finally, future studies in our lab will focus on unraveling the mechanism of how exosomal B19R can prime cells to become infected. This will include assessing the expression levels of interferon pathway effectors following treatment with exosomal B19R.

5. CONCLUSIONS

This is the first time that VacV infection has been shown to increase sEV production, as has been shown with other viruses in the past. This is also the first account of the presence of VacV-encoded RNA molecules in sEVs upon infection. We found that B19R, one of the two RNA molecules which we identified in sEVs, is present in exosomes upon infection and can functionally prime uninfected recipient cells to become infected. Therefore, sEVs are implicated in VacV infection and could represent another way in which VacV can dampen the cell's antiviral response and facilitate the infection of its host.

REFERENCES CITED

Abboud, G. et al. Natural Killer Cells and Innate Interferon Gamma Participate in the Host Defense against Respiratory Vaccinia Virus Infection. J. Virol. 90, 129 (2016).

Admyre, C. et al. Exosomes with immune modulatory features are present in human breast milk. J. Immunol. 179, 1969–78 (2007).

Aguado, B., Lan, '', Selmes, P. & Smith, G. L. Nucleotide sequence of 21.8 kbp of variola major virus strain Harvey and comparison with vaccinia virus. Journal of General Virology 33, (1992).

Alcamí, A., Symons, J. A. & Smith, G. L. The vaccinia virus soluble alpha/beta interferon (IFN) receptor binds to the cell surface and protects cells from the antiviral effects of IFN. J. Virol. 74, 11230–9 (2000).

Alcamí, A. & Smith, G. L. Soluble interferon-gamma receptors encoded by poxviruses. Comp. Immunol. Microbiol. Infect. Dis. 19, 305–17 (1996).

Alcami, A. & Smith, G. L. A soluble receptor for interleukin-1β encoded by vaccinia virus: A novel mechanism of virus modulation of the host response to infection. Cell 71, 153–167 (1992).

Ali, S. A. et al. Genetic Characterization of HIV Type 1 Nef-Induced Vesicle Secretion. AIDS Res. Hum. Retroviruses 26, 173–192 (2010).

Ansarah-Sobrinho, C. & Moss, B. Role of the I7 Protein in Proteolytic Processing of Vaccinia Virus Membrane and Core Components Downloaded from. J. Virol. 78, 6335–6343 (2004).

Arroyo, J. D. et al. Argonaute2 complexes carry a population of circulating microRNAs independent of vesicles in human plasma. Proc. Natl. Acad. Sci. 108, 5003–5008 (2011).

Artenstein, A. W. New generation smallpox vaccines: a review of preclinical and clinical data. Rev. Med. Virol 18, 217–231 (2008).

Baxby. Archives of Virology Poxvirus Hosts and Reservoirs Brief Review. Archives of Virology 55, (1977).

Batagov, A. O., Kuznetsov, V. A. & Kurochkin, I. V. Identification of nucleotide patterns enriched in secreted RNAs as putative cis-acting elements targeting them to exosome nano-vesicles. BMC Genomics 12 Suppl 3, S18 (2011).

Beauchamp, N. M., Busick, R. Y. & Alexander-Miller, M. A. Functional Divergence among CD103+ Dendritic Cell Subpopulations following Pulmonary Poxvirus Infection. J. Virol. 84, 10191–10199 (2010).
Beattie, E., Tartaglia, J. & Paoletti, E. Vaccinia virus-encoded eIF-2 alpha homolog abrogates the antiviral effect of interferon. Virology 183, 419–22 (1991).

Bengali, Z., Townsley, A. C. & Moss, B. Vaccinia virus strain differences in cell attachment and entry. doi:10.1016/j.virol.2009.04.012 (2009).

Bianco, F. et al. Astrocyte-derived ATP induces vesicle shedding and IL-1 beta release from microglia. J. Immunol. 174, 7268–77 (2005).

Bobrie, A. et al. Rab27a Supports Exosome-Dependent and -Independent Mechanisms That Modify the Tumor Microenvironment and Can Promote Tumor Progression. Cancer Res. 72, 4920–4930 (2012).

Bolukbasi, M. et al. miR-1289 and "Zipcode"-like sequence enrich mRNAs in microvesicles. (2012). doi:10.1038/mtna.2011.2

Bonduelle, O., Duffy, D., Verrier, B., Combadiere, C. & Combadiere, B. Cutting Edge: Protective Effect of CX3CR1+ Dendritic Cells in a Vaccinia Virus Pulmonary Infection Model. J. Immunol. 188, 952–956 (2012).

Brentnall, M., Rodriguez-Menocal, L., De Guevara, R., Cepero, E. & Boise, L. H. Caspase-9, caspase-3 and caspase-7 have distinct roles during intrinsic apoptosis. BMC Cell Biol. 14, 32 (2013).

Camussi, G., Deregibus, M. C., Bruno, S., Cantaluppi, V. & Biancone, L. Exosomes/microvesicles as a mechanism of cell-to-cell communication. Kidney Int. 78, 838–848 (2010).

Carroll, K., Elroy-Steinll, O., Mossll, B. & Jagus$, R. Recombinant Vaccinia Virus K3L Gene Product Prevents Activation of Double-stranded RNA-dependent, Initiation Factor 2a-specific Protein Kinase*. 268, (1993).

Carter, G. C., Law, M., Hollinshead, M. & Smith, G. L. Entry of the vaccinia virus intracellular mature virion and its interactions with glycosaminoglycans. J. Gen. Virol. 86, 1279–1290 (2005).

Ceccarelli, S. et al. Epstein-Barr virus latent membrane protein 1 promotes concentration in multivesicular bodies of fibroblast growth factor 2 and its release through exosomes. Int. J. Cancer 121, 1494–1506 (2007).

Chai, N. et al. Properties of Subviral Particles of Hepatitis B Virus. J. Virol. 82, 7812–7817 (2008).

Chang, H. W., Watson, J. C. & Jacobs, B. L. The E3L gene of vaccinia virus encodes an inhibitor of the interferon-induced, double-stranded RNA-dependent protein kinase. Proc. Natl. Acad. Sci. U. S. A. 89, 4825–9 (1992).

Chang, S.-J., Chang, Y.-X., Izmailyan, R., Tang, Y.-L. & Chang, W. Vaccinia virus A25 and A26 proteins are fusion suppressors for mature virions and determine strain-specific virus entry pathways into HeLa, CHO-K1, and L cells. J. Virol. 84, 8422–32 (2010).

Chen, Y. et al. Vaccinia virus p37 interacts with host proteins associated with LE-derived transport vesicle biogenesis. Virol. J. 6, 44 (2009).

Chen, B. J. & Lamb, R. A. Mechanisms for enveloped virus budding: can some viruses do without an ESCRT? Virology 372, 221–32 (2008).

Chevillet, J. R. et al. Quantitative and stoichiometric analysis of the microRNA content of exosomes. Proc. Natl. Acad. Sci. 111, 14888–14893 (2014).

Chiu, W.-L., Lin, C.-L., Yang, M.-H., Tzou, D.-L. M. & Chang, W. Vaccinia virus 4c (A26L) protein on intracellular mature virus binds to the extracellular cellular matrix laminin. J. Virol. 81, 2149–57 (2007).

Cho, Y. et al. Phosphorylation-Driven Assembly of the RIP1-RIP3 Complex Regulates Programmed Necrosis and Virus-Induced Inflammation. Cell 137, 1112–1123 (2009).

Choi, D. et al. Extracellular vesicle communication pathways as regulatory targets of oncogenic transformation. Semin. Cell Dev. Biol. 67, 11–22 (2017).

Choi, D.-S. et al. Proteomic Analysis of Microvesicles Derived from Human Colorectal Cancer Cells. J. Proteome Res. 6, 4646–4655 (2007).

Chung, C.-S., Huang, C.-Y. & Chang, W. Vaccinia Virus Penetration Requires Cholesterol and Results in Specific Viral Envelope Proteins Associated with Lipid Rafts. J. Virol. 79, 1623–1634 (2005).

Cocucci, E., Racchetti, G. & Meldolesi, J. Shedding microvesicles: artefacts no more. Trends Cell Biol. 19, 43–51 (2009).

Colamonici, O. R., Domanski, P., Sweitzer, S. M., Larner, A. & Buller, R. M. Vaccinia virus B18R gene encodes a type I interferon-binding protein that blocks interferon alpha transmembrane signaling. J. Biol. Chem. 270, 15974–8 (1995).

Conde-Vancells, J. et al. Candidate biomarkers in exosome-like vesicles purified from rat and mouse urine samples. PROTEOMICS - Clin. Appl. 4, 416–425 (2010).
Conley, A. et al. High-throughput sequencing of two populations of extracellular vesicles provides an mRNA signature that can be detected in the circulation of breast cancer patients. RNA Biol. 14, 305–316 (2017).

Conry, R. M., Westbrook, B., McKee, S. & Norwood, T. G. Talimogene laherparepvec: First in class oncolytic virotherapy. Hum. Vaccin. Immunother. 14, 839–846 (2018).

Crescitelli, R. et al. Distinct RNA profiles in subpopulations of extracellular vesicles: apoptotic bodies, microvesicles and exosomes. J. Extracell. Vesicles 2, 20677 (2013).

Cudmore, S., Cossart, P., Griffiths, G. & Way, M. Actin-based motility of vaccinia virus. Nature 378, 636–638 (1995).

Cyrklaff, M. et al. Cryo-electron tomography of vaccinia virus. 102, (2005).
Dai, P. et al. Intratumoral delivery of inactivated modified vaccinia virus Ankara (iMVA) induces systemic antitumor immunity via STING and Batf3-dependent dendritic cells. Sci. Immunol. 2, (2017).

Dai, A. et al. Ribosome Profiling Reveals Translational Upregulation of Cellular Oxidative Phosphorylation mRNAs during Vaccinia Virus-Induced Host Shutoff. J. Virol. 91, e01858-16 (2017).

De Jong, O. G. et al. Cellular stress conditions are reflected in the protein and RNA content of endothelial cell-derived exosomes. J. Extracell. Vesicles 1, 18396 (2012).

Del Conde, I., Shrimpton, C. N., Thiagarajan, P. & López, J. A. Tissue-factor-bearing microvesicles arise from lipid rafts and fuse with activated platelets to initiate coagulation. Blood 106, 1604–11 (2005).

De Silva, F. S. & Moss, B. Origin-independent plasmid replication occurs in vaccinia virus cytoplasmic factories and requires all five known poxvirus replication factors. Virol. J. 2, 23 (2005).

Doms, R. W., Blumenthal, R., Moss, B. & Moss, B. Fusion of intra- and extracellular forms of vaccinia virus with the cell membrane. J. Virol. 64, 4884–92 (1990).

Drillien, R., Le Spehner, D. & Hanau, D. Modified vaccinia virus Ankara induces moderate activation of human dendritic cells. doi:10.1099/vir.0.79998-0 (2004).

Dukers, D. F. et al. Direct immunosuppressive effects of EBV-encoded latent membrane protein 1. J. Immunol. 165, 663–70 (2000).

Easterbrook, K. B. Controlled degradation of vaccinia virions in vitro: an electron microscopic study. J. Ultrastruct. Res. 14, 484–496 (1966).

Escrevente, C., Keller, S., Altevogt, P. & Costa, J. Interaction and uptake of exosomes by ovarian cancer cells. BMC Cancer 11, 108 (2011).

Ekström, K. et al. Characterization of mRNA and microRNA in human mast cell-derived exosomes and their transfer to other mast cells and blood CD34 progenitor cells. J. Extracell. Vesicles 1, 18389 (2012).

Fanini, F. & Fabbri, M. Cancer-derived exosomic microRNAs shape the immune system within the tumour microenvironment: state of the art. HHS Public Access. Semin Cell Dev Biol 67, 23–28 (2017).

Feng, D. et al. Cellular Internalization of Exosomes Occurs Through Phagocytosis. Traffic 11, 675–687 (2010).

Feng, Z. et al. A pathogenic picornavirus acquires an envelope by hijacking cellular membranes. Nature 496, 367–371 (2013).

Ferguson, B. J. et al. Vaccinia virus protein N2 is a nuclear IRF3 inhibitor that promotes virulence. J. Gen. Virol. 94, 2070–2081 (2013).

French, K. C., Antonyak, M. A. & Cerione, R. A. Extracellular vesicle docking at the cellular port: Extracellular vesicle binding and uptake. Semin. Cell Dev. Biol. 67, 48–55 (2017).

Fu, Y. et al. Exosome-mediated miR-146a transfer suppresses type I interferon response and facilitates EV71 infection. PLOS Pathog. 13, e1006611 (2017).

Garcia, A. D. & Moss, B. Repression of Vaccinia Virus Holliday Junction Resolvase Inhibits Processing of Viral DNA into Unit-Length Genomes. J. Virol. 75, 6460–6471 (2001).

Gerlic, M. et al. Vaccinia virus F1L protein promotes virulence by inhibiting inflammasome activation. Proc. Natl. Acad. Sci. 110, 7808–7813 (2013).

Goebel, S. J. et al. The complete DNA sequence of vaccinia virus. Virology 179, 247–66, 517–63 (1990).

Graham, S. C. et al. Vaccinia Virus Proteins A52 and B14 Share a Bcl-2–Like Fold but Have Evolved to Inhibit NF-κB rather than Apoptosis. PLoS Pathog. 4, e1000128 (2008).

Greenberg, R. N. & Kennedy, J. S. ACAM2000: a newly licensed cell culture-based live vaccinia smallpox vaccine. Expert Opin. Investig. Drugs 17, 555–564 (2008).
Griffiths, G., Roos, N., Schleich, S. & Locker, J. K. Structure and assembly of intracellular mature vaccinia virus: thin-section analyses. J. Virol. 75, 11056–70 (2001).

Grigorov, B. et al. A role for CD81 on the late steps of HIV-1 replication in a chronically infected T cell line. Retrovirology 6, 28 (2009).

Guo, Z. S. et al. The Enhanced Tumor Selectivity of an Oncolytic Vaccinia Lacking the Host Range and Antiapoptosis Genes SPI-1 and SPI-2. Cancer Res. 65, 9991–9998 (2005).

Gutierrez, K. D. et al. MLKL Activation Triggers NLRP3-Mediated Processing and Release of IL-1β Independently of Gasdermin-D. J. Immunol. 198, 2156–2164 (2017).

Gutwein, P. et al. Cleavage of L1 in Exosomes and Apoptotic Membrane Vesicles Released from Ovarian Carcinoma Cells. Clin. Cancer Res. 11, 2492–2501 (2005).

Hatcher, E. L., Hendrickson, R. C. & Lefkowitz, E. J. Identification of nucleotide-level changes impacting gene content and genome evolution in orthopoxviruses. J. Virol. 88, 13651–68 (2014).

Heijnen, H. F., Schiel, A. E., Fijnheer, R., Geuze, H. J. & Sixma, J. J. Activated platelets release two types of membrane vesicles: microvesicles by surface shedding and exosomes derived from exocytosis of multivesicular bodies and alpha-granules. Blood 94, 3791–9 (1999).

Hessvik, N. P. & Llorente, A. Current knowledge on exosome biogenesis and release. Cell. Mol. Life Sci. 75, 193–208 (2018).

Hetz, C. et al. Proapoptotic BAX and BAK Modulate the Unfolded Protein Response by a Direct Interaction with IRE1. Science (80-.). 312, 572–576 (2006).

Hiller, G. & Weber, K. Golgi-Derived Membranes That Contain an Acylated Viral Polypeptide Are Used for Vaccinia Virus Envelopment. Journal of Virology (1985).

Hitomi, J. et al. Identification of a molecular signaling network that regulates a cellular necrotic cell death pathway. Cell 135, 1311–23 (2008).

Hollinshead, M. et al. Vaccinia virus utilizes microtubules for movement to the cell surface. J. Cell Biol. 154, 389–402 (2001).

Hollinshead, R., Hollinshead, M., Krauss, O. & Smith, G. L. An investigation of incorporation of cellular antigens into vaccinia virus particles. J. Gen. Virol. 83, 2347–2359 (2002).

Honeychurch, K. M., Yang, G., Jordan, R. & Hruby, D. E. The vaccinia virus F13L YPPL motif is required for efficient release of extracellular enveloped virus. J. Virol. 81, 7310–5 (2007). Horibe, S., Tanahashi, T., Kawauchi, S., Murakami, Y. & Rikitake, Y. Mechanism of recipient cell-dependent differences in exosome uptake. BMC Cancer 18, 47 (2018).

Hornung, V. et al. AIM2 recognizes cytosolic dsDNA and forms a caspase-1-activating inflammasome with ASC. Nature 458, 514–518 (2009).

Huang, C.-Y. et al. A novel cellular protein, VPEF, facilitates vaccinia virus penetration into HeLa cells through fluid phase endocytosis. J. Virol. 82, 7988–99 (2008).

Huang, L. et al. Labeling and Single-Particle-Tracking-Based Entry Mechanism Study of Vaccinia Virus from the Tiantan Strain. Anal. Chem. 90, 3452–3459 (2018).

Hung, M. E. & Leonard, J. N. A platform for actively loading cargo RNA to elucidate limiting steps in EV-mediated delivery. J. Extracell. Vesicles 5, 31027 (2016).

Hutchens, M. A. et al. Protective Effect of Toll-like Receptor 4 in Pulmonary Vaccinia Infection. PLoS Pathog. 4, e1000153 (2008).

Ichihashi, Y. Extracellular Enveloped Vaccinia Virus Escapes Neutralization. Virology 217, 478–485 (1996).

Izmailyan, R. et al. Integrin β1 Mediates Vaccinia Virus Entry through Activation of PI3K/ Akt Signaling. J. Virol. 86, 6677–6687 (2012).

Jacobs, B. L. et al. Vaccinia Virus Vaccines: Past, Present and Future. Antiviral Res. 84, 1 (2009).

Jacobs, N., Chen, R. A.-J., Gubser, C., Najarro, P. & Smith, G. L. Intradermal immune response after infection with Vaccinia virus. J. Gen. Virol. 87, 1157–1161 (2006).

Jarahian, M. et al. Modulation of NKp30- and NKp46-Mediated Natural Killer Cell Responses by Poxviral Hemagglutinin. PLoS Pathog. 7, e1002195 (2011).

Jeppesen, D. K. et al. Reassessment of Exosome Composition. Cell 177, 428-445.e18 (2019). Jezek, Z. et al. Human Monkeypox: A Study of 2,510 Contacts of 214 Patients. J. Infect. Dis. 154, 551–555 (1986).

Katsafanas, G. C. & Moss, B. Colocalization of Transcription and Translation within Cytoplasmic Poxvirus Factories Coordinates Viral Expression and Subjugates Host Functions. Cell Host Microbe 2, 221–228 (2007).

Kawai, T. et al. IPS-1, an adaptor triggering RIG-I- and Mda5-mediated type I interferon induction. Nat. Immunol. 6, 981–988 (2005).
Kawakami, Y. et al. Inhibition of NK cell activity by IL-17 allows vaccinia virus to induce severe skin lesions in a mouse model of eczema vaccinatum. J. Exp. Med. 206, 1219–1225 (2009).

Kerr, S. M. & Smith, G. L. Vaccinia virus encodes a polypeptide with DNA ligase activity. Nucleic Acids Res. 17, 9039–50 (1989).

Kettle, S. et al. Vaccinia virus serpin B13R (SPI-2) inhibits interleukin-1beta-converting enzyme and protects virus-infected cells from TNF- and Fas-mediated apoptosis, but does not prevent IL-1beta-induced fever. J. Gen. Virol. 78, 677–685 (1997).

Kidokoro, M., Tashiro, M. & Shida, H. Genetically stable and fully effective smallpox vaccine strain constructed from highly attenuated vaccinia LC16m8. Proc. Natl. Acad. Sci. U. S. A. 102, 4152–7 (2005).

Kilcher, S. et al. siRNA screen of early poxvirus genes identifies the AAA+ ATPase D5 as the virus genome-uncoating factor. Cell Host Microbe 15, 103–12 (2014).

Kim, Y., Lee, H., Heo, L., Seok, C. & Choe, J. Structure of vaccinia virus A46, an inhibitor of TLR4 signaling pathway, shows the conformation of VIPER motif. Protein Sci. 23, 906–914 (2014).

Klibi, J. et al. Blood diffusion and Th1-suppressive effects of galectin-9-containing exosomes released by Epstein-Barr virus-infected nasopharyngeal carcinoma cells. Blood 113, 1957–1966 (2009).

Kobayashi, T. et al. Vesiculation of platelet plasma membranes. Dilauroylglycerophosphocholine-induced shedding of a platelet plasma membrane fraction enriched in acetylcholinesterase activity. Biochim. Biophys. Acta - Biomembr. 778, 210–218 (1984).

Kretzschmar, M., Wallinga, J., Teunis, P., Xing, S. & Mikolajczyk, R. Frequency of Adverse Events after Vaccination with Different Vaccinia Strains. PLoS Med. (2006).

Lai, C. P. et al. Visualization and tracking of tumour extracellular vesicle delivery and RNA translation using multiplexed reporters. Nat. Commun. 6, 7029 (2015).

Laliberte, J. P., Weisberg, A. S. & Moss, B. The Membrane Fusion Step of Vaccinia Virus Entry Is Cooperatively Mediated by Multiple Viral Proteins and Host Cell Components. PLoS Pathog. 7, ee1002446 (2011).

Lancaster, G. I. & Febbraio, M. A. Exosome-dependent Trafficking of HSP70. J. Biol. Chem. 280, 23349–23355 (2005).

Le Boeuf, F. et al. Synergistic interaction between oncolytic viruses augments tumor killing. Mol. Ther. 18, 888–95 (2010).

Lee, S. B. & Esteban, M. The Interferon-Induced Double-Stranded RNA-Activated Human p68 Protein Kinase Inhibits the Replication of Vaccinia Virus. Virology 193, 1037–1041 (1993).

Lenassi, M. et al. HIV Nef is Secreted in Exosomes and Triggers Apoptosis in Bystander CD4+ T Cells. Traffic 11, 110–122 (2010).

Li, J. et al. Exosomes mediate the cell-to-cell transmission of IFN-α-induced antiviral activity. Nature.com (2013).

Li, M. & Beg, A. A. Induction of Necrotic-Like Cell Death by Tumor Necrosis Factor Alpha and Caspase Inhibitors: Novel Mechanism for Killing Virus-Infected Cells. JOURNAL OF VIROLOGY 74, (2000).

Liu, B. et al. Identification of Poxvirus Genome Uncoating and DNA Replication Factors with Mutually Redundant Roles. J. Virol. 92, (2018).

Liu, R. & Moss, B. Vaccinia Virus C9 Ankyrin Repeat/F-Box Protein Is a Newly Identified Antagonist of the Type I Interferon-Induced Antiviral State. J. Virol. 92, (2018).

Liu, S.-W., Wyatt, L. S., Orandle, M. S., Minai, M. & Moss, B. The D10 Decapping Enzyme of Vaccinia Virus Contributes to Decay of Cellular and Viral mRNAs and to Virulence in Mice. J. Virol. 88, 202–211 (2014).

Locker, J. K. et al. Entry of the Two Infectious Forms of Vaccinia Virus at the Plasma Membane Is Signaling-Dependent for the IMV but Not the EEV. Mol. Biol. Cell 11, 2497–2511 (2002).

Logozzi, M. et al. High Levels of Exosomes Expressing CD63 and Caveolin-1 in Plasma of Melanoma Patients. PLoS One 4, e5219 (2009).

Logue, S. E. & Martin, S. J. Caspase activation cascades in apoptosis. Biochem. Soc. Trans. 36, 1–9 (2008).

Lorenzo, M. M., Galindo, I., Griffiths, G. & Blasco, R. Intracellular localization of vaccinia virus extracellular enveloped virus envelope proteins individually expressed using a Semliki Forest virus replicon. J. Virol. 74, 10535–50 (2000).

Macen, J. L. et al. Differential inhibition of the Fas- and granule-mediated cytolysis pathways by the orthopoxvirus cytokine response modifier A/SPI-2 and SPI-1 protein. Proc. Natl. Acad. Sci. U. S. A. 93, 9108–13 (1996).

Mack, M. et al. Transfer of the chemokine receptor CCR5 between cells by membrane-derived microparticles: A mechanism for cellular human immunodeficiency virus 1 infection. Nat. Med. 6, 769–775 (2000).

Maluquer de Motes, C. et al. Inhibition of Apoptosis and NF-κB Activation by Vaccinia Protein N1 Occur via Distinct Binding Surfaces and Make Different Contributions to Virulence. PLoS Pathog. 7, e1002430 (2011).

Mann, B. A. et al. Vaccinia Virus Blocks Stat1-Dependent and Stat1-Independent Gene Expression Induced by Type I and Type II Interferons. J. Interf. Cytokine Res. 28, 367–380 (2008).

Martin-Serrano, J., Yaravoy, A., Perez-Caballero, D., Bieniasz, P. D. & Yaravoy, A. Divergent retroviral late-budding domains recruit vacuolar protein sorting factors by using alternative adaptor proteins. Proc. Natl. Acad. Sci. 100, 12414–12419 (2003).

Masciopinto, F. et al. Association of hepatitis C virus envelope proteins with exosomes. Eur. J. Immunol. 34, 2834–2842 (2004).

Mateescu, B. et al. Obstacles and opportunities in the functional analysis of extracellular vesicle RNA – an ISEV position paper. J. Extracell. Vesicles 6, 1286095 (2017).

Mazurov, D., Heidecker, G. & Derse, D. HTLV-1 Gag protein associates with CD82 tetraspanin microdomains at the plasma membrane. Virology 346, 194–204 (2006).

McKelvey, T. A., Andrews, S. C., Miller, S. E., Ray, C. A. & Pickup, D. J. Identification of the orthopoxvirus p4c gene, which encodes a structural protein that directs intracellular mature virus particles into A-type inclusions. J. Virol. 76, 11216–25 (2002).

Meckes, D. G., Raab-Traub, N. & Raab-Traub, N. Microvesicles and viral infection. J. Virol. 85, 12844–54 (2011).

Mercer, J. & Helenius, A. Vaccinia virus uses macropinocytosis and apoptotic mimicry to enter host cells. Science 320, 531–5 (2008).

Mercer, J. & Helenius, A. Virus entry by macropinocytosis. Nat. Cell Biol. 11, 510–520 (2009).

Mercer, J. & Helenius, A. Apoptotic mimicry: phosphatidylserine-mediated macropinocytosis of vaccinia virus. Ann. N. Y. Acad. Sci. 1209, 49–55 (2010).

Mercer, J. et al. Vaccinia virus strains use distinct forms of macropinocytosis for host-cell entry. Proc. Natl. Acad. Sci. U. S. A. 107, 9346–51 (2010).

Mercer, J. et al. RNAi Screening Reveals Proteasome- and Cullin3-Dependent Stages in Vaccinia Virus Infection. Cell Rep. 2, 1036–1047 (2012).

Mercer, J. et al. RNAi Screening Reveals Proteasome- and Cullin3-Dependent Stages in Vaccinia Virus Infection. Cell Rep. 2, 1036–1047 (2012).

Meyer, H. et al. Outbreaks of disease suspected of being due to human monkeypox virus infection in the Democratic Republic of Congo in 2001. J. Clin. Microbiol. 40, 2919–21 (2002).

Meyer, H, Sutter, G, Mayr, A. Mapping of deletions in the genome of the highly attenuated vaccinia virus MVA and their influence on virulence. J. Gen. Virol. 72, 1031–1038 (1991).

Miao, E. A., Rajan, J. V. & Aderem, A. Caspase-1-induced pyroptotic cell death. Immunol. Rev. 243, 206–214 (2011).

Michael, A. et al. Exosomes from human saliva as a source of microRNA biomarkers. Oral Dis. 16, 34–38 (2010).

Mittelbrunn, M. et al. Unidirectional transfer of microRNA-loaded exosomes from T cells to antigen-presenting cells. Nat. Commun. 2, 282 (2011).

Mohandas, A. R. & Dales, S. Involvement of Spicules in the Formation of Vaccinia Virus Envelopes Elucidated by a Conditional Lethal Mutant1. Virology 214, 494–502 (1995).

Montanuy, I., Alejo, A. & Alcami, A. Glycosaminoglycans mediate retention of the poxvirus type I interferon binding protein at the cell surface to locally block interferon antiviral responses. FASEB J. 25, 1960–1971 (2011).

Montecalvo, A. et al. Mechanism of transfer of functional microRNAs between mouse dendritic cells via exosomes. Blood 119, 756–66 (2012).

Morelli, A. E. et al. Endocytosis, intracellular sorting, and processing of exosomes by dendritic cells. Blood 104, 3257–66 (2004).

Morgan, C. The insertion of DNA into vaccinia virus. Science 193, 591–2 (1976).

Mori, Y. et al. Human Herpesvirus-6 Induces MVB Formation, and Virus Egress Occurs by an Exosomal Release Pathway. Traffic 9, 1728–1742 (2008).

Moss, B. Poxvirus DNA replication. Cold Spring Harb. Perspect. Biol. 5, (2013).

Moss, B. Poxvirus Cell Entry: How Many Proteins Does it Take? Viruses 4, 688–707 (2012).

Moss, B. Poxvirus entry and membrane fusion. Virology 344, 48–54 (2007).

Muratori, C. et al. Massive Secretion by T Cells Is Caused by HIV Nef in Infected Cells and by Nef Transfer to Bystander Cells. Cell Host Microbe 6, 218–230 (2009).

Myskiw, C. et al. RNA species generated in vaccinia virus infected cells activate cell type-specific MDA5 or RIG-I dependent interferon gene transcription and PKR dependent apoptosis. Virology 413, 183–193 (2011).

Ndiaye, B. P. et al. Safety, immunogenicity, and efficacy of the candidate tuberculosis vaccine MVA85A in healthy adults infected with HIV-1: a randomised, placebo-controlled, phase 2 trial. Lancet Respir. Med. 3, 190–200 (2015).

Nolte-’t Hoen, E. N. M. et al. Deep sequencing of RNA from immune cell-derived vesicles uncovers the selective incorporation of small non-coding RNA biotypes with potential regulatory functions. Nucleic Acids Res. 40, 9272–9285 (2012).

Ockenhouse, C. F. et al. Phase I/IIa safety, immunogenicity, and efficacy trial of NYVAC-Pf7, a pox-vectored, multiantigen, multistage vaccine candidate for Plasmodium falciparum malaria. J. Infect. Dis. 177, 1664–73 (1998).

Ostrowski, M. et al. Rab27a and Rab27b control different steps of the exosome secretion pathway. Nat. Cell Biol. 12, 19–30 (2010).

Paez, E. & Esteban, M. Resistance of vaccinia virus to interferon is related to an interference phenomenon between the virus and the interferon system. Virology 134, 12–28 (1984).

Panchanathan, V., Chaudhri, G. & Karupiah, G. Protective immunity against secondary poxvirus infection is dependent on antibody but not on CD4 or CD8 T-cell function. J. Virol. 80, 6333–8 (2006).

Pedersen, K. et al. Characterization of vaccinia virus intracellular cores: implications for viral uncoating and core structure. J. Virol. 74, 3525–36 (2000).

Pegtel, D. M. et al. Functional delivery of viral miRNAs via exosomes. Proc. Natl. Acad. Sci. 107, 6328–6333 (2010).

Perrin, L. H., Zinkernagel, R. M. & Oldstone, M. B. Immune response in humans after vaccination with vaccinia virus: generation of a virus-specific cytotoxic activity by human peripheral lymphocytes. J. Exp. Med. 146, 949–69 (1977).

Peters, N. E. et al. A Mechanism for the Inhibition of DNA-PK-Mediated DNA Sensing by a Virus. PLoS Pathog. 9, e1003649 (2013).
Pham, A. M. et al. PKR Transduces MDA5-Dependent Signals for Type I IFN Induction. PLOS Pathog. 12, e1005489 (2016).

Pilato, M. Di et al. NFκB activation by modified vaccinia virus as a novel strategy to enhance neutrophil migration and HIV-specific T-cell responses. Proc. Natl. Acad. Sci. 112, E1333–E1342 (2015).

Prazsák, I. et al. Full Genome Sequence of the Western Reserve Strain of Vaccinia Virus Determined by Third-Generation Sequencing. Genome Announc. 6, (2018).

Pucci, F. et al. SCS macrophages suppress melanoma by restricting tumor-derived vesicle-B cell interactions. Science 352, 242–6 (2016).

Qin, L., Favis, N., Famulski, J. & Evans, D. H. Evolution of and evolutionary relationships between extant vaccinia virus strains. J. Virol. 89, 1809–24 (2015).

Ramakrishnaiah, V. et al. Exosome-mediated transmission of hepatitis C virus between human hepatoma Huh7.5 cells. Proc. Natl. Acad. Sci. 110, 13109–13113 (2013).

Raposo, G. et al. B lymphocytes secrete antigen-presenting vesicles. J. Exp. Med. 183, 1161–72 (1996).

Ratajczak, J. et al. Embryonic stem cell-derived microvesicles reprogram hematopoietic progenitors: evidence for horizontal transfer of mRNA and protein delivery. Leukemia 20, 847–856 (2006).

Reading, P. C. & Smith, G. L. A kinetic analysis of immune mediators in the lungs of mice infected with vaccinia virus and comparison with intradermal infection. J. Gen. Virol. 84, 1973–1983 (2003).

Reed, K. D. et al. The Detection of Monkeypox in Humans in the Western Hemisphere. N. Engl. J. Med. 350, 342–350 (2004).

Reggiori, F. & Pelham, H. R. Sorting of proteins into multivesicular bodies: ubiquitin-dependent and -independent targeting. EMBO J. 20, 5176–86 (2001).

Ridder, K. et al. Extracellular vesicle-mediated transfer of functional RNA in the tumor microenvironment. Oncoimmunology 4, e1008371 (2015).

Ridder, K. et al. Extracellular Vesicle-Mediated Transfer of Genetic Information between the Hematopoietic System and the Brain in Response to Inflammation. PLoS Biol. 12, e1001874 (2014).

Risco, C. et al. Endoplasmic Reticulum-Golgi Intermediate Compartment Membranes and Vimentin Filaments Participate in Vaccinia Virus Assembly. J. Virol. 76, 1839–1855 (2002).

Rojas, J. J. et al. Manipulating TLR Signaling Increases the Anti-tumor T Cell Response Induced by Viral Cancer Therapies. Cell Rep. 15, 264–273 (2016).

Rowan, K. Oncolytic Viruses Move Forward in Clinical Trials. JNCI J. Natl. Cancer Inst. 102, 590–595 (2010).

Russell, S. J., Peng, K.-W. & Bell, J. C. Oncolytic virotherapy. Nat. Biotechnol. 30, 658–70 (2012).

Rountree, R. B. et al. Exosome Targeting of Tumor Antigens Expressed by Cancer Vaccines Can Improve Antigen Immunogenicity and Therapeutic Efficacy. Cancer Res. 71, 5235–5244 (2011).

Ryerson, M. R., Richards, M. M., Kvansakul, M., Hawkins, C. J. & Shisler, J. L. Vaccinia Virus Encodes a Novel Inhibitor of Apoptosis That Associates with the Apoptosome. J. Virol. 91, (2017).

Sanjana, N. E., Shalem, O. & Zhang, F. Improved vectors and genome-wide libraries for CRISPR screening. Nat. Methods 11, 783–784 (2014).

Schmelz, M. et al. Assembly of vaccinia virus: the second wrapping cisterna is derived from the trans Golgi network. J. Virol. 68, 130–47 (1994).

Schmidt, F. I. et al. Vaccinia Virus Entry Is Followed by Core Activation and Proteasome-Mediated Release of the Immunomodulatory Effector VH1 from Lateral Bodies. Cell Rep. 4, 464–476 (2013).

Schmidt, F. I., Bleck, C. K. E., Helenius, A. & Mercer, J. Vaccinia extracellular virions enter cells by macropinocytosis and acid-activated membrane rupture. EMBO J. 30, 3647–3661 (2011).

Schroeder, N., Chung, C.-S., Chen, C.-H., Liao, C.-L. & Chang, W. The lipid raft-associated protein CD98 is required for vaccinia virus endocytosis. J. Virol. 86, 4868–82 (2012).

Schoggins, J. W. Interferon-stimulated genes: roles in viral pathogenesis. Curr. Opin. Virol. 6, 40–46 (2014).

Senkevich, T. G., Weisberg, A. S. & Moss, B. Vaccinia Virus E10R Protein Is Associated with the Membranes of Intracellular Mature Virions and has a Role in Morphogenesis. Virology 278, 244–252 (2000).

Senkevich, T. G., Ojeda, S., Townsley, A., Nelson, G. E. & Moss, B. Poxvirus multiprotein entry-fusion complex. Proc. Natl. Acad. Sci. U. S. A. 102, 18572–7 (2005).

Shen, B., Wu, N., Yang, J.-M. & Gould, S. J. Protein Targeting to Exosomes/Microvesicles by Plasma Membrane Anchors. J. Biol. Chem. 286, 14383–14395 (2011).

Shi, J. et al. Cleavage of GSDMD by inflammatory caspases determines pyroptotic cell death. Nature 526, 660–665 (2015).

Shurtleff, M., Temoche-Diaz, M., Karfilis, K., & Elife, S. R. Y-box protein 1 is required to sort microRNAs into exosomes in cells and in a cell-free reaction. Cdn.elifesciences.org (2016).

Singh, R. K., Balamurugan, V., Bhanuprakash, V., Venkatesan, G. & Hosamani, M. Emergence and reemergence of vaccinia-like viruses: global scenario and perspectives. Indian J. Virol. 23, 1–11 (2012).

Sivan, G., Weisberg, A. S., Americo, J. L. & Moss, B. Retrograde Transport from Early Endosomes to the trans -Golgi Network Enables Membrane Wrapping and Egress of Vaccinia Virus Virions. J. Virol. 90, 8891–8905 (2016).

Skog, J. et al. Glioblastoma microvesicles transport RNA and proteins that promote tumour growth and provide diagnostic biomarkers. Nat. Cell Biol. 10, 1470–1476 (2008).

Smith, G. L. et al. Vaccinia virus immune evasion: mechanisms, virulence and immunogenicity. J. Gen. Virol. 94, 2367–2392 (2013).

Smith, G.L., & Law, M. The exit of Vaccinia virus from infected cells. Virus Res. 106, 189–197 (2004).

Smith, G. L., Vanderplasschen, A. & Law, M. The formation and function of extracellular enveloped vaccinia virus. J. Gen. Virol. 83, 2915–2931 (2002).

Smith, G. L., Khanna, A., Alcami, A. & Paul, N. L. Vaccinia virus strains Lister, USSR and Evans express soluble and cell-surface tumour necrosis factor receptors. J. Gen. Virol. 80, 949–959 (1999).

Sodeik, B. & Krijnse-Locker, J. Assembly of vaccinia virus revisited: de novo membrane synthesis or acquisition from the host? Trends Microbiol. 10, 15–24 (2002).

Sodeik, B. et al. Assembly of vaccinia virus: role of the intermediate compartment between the endoplasmic reticulum and the Golgi stacks. J. Cell Biol. 121, 521–41 (1993).
Spehner, D, & Drillien, R. Extracellular vesicles containing virus-encoded membrane proteins are a byproduct of infection with modified vaccinia virus Ankara. Virus Res. 137, 129–136 (2008).

Squadrito, M. L. et al. Endogenous RNAs Modulate MicroRNA Sorting to Exosomes and Transfer to Acceptor Cells. Cell Rep. 8, 1432–1446 (2014).

Stack, J. et al. Vaccinia virus protein A46R targets multiple Toll-like–interleukin-1 receptor adaptors and contributes to virulence. J. Exp. Med. 201, 1007–1018 (2005).

Stuart, J. H., Sumner, R. P., Lu, Y., Snowden, J. S. & Smith, G. L. Vaccinia Virus Protein C6 Inhibits Type I IFN Signalling in the Nucleus and Binds to the Transactivation Domain of STAT2. PLOS Pathog. 12, e1005955 (2016).

Symons, J. A., Bartlett, N., Tscharke, D. C. & Smith, G. L. The vaccinia virus N1L protein is an intracellular homodimer that promotes virulence. J. Gen. Virol. 83, 1965–1976 (2002).

Symons, J. A., Alcamí, A. & Smith, G. L. Vaccinia virus encodes a soluble type I interferon receptor of novel structure and broad species specificity. Cell 81, 551–60 (1995).

Szajner, P., Weisberg, A. S., Lebowitz, J., Heuser, J. & Moss, B. External scaffold of spherical immature poxvirus particles is made of protein trimers, forming a honeycomb lattice. J. Cell Biol. 170, 971-981 (2005).

Szostak, N. et al. Sorting signal targeting mRNA into hepatic extracellular vesicles. RNA Biol. 11, 836–44 (2014).

Tartaglia, J. et al. NYVAC: A highly attenuated strain of vaccinia virus. Virology 188, 217–232 (1992).

Teale, A. et al. Orthopoxviruses require a functional ubiquitin-proteasome system for productive replication. J. Virol. 83, 2099–108 (2009).

Thacore, H. R. & Youngner, J. S. Rescue of vesicular stomatitis virus from interferon-induced resistance by superinfection with vaccinia virus. I. Rescue in cell cultures from different species. Virology 56, 505–11 (1973).

Théry, C. et al. Minimal information for studies of extracellular vesicles 2018 (MISEV2018): a position statement of the International Society for Extracellular Vesicles and update of the MISEV2014 guidelines. J. Extracell. vesicles 7, 1535750 (2018).

Théry, C. et al. Indirect activation of naïve CD4+ T cells by dendritic cell–derived exosomes. Nat. Immunol. 3, 1156–1162 (2002).
Théry, C. et al. Proteomic analysis of dendritic cell-derived exosomes: a secreted subcellular compartment distinct from apoptotic vesicles. J. Immunol. 166, 7309–18 (2001).

Tolonen, N., Doglio, L., Schleich, S. & Locker, J. K. Vaccinia Virus DNA Replication Occurs in Endoplasmic Reticulum-enclosed Cytoplasmic Mini-Nuclei. Mol. Biol. Cell 12, 2031–2046 (2001).

Tooze, J., Hollinshead, M., Reis, B., Radsak, K. & Kern, H. Progeny vaccinia and human cytomegalovirus particles utilize early endosomal cisternae for their envelopes. Eur. J. Cell Biol.60, 163–178 (1993).

Torralba, D. et al. Priming of dendritic cells by DNA-containing extracellular vesicles from activated T cells through antigen-driven contacts. Nat. Commun. 9, 2658 (2018).

Torres-Domínguez, L. E. & McFadden, G. Poxvirus Oncolytic virotherapy. Expert Opin. Biol. Ther. 14712598.2019.1600669 (2019). doi:10.1080/14712598.2019.1600669

Tulman, E. R. et al. Genome of Horsepox Virus. J. Virol. 80; 9244–9258 (2006).

Valadi, H. et al. Exosome-mediated transfer of mRNAs and microRNAs is a novel mechanism of genetic exchange between cells. Nat. Cell Biol. 9, 654–659 (2007).

Vanderplasschen, A. & Smith, G. L. A novel virus binding assay using confocal microscopy: demonstration that the intracellular and extracellular vaccinia virions bind to different cellular receptors. J. Virol. 71, 4032–41 (1997).

Vanderplasschen, A., Mathew, E., Hollinshead, M., Sim, R. B. & Smith, G. L. Extracellular enveloped vaccinia virus is resistant to complement because of incorporation of host

complement control proteins into its envelope. Proc. Natl. Acad. Sci. U. S. A. 95, 7544–9 (1998).

Venkatesan, G. et al. Emerging and re-emerging zoonotic buffalopox infection: a severe outbreak in Kolhapur (Maharashtra), India. Vet. Ital. 46, 439–48.

Veyer, D.L. et al. Vaccinia virus evasion of regulated cell death. Immunol. Lett. 186, 68–80 (2017).

Veyer, D. L. et al. Analysis of the anti-apoptotic activity of four vaccinia virus proteins demonstrates that B13 is the most potent inhibitor in isolation and during viral infection. J. Gen. Virol. 95, 2757–68 (2014).

Villarroya-Beltri, C. et al. Sumoylated hnRNPA2B1 controls the sorting of miRNAs into exosomes through binding to specific motifs. Nat. Commun. 4, 2980 (2013).

Vincent-Schneider, H. et al. Exosomes bearing HLA-DR1 molecules need dendritic cells to efficiently stimulate specific T cells. Int. Immunol. 14, 713–722 (2002).

Vyas, N. et al. Vertebrate Hedgehog is secreted on two types of extracellular vesicles with different signaling properties. Sci. Rep. 4, 7357 (2015).

Walsh, D. et al. Eukaryotic translation initiation factor 4F architectural alterations accompany translation initiation factor redistribution in poxvirus-infected cells. Mol. Cell. Biol. 28, 2648–58 (2008).

Wang, J. et al. Exosome-Mediated Delivery of Inducible miR-423-5p Enhances Resistance of MRC-5 Cells to Rabies Virus Infection. Int. J. Mol. Sci. 20, 1537 (2019).

Ward, B. M. Visualization and characterization of the intracellular movement of vaccinia virus intracellular mature virions. J. Virol. 79, 4755–63 (2005).

Wasilenko, S. T., Stewart, T. L., Meyers, A. F. A. & Barry, M. A cytomegalovirus-encoded mitochondria-localized inhibitor of apoptosis structurally unrelated to Bcl-2. PNAS 96, 12536–12541 (2003).

Wasilenko, S. T., Stewart, T. L., Meyers, A. F. A. & Barry, M. Vaccinia virus encodes a previously uncharacterized mitochondrial-associated inhibitor of apoptosis. Proc. Natl. Acad. Sci. 100, 14345–14350 (2003).

Wei, M. C. et al. Proapoptotic BAX and BAK: A Requisite Gateway to Mitochondrial Dysfunction and Death. Science (80-.). 292, 727–730 (2001).

Whitaker-Dowling, P. & Youngner, J. S. Vaccinia rescue of VSV from interferon-induced resistance: reversal of translation block and inhibition of protein kinase activity. Virology 131, 128–36 (1983).

Whitbeck, J. C., Foo, C.-H., Ponce de Leon, M., Eisenberg, R. J. & Cohen, G. H. Vaccinia virus exhibits cell-type-dependent entry characteristics. Virology 385, 383–91 (2009).

Williams, R. L. & Urbé, S. The emerging shape of the ESCRT machinery. Nat. Rev. Mol. Cell Biol. 8, 355–368 (2007).

Williamson, J. D., Reith, R. W., Jeffrey, L. J., Arrand, J. R. & Mackett, M. Biological characterization of recombinant vaccinia viruses in mice infected by the respiratory route. J. Gen. Virol. 71, 2761–2767 (1990).

Willms, E. et al. Cells release subpopulations of exosomes with distinct molecular and biological properties. Sci. Rep. 6, 22519 (2016).
Winter, J. & Diederichs, S. Argonaute proteins regulate microRNA stability: Increased microRNA abundance by Argonaute proteins is due to microRNA stabilization. RNA Biol. 8, 1149–1157 (2011).

Xiang, Y. et al. Blockade of interferon induction and action by the E3L double-stranded RNA binding proteins of vaccinia virus. J. Virol. 76, 5251–9 (2002).

Xu, R., Johnson, A. J., Liggitt, D. & Bevan, M. J. Cellular and humoral immunity against vaccinia virus infection of mice. J. Immunol. 172, 6265–71 (2004).

Yang, Z., Bruno, D. P., Martens, C. A., Porcella, S. F. & Moss, B. Simultaneous high-resolution analysis of vaccinia virus and host cell transcriptomes by deep RNA sequencing. Proc. Natl. Acad. Sci. 107, 11513–11518 (2010).

Yang, Z., Bruno, D. P., Martens, C. A., Porcella, S. F. & Moss, B. Simultaneous high-resolution analysis of vaccinia virus and host cell transcriptomes by deep RNA sequencing. Proc. Natl. Acad. Sci. U. S. A. 107, 11513–8 (2010).

Zhang, Q. et al. Genomic Sequence and Virulence of Clonal Isolates of Vaccinia Virus Tiantan, the Chinese Smallpox Vaccine Strain. PLoS One 8, e60557 (2013).

CONTRIBUTIONS FROM COLLABORATORS

The work of several other members of our lab was crucial for this research project. Marie-Eve Wedge collected and prepared the MiaPACA-2 sEV and cell samples for the small RNA-Seq experiment. Adrian Pelin, a member of John Bell's lab, performed the Small RNA-Seq analyses. Finally, Natalie Crawford performed the CRISPR-Cas9-mediated targeting of Rab27a, clonal selection by serial dilution, and initial screening of monoclonal lines for Rab27a expression.

APPENDIX

Table 1. qPCR and PCR primers used in this study.

TARGET	Forward Primer Sequence	Reverse Primer Sequence
18S (qPCR)	CTCAACACGGGAAACCTCAC	CGCTCCACCAACTAAGAACG
R-PIPO (qPCR)	TTAAACCCTGCGTGGCAATCC	CCACATTCCCCCGGATATGA
B19R (qPCR)	CACAGTTACGCCATAGACATCG	GCCTCTCCCATTTAACCACATAG
C12L (qPCR)	TGAGAATACACCCGATGACAATAA	AAATGGACGGCGCTAACA
A11R (qPCR)	CTATGCCAACACAAACACCAT	ACCACTTCATCCTCCAACATC
C12L (Full CDS)	CTAATCGTAAAACACCCTGATG	AAAGTATACGTCCTGTGGTGT
Rab27a	CCTCACACTTGAGAGGTAGC	CCAAGAGTTTGAGAAAATGG
Rab27a Seq	GCATTATGTCAATTCCCAAT	AAAGGACACATTCAACATGC

Table 2. Human Rab27a gRNA Design and Cloning Strategy.

gRNA Oligo Design	5’ -CACCGNNNNNNNNNNNNNNNNNNN- 3’ 3’ -CNNNNNNNNNNNNNNNNNNNCAAA- 5’
Rab27a Region to Target	5’ -TAGCACTCGCAGAGAAATAT- 3’
gRNA Spacer Sequence	5’ -ATATTTCTCTGCGAGTGCTA- 3’
Top Oligo	5’ -CACCGATATTTCTCTGCGAGTGCTA- 3’
Bottom Oligo	5’ -AAACTAGCACTCGCAGAGAAATATC- 3’

CURRICULUM VITAE

EDUCATION

MSc in Microbiology and Immunology
2017-2019

University of Ottawa, Faculty of Medicine

Ottawa Hospital Research Institute

BScH Specialization in Biology with Distinction
2013-2017

Queen's University, Kingston, ON

GPA: 3.88

AWARDS

Canada Graduate Scholarship – CIHR – Master's Program
2018-2019

Frederick Banting and Charles Best Canada Graduate Scholarship

Excellence Scholarship
2018-2019

University of Ottawa, Ottawa, ON

Travel Award, BioCANRx Summit for Cancer Immunotherapy
2018

Banff, Alberta, Canada

Travel Award, Intellectual Property for Biotherapeutic Scientists
2018

Clinical Translation Education Group and BioCANRx

Toronto, Ontario

Registration Award – Canadian Bioinformatics Workshop
2018

Ontario Institute of Cancer Research (OICR)

Introduction to RNA-Seq

Top Ten Poster Award, International Oncolytic Virus Conference
2018

University of Oxford, Oxford, UK

Nomination: Ontario Women's Health Scholars (Provincial Competition)
2017

Nominated By: Scholarship Committee of the Office of the Vice-Provost, Graduate and Postdoctoral Studies, University of Ottawa

Admission Scholarship
2017

University of Ottawa, Ottawa, ON

Dean's List
2014-2017

Queen's University, Kingston, ON

Excellence Scholarship
2013

Queen's University, Kingston, ON

RESEARCH EXPERIENCE

Graduate Research Student, Ottawa Hospital Research Institute
2017-2019

Centre for Innovative Cancer Therapeutics

Department of Biochemistry, Microbiology, and Immunology

Supervisor: Carolina Ilkow, PhD

Honours Thesis Student, Queen's University
2016-2017

Biology Department

Supervisor: Paul Young, PhD

Research Student, Ottawa Hospital Research Institute
2016

Centre for Innovative Cancer Therapeutics

Supervisor: John Bell, PhD

Research Mentorship Student, Queen's University
2016 Biology Department

Supervisor: Paul Young, PhD

Independent Research Course, Carleton University
2014

Institute of Biochemistry

Supervisor: Ashkan Golshani, PhD

ORAL PRESENTATIONS

Extracellular Vesicles and Intercellular Communication during Oncolytic Virus Infection

Hayley McKay, Adrian Pelin, Natalie Crawford, John Bell, Carolina Ilkow

BioCANRx Summit for Cancer Immunotherapy in Banff, Alberta

"Speed Poster" Oral Presentation on October 27 2018

Extracellular Vesicle Day, Ottawa, ON

Hayley McKay, Adrian Pelin, Marie-Eve Wedge, John Bell, Carolina Ilkow

Ottawa Extracellular Vesicle Day, June 2018

Finding Sal1: The search for the lost allosuppressor

Hayley McKay and Paul Young

Queen's University Biology Department Thesis Seminar Series, October 2016

Targeting Arid1A with CRISPR-Cas9: Understanding Oncolytic Virotherapy

Hayley McKay, Larissa Pikor, Carolina Ilkow, John Bell

Ottawa Hospital Research Institute Summer Student Program, June 2016

POSTER PRESENTATIONS

Exosome-mediated transfer of an alpha/beta IFN receptor promotes vaccinia virus spread

Hayley McKay, Adrian Pelin, Marie-Eve Wedge, John Bell, Carolina Ilkow

Biochemistry, Microbiology, and Immunology Symposium, May 2018

Exosome-mediated transfer of an alpha/beta IFN receptor promotes vaccinia virus spread

Hayley McKay, Adrian Pelin, Marie-Eve Wedge, John Bell, Carolina Ilkow

Biochemistry, Microbiology, and Immunology Poster Day, May 2018

Extracellular Vesicles and Intercellular Communication during Oncolytic Virus Infection

Hayley McKay, Adrian Pelin, Marie-Eve Wedge, John Bell, Carolina Ilkow

International Oncolytic Virus Conference, University of Oxford, Oxford, UK, April 2018

Targeting Oncogenes in Cervical Cancer

Hayley McKay, Brian Keller, John Bell, Carolina Ilkow

Ottawa Hospital Research Institute Research Day, Ottawa, Ontario, November 2017

Finding Sal1: The search for the lost allosuppressor

Hayley McKay and Paul Young

Queen's University Biology Department Capstone Research Day, March 2017

EXTRACURRICULAR ACTIVITIES

VP Wellness, Biochemistry, Microbiology, and Immunology Grad Student Assoc.
2018-2019

Organize and promote various wellness initiatives to enhance the graduate student experience within the Faculty of Medicine and BMI Department.

Working Group Member, BioCANRx Summit for Cancer Immunotherapy
2017-2018

BioCANRX, Highly Qualified Personnel Working Group

Organized educational and networking events at the annual conference in Oct. 2019.

Mediated the 'Meet the Experts' panel for 120 HQP at the summit.

Volunteer, Let's Talk Science School Program, Ottawa ON
2017-2019

Led engaging and educational science sessions with elementary school children.

Member of Let's Talk Cancer, and present workshops to Canadian high school children who come to Ottawa for the Encounters with Canada 'Health and Medicine' Program.

Volunteer Sports Leader, Ausome Ottawa
2017-2019

Work one-on-one with children with Autism Spectrum Disorder in sports programs. Adapt the activities based on their individual needs.

Graduate Student Representative, Faculty of Medicine Wellness Committee
2017-2019

Work with fellow committee members, including psychologists and a psychiatrist,

to improve the health & wellness of students in the Faculty of Medicine.

Member, Biochemistry, Microbiology and Immunology Grad Student Assoc.
2017-2018

Began working with the BMIGSA as a Member-At-Large.

Co-President, Queen's Biology Departmental Student Council
2016-2017

Led a team of 28 executive members, oversaw the planning of social events, academic workshops, and marketing initiatives, and participate in departmental and faculty meetings to advocate for Biology students.

Capstone Committee Member, Queen's Biology Department
2016-2017

Organized the keynote speaker series at the Annual Thesis Poster Day.

Student Representative, Renewal Tenureship Promotions Committee
2015-2016

Reviewed RTP files and gave recommendations to the Head of Biology and the

Dean of the Faculty of Arts and Science.

Children's Outpatient Volunteer, Hotel Dieu Hospital
2015-2016

Supervised patients in the playroom, organized activities for them.

Cardiac Rehab Volunteer, **Hotel Dieu Hospital**
2014-2015

Assisted in the Cardiac Rehab Exercise Program, helped the patients with their exercises and provided a supportive role for the nurses and physiotherapists.

Executive Member, Biology Departmental Student Council
2014-2016

Advocated for students within the Biology Department and Faculty as a member of the student affairs and academics sub-committees.

Surplus Food Distributor, Queen's Soul Foods, Kingston ON
2014

Brought excess food from Queen's cafeterias to In From The Cold Emergency Shelter.

OTHER EMPLOYMENT ACTIVITIES

Assistant Camp Supervisor, RA Centre, Ottawa, ON
2012-2015

Led a team of camp counsellors and counsellors-in-training as a part of the supervisory staff.

Technical Soccer Coach, Gloucester Soccer Association, Ottawa, ON
2010-2016

Ran technical sessions for assigned teams.

Ski Instructor, Camp Fortune Ski School, Chelsea, QC
2010-2012

Taught children ages 4-6.

ACTIVITIES AND INTERESTS

Competitive Soccer Player, Gloucester Hornets, Ottawa, ON
2005-2018

Kayaking, Hiking, Alpine Skiing, CrossFit, and Traveling